Inaugural dissertation

for

obtaining the doctoral degree

of the

Combined Faculty of Mathematics, Engineering and Natural Sciences

of the

Ruprecht – Karls – University

Heidelberg

Presented by

Mgr. Dajana Tanasić, MSc

Born in: Banja Luka, Bosnia and Herzegovina

Oral examination: 01.07.2022

Intracellular membrane trafficking of E-cadherin in *Drosophila*

Referees:

Prof. Dr. Dr. Georg Stoecklin

PD Dr. Veit Riechmann

Ehrenwörtliche Erklärung zu meiner Dissertation mit dem Titel:
„Intracellular membrane trafficking of E-cadherin in *Drosophila*"

Hiermit erkläre ich, dass ich die vorliegende Arbeit ohne unzulässige Hilfe Dritter und nur unter Verwendung der angegebenen Quellen und Hilfsmittel verfasst habe. Jegliche Ausführungen, die wörtlich oder sinngemäß übernommen wurden, sind als solche kenntlich gemacht. Ich habe diese Arbeit bisher an keinem anderen in- oder ausländischen Naturwissenschaftlich-Mathematischen Fachbereich als Prüfungsarbeit verwendet oder als Dissertation eingereicht.

I hereby declare that I have written this thesis without the unauthorized help of third parties and only using the sources and aids indicated. Any statements that have been taken over verbatim or in spirit are marked as such. I have not used this thesis as an examination paper or submitted it as a dissertation to any other department of natural science or mathematics in Germany or abroad.

Ort, Datum

Unterschrift

Acknowledgements

This research was carried out at the Department of Cell and Molecular Biology of Medical Faculty Mannheim, University of Heidelberg. First, I would like to express my gratitude to my supervisor, PD Dr. Veit Riechmann, for allowing me to work on a PhD project in his lab. I am grateful for all of his help and support over the last five years. Even when my scientific enthusiasm was low, discussions with him were always inspirational and informative, teaching me how to think critically and approach problems from other perspectives. I am also grateful for his time and patience. I would not have completed my PhD as successfully as I did without his mentoring.

I would like to thank Nicola Berns, the lab postdoc, for her support, and assistance throughout my PhD. Her ideas contributed to the quality of my work. I'm also thankful for the opportunity to share the lab and enjoy the conversation during the long lab hours.

I'd also like to express my heartfelt gratitude to my colleague, Dr. Sara Laiouar-Pedari. With her wonderful personality and cheerful spirit, she was the nicest labmate anyone could ask for. She truly brightened my PhD days.

A big thank goes to the lab technician Nadine Kraft. She did an amazing job in performing the immunohistochemistry experiments and managing the lab. It was a pleasure to share the workplace with her.

I would also like to thank our secretary Felicitas Olschowsky for all the paperwork that she has performed for our lab.

Prof. Dr. Dr. Georg Stoecklin and Prof. Dr. Steven Dooley, members of my TAC committee, deserve special recognition. During our annual meetings, their feedback and encouragement have always motivated me and contributed to the improvement of my project.

I further want to express my gratitude to Dr. Nitin Patil, Bojana Pavlovic, Öznur Singin and Johanna Dieplinger for reviewing my thesis and providing constructive criticism, suggestions, and feedback.

In addition, I would like to thank Radana and Nedo Drvar for their friendship and love, as well as for providing me with a family atmosphere when I needed it most.

I am forever thankful for love and support that my parents Jelena and Miroslav and my sister Aleksandra, as well as the rest of my family, have always shown me. They had unconditional faith in me and selflessly encouraged me to pursue my dreams. None of my accomplishments would have been possible without their love, patience and encouragement, and I dedicate this milestone to them.

Last but not the least, I would like to praise and thank God for countless blessings in my life, amongst which are the successful end of my PhD.

Zusammenfassung

Die Aufrechterhaltung der Zell-Zell-Adhäsion ist entscheidend für die Gewebeintegrität und die epitheliale Homöostase. Der Hauptbaustein der Zellverbindungen, der sogenannten Adherens-Verbindungen, ist E-Cadherin. Eine Unterbrechung der E-Cadherin-Sekretion zur Plasmamembran verursacht Gewebezerfall und Metastasierung.

Trotz der Wichtigkeit der ordnungsgemäßen E-Cadherin-Lieferung an die Plasmamembran, bleiben die Transportmechanismen unbekannt. In dieser Arbeit untersuche ich den Transport von E-Cadherin unter Verwendung des follikulären Epithels von *Drosophila*-Ovarien.

Ich zeige, dass das neu synthetisierte und endozytierte *Drosophila* E-Cadherin (DE-Cadherin) die apikalen endosomalen Kompartimente Rab7 und Rab11 durchquert. Die Signale für die richtige Abgabe von DE-Cadherin an apikale Endosomen befinden sich im zytoplasmatischen Schwanz des Proteins. Darüber hinaus rekrutiert Rab7 das Sorting Nexin 16 (Snx16) für den anschließenden DE-Cadherin-Transport. Snx16 liefert DE-Cadherin über die Tubulationsaktivität an das Rab11-Kompartiment. Meine Ergebnisse legen nahe, dass Snx16 auch für die Stabilisierung des DE-Cadherin- und Armadillo-Komplexes erforderlich ist, was wiederum für einen effizienten DE-Cadherin-Transport notwendig ist. Außerdem werden die Exozystenkomponente Sec15 und der Motor MyosinV (MyoV) von Rab11 rekrutiert. Dies führt zur Bildung des MyoV/Sec15/Rab11-Komplexes, der apikale Aktinbahnen nutzt, um DE-Cadherin zu der Zonula-Adhärenz zu transportieren, wo es einen kontinuierlichen Adhäsionsgürtel bildet. Meine Daten zeigen, dass für die ordnungsgemäße Bildung des MyoV/Sec15/Rab11-Komplexes und die ungehinderte DE-Cadherin-Abgabe an die Plasmamembran äquivalente Spiegel von MyoV, Rab11 und Sec15 erforderlich sind. Bei der Expression des nicht funktionsfähigen MyoV, reichert sich DE-Cadherin in den endosomalen Kompartimenten Rab7 und Rab11 an, wodurch die Zonula-Adhärenz nicht kontinuierlich gebildet werden kann. Dies deutet darauf hin, dass der MyoV-Motor DE-Cadherin auch aus apikalen endosomalen Kompartimenten transportiert. Darüber hinaus zeigen meine Daten, dass DE-Cadherin auch entlang der basalen Aktinkabel über den MyoV/Sec15/Rab11-Komplex zur Abgabe an die basolaterale Plasmamembran transportiert wird.

Zusammengenommen geben meine Ergebnisse Aufschluss über die DE-Cadherin-Sekretionswege. Ich konnte mehrere zusätzliche Aspekte des E-Cadherin-Transports innerhalb endosomaler Kompartimente und zur Plasmamembran zeigen. Dadurch tragen meine Daten zu einem besseren Verständnis der epithelialen Homöostase und der Prävention von Krankheiten und deren Folgen, einschließlich Krebsmetastasen, bei.

Summary

The maintenance of the cell-cell adhesion is crucial for tissue integrity and epithelial homeostasis. E-cadherin is the main building block of the cell junctions called adherens junctions. Disruption in E-cadherin secretion to the plasma membrane causes tissue disintegration and metastasis.

Despite the importance of the proper E-cadherin delivery to the plasma membrane, the mechanisms of transport remain unknown. Here, I investigate E-cadherin trafficking using the follicular epithelium of *Drosophila* ovaries.

I show that the newly synthesized and endocytosed *Drosophila* E-cadherin (DE-cadherin) transverses through the apical Rab7 and Rab11 endosomal compartments. The signals for the proper DE-cadherin delivery to apical endosomes are located within the protein`s cytoplasmic tail. Furthermore, the Rab7 recruits a sorting nexin 16 (Snx16) for subsequent DE-cadherin transport. Snx16 delivers DE-cadherin to the Rab11 compartment via the tubulation activity. My finding suggests that Snx16 is also required for the stabilization of the DE-cadherin and Armadillo complex, which is necessary for efficient DE-cadherin trafficking. Further, the exocyst component Sec15 and the motor MyosinV (MyoV) are then recruited by Rab11. This results in the formation of the MyoV/Sec15/Rab11 complex that uses apical actin tracks to transport DE-cadherin to the zonula adherens, where it creates a continuous adhesion belt. My data shows that equivalent levels of MyoV, Rab11 and Sec15 are required for the proper MyoV/Sec15/Rab11 complex formation and unhampered DE-cadherin delivery to the plasma membrane. Upon the expression of the nonfunctional MyoV, DE-cadherin accumulates in Rab7 and Rab11 endosomal compartments, and zonula adherens cannot be continuously formed. Additionally, my data reveal that the DE-cadherin is also transported along basal actin cables via the MyoV/Sec15/Rab11 complex for delivery to the basolateral plasma membrane. Taken together, my findings shed light on the DE-cadherin secretion pathways. I was able to show several additional aspects of E-cadherin transport within endosomal compartments and towards the plasma membrane. As a result, my data contribute to a better understanding of epithelial homeostasis and the prevention of diseases and their consequences, including cancer metastasis.

Table of Contents

1 Introduction

1.1 *Drosophila* oogenesis

The epithelium of the *Drosophila* ovary is an excellent model to study how membrane proteins are secreted, endocytosed and recycled. Such transport processes in membrane vesicles are summarized by the term 'membrane trafficking'. The fly has a pair of ovaries and each ovary consists of 15-20 ovarioles (Figure 1a). A single ovariole contains gradually matured egg chambers of different stages (Figure 1b). The most anterior part of the ovariole is termed germarium and is the place where the stem-cell niche is located (Lin, 2002). The germarium develops into egg chambers, which form a series of progressively older-stage egg chambers. Each egg chamber consists of an inner cyst that contains 16 germline cells: 1 oocyte and 15 nurse cells. A monolayer of epithelial cells surrounds the inner cyst of each egg chamber. As the oocyte matures and grows in size, the epithelial cells enclosing the inner cyst need to adapt to the changes. One of the adaptions involves the change in the egg chamber rotation. In stages 1-5 egg chambers rotate slowly, whereas the egg chambers' rotation speeds up in stages 6-8 resulting in a fast rotation. Interestingly, the rotation completely stops after stage 9 (Cetera et al., 2014; L. He et al., 2010). Besides the changes in the egg chamber rotation, the cell shape of the epithelium changes as well. The epithelial cells in *Drosophila* egg chambers of the early stages all have cuboidal cell shape. At the beginning of stage 9, the cell shape throughout the epithelium becomes heterogeneous: approximately 50 anterior cells become flat and adopt a squamous shape, while the posterior cells become columnar. At stage 10, the egg chambers consist of squamous cells in the anterior part and the columnar cells in the posterior part of the egg chamber (Horne-Badovinac & Bilder, 2005).

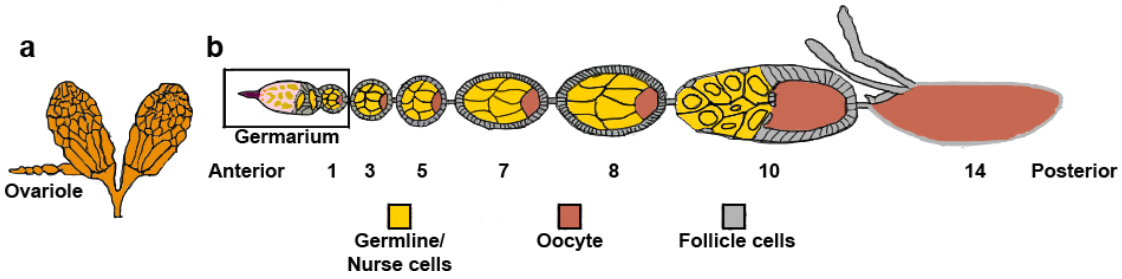

Figure 1. Schematic diagram of the *Drosophila* ovary. (a) The female fly has a pair of ovaries and each ovary consists of 15-20 ovarioles. (b) A single ovariole of the *Drosophila* ovary, with the germarium at the anterior part and different developmental stages of the egg chambers. Follicle cells are represented in grey, nurse cells in yellow and the oocyte in red. The figure is adapted from Lebo & McCall, 2021.

Epithelial shape changes are characterized by the removal and recycling of the adhesion membrane proteins. Two important families of adhesion membrane proteins are the immunoglobulin and cadherins superfamily. Fasciclin 2 (Fas2), the insect homolog of the vertebrate neural cell-adhesion molecule (N-CAM), and Fasciclin 3 (Fas3), which doesn't have a vertebrate homolog until now, both belong to the immunoglobulin superfamily (Grenningloh et al., 1991; Patel et al., 1987; Snow et al., 1989). By stage 8 of egg chambers, Fas2 and Fas3 are completely removed from the cell membrane by endocytosis. This removal is critical for the posterior cells transition from cuboidal into squamous shape and for anterior cells to flatten into squamous shape (Gomez et al., 2012; Grenningloh et al., 1991; Laiouar et al., 2020; Szafranski & Goode, 2004).

Cadherin molecules also play an essential role in cell shape establishment, as the presence of cadherins at the membrane determines the shape of the cells (Hayashi & Carthew, 2004). Particularly important is the epithelial cadherin, E-cadherin. It serves as a building block for the homophilic cell-cell adhesion in the epithelial cells. Preventing the removal of E-cadherin from the plasma membrane can result in increased adherence amongst cells and cell shape distortion (Levayer et al., 2011; K. Sato et al., 2011). The removal and turnover of E-cadherin must therefore be regulated. However, the exact mechanisms involved in E-cadherin delivery to the plasma membrane, internalization and intracellular transport remain unknown.

In the *Drosophila* ovary follicular epithelium, *Drosophila* E-cadherin (DE-cadherin) is detected along the lateral membrane but concentrated at the apical-most region, termed zonula adherens, throughout all egg chamber stages (Figure 2). However, at the beginning of stage 9, the expression of DE-cadherin at the posterior part of the egg chamber reduces significantly (arrows in Figure 2). This change in DE-cadherin expression in the posterior part of the egg chamber corresponds to the change in the cell shape of the follicle cells. At stage 9, the cell shape becomes heterogeneous throughout the egg chamber (Horne-Badovinac & Bilder, 2005).

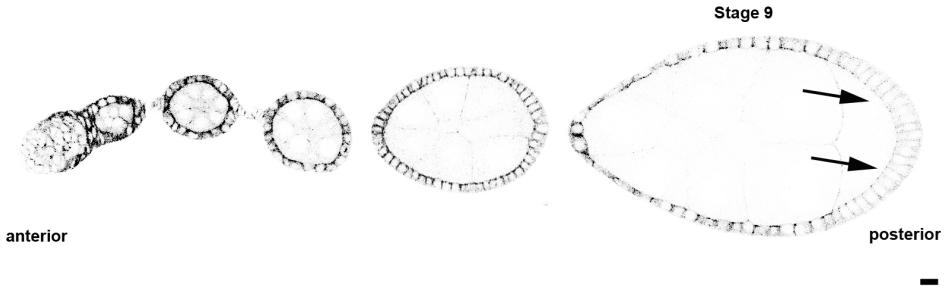

Figure 2. DE-cadherin localization throughout different developmental *Drosophila* egg chamber stages. The ovaries were stained with α-DE-cadherin antibody and one ovariole is represented. Until stage 9, DE-cadherin can be detected at the membrane encircling the inner cyst. At stage 9, DE-cadherin is barely detected at the posterior part of the egg chamber (arrows). The scale bar in the lower right corner represents 10μm.

1.2 Cell-cell adhesion

Cells are attached to each other or to the common surface, termed extracellular matrix, via the cell adhesion process. The extracellular matrix is a three-dimensional network of collagens, proteoglycans, elastin, laminin, and a variety of other glycoproteins that gives structural and biological support to adjacent cells (Romani et al., 2021). Proper cell attachment is necessary for the formation of organized multicellular structures, as well as for cell-cell communication and interaction. Structures called cell junctions are responsible for cell-cell adhesion. Anchoring junctions are one type of cell junctions that can stretch across the membrane and connect the adhesion surface (neighboring cell or matrix) to the inner cellular structures. The adherens junction, which is a form of anchoring junction, is critical for cell polarity and tissue homeostasis (Green et al., 2010).

The main building block of the adherens junction is the protein E-cadherin that interacts with another E-cadherin protein on the neighboring cell. Adherens junctions form a belt, resulting in the belt-like adherens junction, that links the cells into a continuous sheet termed the zonula adherens. Besides the belt-like adherens junction, E-cadherin can be observed localizing along the lateral membrane below the zonula adherens, forming the punctate-like adherens junction (Takeichi, 2014).

The strength of adherens junction depends on E-cadherin available for its formation. The process of adherens junction constant assembly and disassembly is linked to changes in cell shape, tissue remodeling, cell division and cell death. Fast E-cadherin turnover is therefore crucial in these processes, as the changes in adherens junction are reflected by the changes in the localization of E-cadherin on the plasma membrane (Harris & Tepass, 2010; Takeichi, 2014). It is thus important to understand the mechanisms behind the processes of E-cadherin transport within the cell and, eventually, to the adherens junction.

1.2.1 The transmembrane adhesion protein E-cadherin

E-cadherin is expressed in epithelial cells and belongs to the cadherin protein family. Cadherins are cell adhesion molecules that form 'calcium-dependent adhesion'. Their function is dependent on calcium ions, since calcium depletion leads to conformational changes of cadherin proteins and thus suppresses cell adhesion via cadherins (Nagar et al., 1996). Structurally, mature E-cadherin consists of an extracellular domain, a transmembrane domain and an intracellular (cytoplasmic) domain (Figure 3). The vertebrate extracellular domain has 5 cadherin repeats, whereas in *Drosophila*, 7 cadherin repeats are present (Harris & Tepass, 2010). Cadherin repeats have binding sites for Ca^{2+} located between them and these cadherin repeats are important for building homophilic interactions between E-cadherins on neighboring cells (Chappuis-Flament et al., 2001).

The intracellular domain of the E-cadherin protein has binding sites for different E-cadherin regulators and links the cell surface to the cytoskeleton. It is a rather short (150 amino acids) unstructured domain that is highly conserved throughout species, unlike the extracellular domain. There are two distinct domains within the intracellular E-cadherin tail: a membrane-proximal cytoplasmic domain (the so-called juxtamembrane domain) and a β-catenin binding domain (Biswas & Zaidel-Bar, 2017; Van Roy & Berx, 2008). Within the intracellular domain, there is also a so-called serine cluster that has been shown to significantly increase the affinity of E-cadherin towards the β-catenin regulator *in vivo* and *in vitro* (Choi et al., 2015). β-catenin regulation of E-cadherin is essential for cell-cell attachment (J. Chen et al., 2017; Choi et al., 2015; A. H. Huber & Weis, 2001). Studies have shown that the intracellular domain of E-cadherin contains sorting signals for proper E-cadherin transport (Y. T. Chen et al., 1999; Miranda et al., 2001). The dileucine motif, in particular, provides signals for direct E-cadherin sorting to the plasma membrane, according to *in vitro* research (Miranda et al., 2001). Interestingly, despite high sequence similarity amongst the species, the dileucine motif is not present in *Drosophila* E-cadherin intracellular domain (Bulgakova & Brown, 2016; Myster et al., 2003). Therefore, the exact sorting signals required for E-cadherin delivery to the plasma membrane in both vertebrates and *Drosophila* still remain unknown.

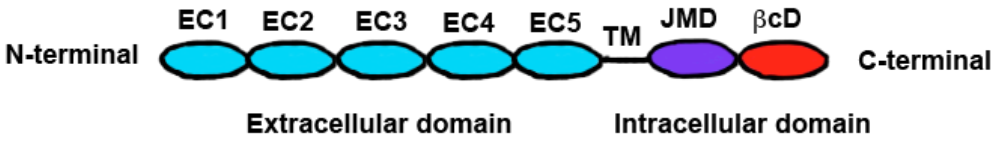

Figure 3. Schematic representation of vertebrate E-cadherin protein domains. The vertebrate extracellular domain consists of five E-cadherin repeats (blue). In *Drosophila*, however, there are 7 cadherin repeats. The transmembrane domain (TM) connects the extracellular domain to the intracellular domain, which is made of juxtamembrane domain (purple) and β-catenin domain (red).

1.2.2 Regulation of E-cadherin transport and its delivery to the cell surface

Precise delivery of E-cadherin to the plasma membrane is achieved by regulated intracellular E-cadherin transport. Newly synthesized E-cadherin first needs to be transported out of the endoplasmic reticulum (ER). At the ER, β-catenin binds to the E-cadherin cytoplasmic domain and forms the E-cadherin/β-catenin complex that is shown to be required for efficient E-cadherin transport out of the ER and localization to the plasma membrane (Y. T. Chen et al., 1999). However, further studies on the importance of E-cadherin/β-catenin complex *in vitro* and *in vivo* revealed that E-cadherin is able to not only leave the ER but also localize to the plasma membrane without β-catenin (Miranda et al., 2001; Pacquelet & Rørth, 2005). After leaving the ER, E-cadherin undergoes sorting for the subsequent transport steps. This sorting can take place at the Golgi network (Beronja et al., 2005; Satoh et al., 2005) or at the endosomes (Classen et al., 2005; Langevin et al., 2005). Transport of E-cadherin out of the *trans*-Golgi compartment is regulated by the tubulovesicular carrier Golgin-97 (Lock et al., 2005). Once the E-cadherin/β-catenin complex reaches the adherens junction at the plasma membrane, β-catenin links E-cadherin to the actin cytoskeleton via α-catenin (Drees et al., 2005). Interestingly, a study conducted in *Drosophila* suggests that the linkage of E-cadherin to the actin cytoskeleton via α-catenin might be the primary role of β-catenin at the adherens junctions (Pacquelet & Rørth, 2005). Another member of the catenin protein family, p120, also binds E-cadherin at the adherens junction. The binding of p120 to E-cadherin regulates E-cadherin turnover and degradation (Bulgakova & Brown, 2016; K. Sato et al., 2011; Thoreson et al., 2000).

Once at the plasma membrane, E-cadherin can be internalized via endocytosis. E-cadherin endocytosis is an essential process in cell reshaping and tissue remodeling. Endocytosis of E-cadherin can be performed via two different mechanisms: clathrin-dependent or clathrin-independent endocytosis. Clathrin-dependent endocytosis involves vesicles consisting mainly of clathrin proteins. Clathrin requires adaptor proteins to recognize different motifs for cargo

binding (B. T. Kelly & Owen, 2011). E-cadherin endocytosis through clathrin-vesicles has been associated with the AP-2 adaptor. Studies in vertebrates have shown that E-cadherin binds AP-2 through the dileucine motif located within the cytoplasmic tail (Miranda et al., 2001; Miyashita & Ozawa, 2007). Other studies reveal that the endocytic adaptor Numb binds to E-cadherin and promotes endocytosis of the protein from the plasma membrane (Lau & McGlade, 2011; Z. Wang et al., 2009). Another adaptor Disabled-2 (Dab2) has also been associated with E-cadherin. Dab2 downregulation results in E-cadherin accumulation and loss of apical-basal polarity (Yang et al., 2007). Formation of clathrin-coated vesicles also involves Dynamin, the main component of the endocytic machinery, and Rab5 GTPase. Rab5 recruits clathrin-coated vesicles and Dynamin drives the cleavage of the endocytic vesicle (Kirchhausen et al., 2014). The less studied endocytosis mechanism of E-cadherin is the clathrin-independent endocytosis. According to a few studies, clathrin-independent endocytosis can be performed either via caveolin-mediated internalization or via micropinocytosis (Bryant et al., 2005; Lu et al., 2003; Paterson et al., 2003).

E-cadherin first enters the Rab5 positive compartment, also known as the early endosome, if it is internalized by clathrin-mediated endocytosis (S. R. Pfeffer, 2013; Wandinger-Ness & Zerial, 2014). Studies in cultured cells have shown that endocytosis through Rab5 compartments is the driving force of E-cadherin dynamics (De Beco et al., 2009; Le et al., 1999). Along the endocytic pathway, E-cadherin is constantly trafficked. Fluorescence recovery after photobleaching experiments demonstrated that adherens junction disassembly and E-cadherin extraction from the plasma membrane occur via endocytosis (De Beco et al., 2009).

From the Rab5 compartment, E-cadherin can face two different fates. It is either transported back to the plasma membrane or degraded in the lysosomes. The decision between recycling and degradation regulates the strength of cell-cell adhesion. The more E-cadherin is degraded, the weaker the cell adhesion is. Similarly, more rapid recycling results in stronger cell-cell adhesion (Brüser & Bogdan, 2017). A study in *Drosophila* ovaries has shown that endocytosed E-cadherin passes through the Rab11 endosomal compartment if destined to be recycled for the adherens junction formation (Langevin et al., 2005). This is in line with findings in cultured mammalian cells, which show that newly synthesized E-cadherin vesicles also fuse with intermediate Rab11 compartments before reaching the plasma membrane (Stow & Lock, 2005). Live imaging conducted in the same study with cultured mammalian cells detected both Ecad and Rab11 in highly dynamic tubulovesicular carriers, indicating active involvement of Rab11 in E-cadherin exocytosis. E-cadherin cannot be secreted to the cell surface when the dominant-negative form of Rab11 is expressed, confirming the role of Rab11 in E-cadherin delivery to the plasma membrane (Stow & Lock, 2005). A recent study from our lab in *Drosophila* ovaries also shows that Rab11 is involved in the delivery of newly synthesized E-

cadherin directly to the zonula adherens (Woichansky et al., 2016). The same study suggests that E-cadherin delivery to the lateral area of the plasma membrane, however, is Rab11-independent, indicating that the cell has several E-cadherin delivery routes to the plasma membrane (Woichansky et al., 2016). Despite significant research, it is still unclear how E-cadherin reaches Rab11 compartments. Furthermore, transfer of E-cadherin within the endosomal compartment has also not been thoroughly studied.

Once E-cadherin reaches the Rab11 compartment, the evolutionarily conserved exocyst complex is recruited for the subsequent trafficking steps. Absence of the exocyst subunits Sec5, Sec6 and Sec15 leads to the accumulation of the E-cadherin protein within the enlarged Rab11 compartment (Langevin et al., 2005). This demonstrates that the exocyst promotes the delivery of E-cadherin to the lateral membrane from recycling endosomes (Langevin et al., 2005). Depletion of Protein Associated with Lin Seven 1 (PALS1), a mammalian homologue for an important polarity protein termed Stardust in *Drosophila*, leads to mislocalization of the exocyst complex and the cytoplasmic E-cadherin accumulation (Q. Wang et al., 2007). This result indicates an important function of the exocyst in E-cadherin recycling in vertebrates as well. However, it still remains unclear how exactly the exocyst complex transports E-cadherin from endosomes to the plasma membrane.

Other proteins in *Drosophila* that regulate the localization of E-cadherin at the membrane are Cip4 and Nostrin. Cip4 and Nostrin belong to the Bin/Amphiphysin/Rvs (BAR) - protein family, whose members are capable of generating vesicles and tubules. Nostrin localizes to the Rab11 compartment and Cip4 and Nostrin might be mediating the transport of E-cadherin at the endosomes via tubulation activity (Zobel et al., 2015).

When not destined for recycling, E-cadherin is sent for degradation. E-cadherin targeted for the degradation associates with the ubiquitin ligase Hakai. The ubiquitination and binding of Hakai to E-cadherin depends on the Src-mediated phosphorylation at the two tyrosine residues within the E-cadherin juxtamembrane domain (Fujita et al., 2002). Interestingly, the binding site for the p120 regulator is near the tyrosine residues that are phosphorylated, suggesting that p120 and Hakai might be competing in binding to E-cadherin (Hartsock & Nelson, 2012).

The organelle responsible for the degradation of biological macromolecules is the lysosome (Hesketh et al., 2018; Saftig & Klumperman, 2009). It is a membrane-enclosed acidic compartment containing up to 50 acid hydrolases in its lumen. The late endosome is capable of fusion with the lysosome, leading to the formation of the hybrid compartment termed endolysosomes. A study in mammalian cells has demonstrated that lysosomal hydrolases can also be detected in the endolysosomes (Bright et al., 2016). This suggests that the degradation of cargo might already start in the endolysosomes.

1.2.3 E-cadherin in tumor development and progression

Disturbance of E-cadherin localization at the plasma membrane leads to cell and tissue disorders that result in the development of disease processes. Lack of E-cadherin has been connected to tumor development and cancer metastasis already in an early study (Berx et al., 1995). Metastasis of the cancer cells requires the loss of E-cadherin on the membrane in the process termed epithelial-mesenchymal transition (EMT). EMT is a well-organized and regulated cell program activated in many cancer cells that leads to the suppression of epithelial markers and the upregulation of mesenchymal markers. The cells undergoing EMT gradually lose epithelial character and acquire mesenchymal character. The hallmark of the EMT process is the downregulation of E-cadherin, since the changes in E-cadherin expression affect cell shape and cell-cell adhesion (Huang et al., 2012). Suppression of E-cadherin expression is accompanied by the upregulation of the mesenchymal marker N-cadherin. The mesenchymal cells form homotypic N-cadherin interactions that are significantly weaker than the interactions through E-cadherin. Such N-cadherin links promote invasive and migratory properties of cells (Wheelock et al., 2008). The reduced level of E-cadherin on the cell membrane also leads to increased cell motility (Qin et al., 2005; Yilmaz & Christofori, 2010). Increased cell motility during EMT requires changes in the cell cytoskeleton. Actin filaments facilitate cell movement by forming sheet-like and spike-like membrane protrusions termed lamellipodia and filopodia. Rearrangement of the cytoskeleton is the prerequisite for the front-rear polarity, characteristic for migrative cells (Ridley, 2011; Thiery & Sleeman, 2006; Yilmaz & Christofori, 2009). Taken together, E-cadherin localization at the plasma membrane is essential for maintaining cell integrity and homeostasis. Disturbance in the expression of E-cadherin at the cell surface underlies tissue disorders and diseases development.

1.3 The actin network and myosin motors

The cytoskeleton is a network of interconnected structures that maintains cells' support and organization. Cell-cell adhesion and cytoskeletal structures are co-dependent. Tight control in regulating the cross-talk between the cell-cell adhesion and cytoskeletal structures is thus crucial. E-cadherin and the catenin regulators play an essential role in this cross-talk (Parsons et al., 2010). E-cadherin, which is a building block of adherens junctions, is attached to the cytoskeleton via the binding to β-catenin and α-catenin (Drees et al., 2005). Past studies have shown that α-catenin is a crucial linker in conducting signals from cytoskeletal structures to the cell membrane, as it interacts with the actin filaments and actin-binding proteins through its C-terminal domain (Borghi et al., 2012; Kobielak & Fuchs, 2004; Rimm et al., 1995; Yonemura

et al., 2010). Besides the interplay of the cytoskeleton and cell adhesion, the cytoskeletal elements are also essential in the transport of E-cadherin. However, it is unclear exactly what motors and which cytoskeletal tracks are involved in this process of E-cadherin trafficking.

Microtubules and actin filaments are the main components of the cell cytoskeleton, which also provide the tracks for the movement of molecular motors that transport vesicles, organelles and other cargo. Actin filaments are polarized and highly dynamic cytoskeletal structures. They are capable of performing rapid structural changes in a very short time and are involved in processes such as cell movement, cell morphology and vesicle trafficking (Galletta & Cooper, 2009). The main unit of the actin filaments is globular actin (G-actin). G-actin forms fiber-like structures of double-helical filaments referred to as F-actin. The continuous assembly and disassembly of the actin network can occur locally. During endocytosis, invagination of the plasma membrane leads to the formation of a local actin network that eventually assists in the formation of the endocytic vesicle from the internalized region of the membrane (Galletta & Cooper, 2009; Simonetti & Cullen, 2019). Molecular motors using F-actin filaments to transport cargo are myosin motors (Pollard, 2016).

Myosin motors consist of a large superfamily. Three different subdomains can be distinguished within myosin proteins: the motor domain, the neck domain and the C-terminal tail domain. Rather conserved amongst myosin proteins is the motor domain, which uses the energy from ATP hydrolysis to “walk” along the actin filaments (Heissler & Sellers, 2016). On the other hand, the tail domain varies widely in both length and sequence (Sellers, 1999). The motor and tail domains are thought to be interrelated, and both are considered necessary for the specific function of myosin motors (Korn, 2000; Krendel & Mooseker, 2005; O`Connell et al., 2007). Furthermore, the tail of the myosin motor binds to the specific adaptor protein, resulting in the myosin recruitment to an organelle or molecular complex (Akhmanova & Hammer III, 2010; Hartman & Spudich, 2012). Directionality also plays an important role in myosin-dependent transport (O`Connell et al., 2007). Actin filaments within the cell are arranged in a polarized order, with the minus-end oriented towards the interior of the cell and the plus-end oriented towards the plasma membrane. A myosin motor implicated in the transport of vesicles will thus move towards the plus end in the process of protein secretion. Myosin proteins are grouped into 20 different classes, based on the phylogenetic analysis of the motor domain (O`Connell et al., 2007). Another classification of myosin motors can also be distinguished: conventional myosins, (consisting of skeletal, cardiac, smooth myosins and non-muscle myosin II) and unconventional myosins (representing a majority of myosin genes) (Fili & Toseland, 2020).

One class of the myosin superfamily, unconventional motor myosin V (MyoV), is found widely within many species. It is involved in the trafficking of many membrane cargos such as secretory vesicles, vacuoles and recycling endosomes (Hammer & Sellers, 2012; Hammer &

Wagner, 2013). There are three classes of MyoV in humans (Va, Vb and Vc), whereas in *Drosophila* there is a single MyoV gene. The association of MyoV motors with Rab GTPases, such as Rab8 and Rab11, has already been described in both mammals and *Drosophila* (Lapierre et al., 2001; Li et al., 2007; Roland et al., 2009). Previous work in yeast used pull-down experiments to show that MyoV is a Rab11 binding partner, which is further confirmed by experiments *in vitro* and *in vivo* (Jin et al., 2011). The same study also demonstrates that there is an interaction between MyoV and the exocyst subunit Sec15, revealing possible binding sites within both proteins (Jin et al., 2011). All of this suggests the existence of a complex involving the MyoV motor, Rab11, and the exocyst complex. However, it is unknown which proteins are transported via this complex. It is also unclear which tracks exactly the complex uses to move within the cell.

1.4 Rab proteins

Rab proteins were initially described as Ras-related genes expressed in the rat brain (Touchot et al., 1987). In vertebrates, there are more than 75 different Rab proteins, whereas in *Drosophila* only 31 are identified. Nevertheless, most *Drosophila* Rab proteins are closely related to at least one vertebrate Rab gene based on sequence similarity (Zhang et al., 2007). Rab proteins act as molecular switches alternating between an active and an inactive state (Figure 4). In their active state, Rab proteins are recruited to the membranes of cell organelles where they interact with different factors to control various steps in vesicle trafficking (Zerial & McBride, 2001). Rab proteins in inactive form, on the other hand, remain in the cytosol and await activation. An active state is when the Rab protein is bound to the guanosine-5`-triphosphate (GTP), while the Rab protein bound to the of guanosine-5`-diphosphate (GDP) is in its inactive state. A number of assistant proteins support the Rab protein switch between the active and the inactive state (Barr & Lambright, 2010). Rab proteins interact with the guanine-nucleotide-exchange factor (GEF), which prompts the exchange of inactive Rab (GDP-bound) to active Rab (GTP-bound). This release of GDP and binding of GTP initiates the downstream cascade. The switch to the inactive state occurs when GTP is hydrolyzed to the GDP. This is stimulated by the GTPase activating protein (GAP). Once in the inactive state, Rab proteins soon re-enter the cycle by the exchange of GDP to GTP that is prompted by GEFs (E. E. Kelly et al., 2012; Wandinger-Ness & Zerial, 2014). The interplay of Rab proteins and their GEFs and GAPs is necessary to have the Rab protein functions in vesicles trafficking properly carried out (Barr & Lambright, 2010; Zerial & McBride, 2001).

The nucleotide exchange and the molecular switch depend on the structural features of Rab proteins. Rab proteins consist of two variable regions that are named switch I and switch II.

These switch regions can change their conformation depending on the active/inactive status of the Rab protein (S. R. Pfeffer, 2005). Another crucial part of the Rab GDP-GTP cycle is the tethering of Rab proteins to the membrane of different cell organelles (S. Pfeffer & Aivazian, 2004). To be bound to the membrane, Rab proteins first need to be prenylated. Prenylation is a posttranslational modification where geranylgeranyl groups are covalently added to the C-terminal cysteine residues. Prenylation allows for the attachment of the Rab protein to the target membrane (Alexandrov et al., 1994). Prenylated Rab proteins can also be found in the cytosol, where they form a complex with the GDP-dissociation inhibitor (GDI) (Alory & Balch, 2001). Attachment of Rab proteins to membranes is essential for their roles in membrane trafficking such as vesicle budding, motility, tethering and fusion. An early study has shown that different Rab proteins are present on different membranous organelles in the cytoplasm, making Rab GTPases suitable as markers for the various compartments (Chavrier et al., 1990). Rab1 is mainly detected on the Golgi, whereas Rab3 is present on the synaptic vesicles. Rab5 is traditionally used as a marker for the early endosome, Rab11 for the recycling endosome, while Rab7 and Rab9 are expressed on the late endosome (Zerial & McBride, 2001). The presence of Rab proteins on different compartments also marks them as molecular addresses for different steps in vesicle trafficking. The early endosomal Rab5, for instance, can be replaced by Rab7 as the compartment matures into the late endosome (Rink et al., 2005). Therefore, Rab GTPases play an important role in the dynamics of the intracellular compartments and vesicles trafficking.

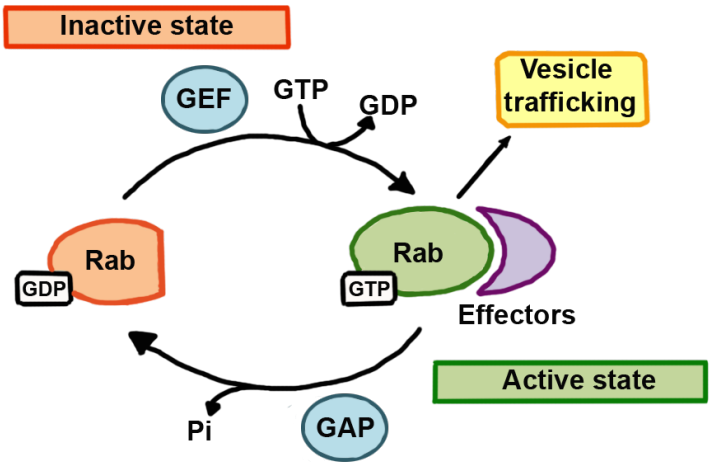

Figure 4. Schematic representation of the interchange of Rab proteins from active to inactive state. When in the inactive state, Rab protein bound to GDP. GEF catalyzes the exchange from GDP to GTP, Rab binds GTP and enters the active state. In its active state, Rab proteins are capable of binding the effectors, which would promote processes such as vesicle trafficking. Eventually, Rab proteins re-enter inactive state by GAP-facilitated hydrolysis of GTP to GDP. The figure is adapted from S. Wang et al., 2017.

1.5 The intracellular trafficking compartments

Cell homeostasis and the cell's interaction with the environment are dependent on the transport of different proteins into and out of the cell. Intracellular delivery of proteins to the plasma membrane or the extracellular space is termed exocytosis. On the other hand, endocytosis describes the process of the internalization of proteins into the cell. Proteins can also be transported within different cellular compartments. One established way of protein transport is performed via vesicular transport (Schu, 2001). Vesicles are transport tools enclosed by a membrane that bud from one compartment and fuse with the target compartment to release the transported cargo. Vesicle budding is performed with the help of adaptor proteins and specialized coat proteins, whereas vesicle fusion with the target compartments requires tethers and specialized proteins called SNAREs (Y. A. Chen et al., 2001; Guo et al., 2000). There are many different routes that vesicles can utilize to transport proteins, some being general and some being specific to the cargo they are transporting. The following sections provide an insight into the different cell compartments involved in vesicle transport and their context within cargo trafficking (Figure 5).

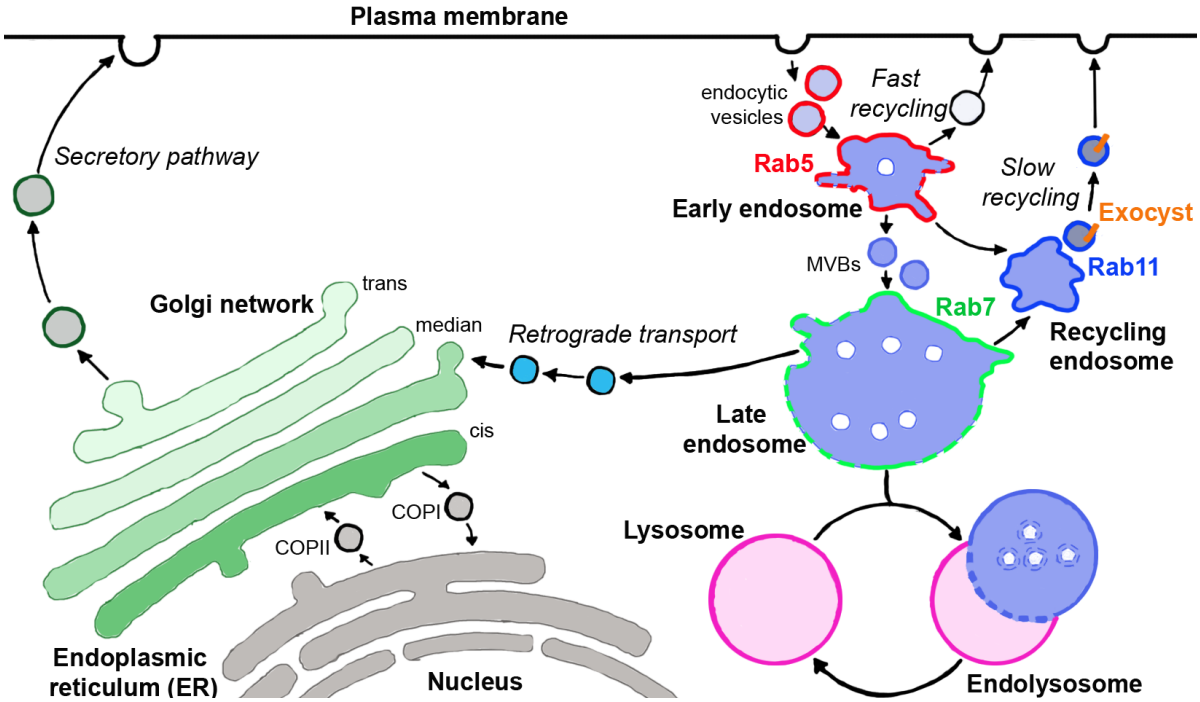

Figure 5. Schematic representation of intracellular trafficking compartments. The endoplasmic reticulum (grey) is the site of protein synthesis. After the synthesis, proteins enter the Golgi network (green) via COPII vesicles (grey). The Golgi network consists of cis- (dark green), median- (medium green) and trans- (light green) sides. From the Golgi network, proteins are transported to the plasma membrane via the secretory pathway. Once at the plasma membrane, proteins can be internalized via endocytic vesicles in the process termed endocytosis. After the endocytosis, the proteins enter the early endosome marked by Rab5 (red rim). From the early endosome, proteins can be sorted for fast or slow recycling. Slow recycling involves the passage of proteins through the recycling endosomes marked by Rab11 (blue rim). From the recycling endosome, proteins can be sent back to the plasma membrane with the help of the exocyst complex (orange). Proteins destined for degradation will be sorted into the intraluminal vesicles (ILVs) at the early endosome. ILVs form multivesicular bodies (MVBs) that bud from the early endosomes and make up the late endosomes marked by Rab7 (green rim). From the late endosomes, the proteins go to the endolysosomes, hybrid transitional compartments that eventually transform into the degradative compartments called lysosomes (pale pink). From the late endosome, proteins can also enter so-called retrograde transport, where they are sent back to the Golgi network from which they re-enter the secretory pathway. The figure is adapted from Cullen & Steinberg, 2018.

1.5.1 Endoplasmic reticulum and Golgi network

The endoplasmic reticulum (ER) is the organelle in which synthesis of transmembrane and secreted proteins takes place (Jan et al., 2015; Reid, 2017). The ER is the largest organelle in the cell and very dynamic and complex in structure. The ER consists of a continuous membrane that can be divided into three main morphological structures: the nuclear envelope, the peripheral ER cisternae and an interconnected tubular network. The biggest domain is the nuclear envelope, which is composed of a double membrane around the cell nucleus. Peripheral ER diverges from the nuclear envelope and can be subdivided into cisternae and tubular domains. The tubules of the peripheral ER are used to contact the plasma membrane and other organelles, establishing membrane contact sites (MCSs) (Eden et al., 2010; Ogata & Yamasaki, 1997; Phillips & Voeltz, 2016; Rocha et al., 2009; West et al., 2011). The ER exit sites (ERES) are used for secretory proteins to exit the ER. ERES are also characterized by the formation of coat protein complex II (COPII)-coated vesicles that are in charge of transporting the cargo leaving the ER for the Golgi network (Bannykh et al., 1996; Barlowe et al., 1994; Kurokawa & Nakano, 2019).

The Golgi network is a primary site for the receiving and the dispatching of proteins arriving from the ER. Structurally, the Golgi stack consists of 4-8 flat cisternal membranes that form ribbon-like compartments. In *Drosophila*, however, Golgi stacks are not connected and arranged into the Golgi ribbon, but are rather diffused throughout the cytoplasm. These diffused Golgi stacks are spatially related to the ER exit sites (Kondylis & Rabouille, 2009). The Golgi network is additionally also organized into *cis*, *median* and *trans* compartments, reflecting the polarity of the apparatus. The cargo is received from the ER on the *cis* side, whereas cargo exits the Golgi apparatus on the *trans* side (Kulkarni-Gosavi et al., 2019; Ravichandran et al., 2020). Once the proteins arrive at the *trans*-Golgi, they are sorted and sent for delivery to their further destinations. The Golgi is involved in vesicle trafficking via the so-called membrane tethers, the Golgi-associated proteins such as GRASPs (Golgi Reassembly and Stacking Proteins) and golgins. GRASPs are involved in the proper stacking of cisternae within the Golgi stacks as well as tethering of vesicles destined for merging with the Golgi apparatus (Feinstein & Listedt, 2008; Puthenveedu et al., 2006; Y. Wang et al., 2003). Golgins have a rod-like coiled-coil structure that allows them to span the long distances in the cytosol, “catch” vesicles and also tether them to the Golgi network. The coiled-coil nature of golgins is not rigid but rather flexible, accommodating for the changes in the conformation of golgin protein when required. Different golgins are localized to different regions of the Golgi network dependent on their function (Barinaga-Rementeria Ramirez & Lowe, 2009; Munro, 2011).

1.5.2 Endosomes

1.5.2.1 Early endosomes

Endosomes are cell compartments that serve as intermediate stations for the trafficking of proteins via vesicular transport. It is directly important to note that 'the endosome compartment' is still not precisely described, despite its importance in vesicle trafficking. Furthermore, although numerous advanced scientific approaches have been used for the investigation of endosomes, their characteristics remain unclear and diversified (Naslavsky & Caplan, 2018). Hence the distinction between early, late and recycling endosomes, widely used in the literature and presented in the following sections, should be regarded with caution.

The early endosome is the first stop for proteins that are internalized from the plasma membrane. Early endosomes are formed by the fusion of endocytic vesicles that originate from the plasma membrane. They can have diverse morphology, composition, localization and function (Huotari & Helenius, 2011). Early endosomes are rather small in size and can be detected at the periphery of the cell near the plasma membrane (Hoepfner et al., 2005; Nielsen et al., 1999). The membrane of the early endosome is marked by Rab5 GTPase, although subdomains enriched in Rab4, Rab11, Arf1/COPI and retromer can be detected as well (Rojas et al., 2008; Vonderheit & Helenius, 2005). These domains can be found on the tubular structures within the early endosome, assisting in the generation of vesicles that will transport the cargo to the subsequent target compartment. The early endosome consists of a central vacuole with tubular extensions facing the cell cytosol. Additionally, intraluminal vesicles (ILVs) budding from the outer early endosome membrane toward the central vacuole can also be detected (Klumperman & Raposo, 2014). Already at the early endosome, the cargo can be sorted either for recycling or for degradation (Rojas et al., 2008).

1.5.2.2 Late endosomes and degradation

The cargo destined for degradation is packed into the ILVs and eventually sent to the lysosomes (Frankel & Audhya, 2018). The regions of the early endosome containing ILVs "mature" by segregation and form multivesicular bodies (MVBs) or endosomal carrier vesicles (ECVs). Through further maturation, those compartments become part of the late endosome, another essential stop in proteins trafficking (Scott et al., 2014). During this process, Rab5 GTPase is replaced with Rab7 GTPase, a marker for the late endosomes. Rab5 recruits Rab7 to the early endosome, swiftly changes to its inactive GDP-bound form and detaches from the endosome (Rink et al., 2005). The maturation process of the early endosome to the late

endosome is very fast, as within 40 minutes all early endosome characteristics and markers are replaced by the late endosomal character. Late endosome characteristics include its more central cell position (in contrast to the early endosome position, which is more peripheral), greater number of ILVs, lower pH, different membrane composition, as well as changes in the compartment structure. Late endosomes are oval, round and bigger opposed to small tubular early endosomes (Huotari & Helenius, 2011). From the late endosome, the cargo destined for degradation is sent to the lysosomes. The lysosome is the organelle responsible for the degradation of biological macromolecules (Hesketh et al., 2018; Saftig & Klumperman, 2009). Late endosomes can temporally or completely merge with lysosomes, resulting in the formation of the endolysosomes (Bright et al., 2016). A recent study has shown that RabX1 GTPase plays a role in the formation of endolysosomal compartments (Laiouar et al., 2020). RabX1 localizes to late endosomal compartments and interacts with lysosomes by forming tubular structures. This results in the formation of endolysosomes, where the content exchange between lysosomes and late endosomes occurs. Loss of RabX1 function prevents degradation of lateral protein Fas2 and results in Fas2 accumulation in swelling late endosomal compartments, since no tubular structures enabling the content exchange can form. The frequent contact between RabX1 and lysosomes, as well as the content exchange, has been termed the ‘kiss and run’ mechanism. (Laiouar et al., 2020). However, it remains to be investigated whether proteins localizing to the apicolateral membrane, such as E-cadherin, are also degraded via the RabX1 compartment.

1.5.2.3 Recycling endosomes

Besides degradation, proteins can be destined for recycling. Cargo sorted for recycling needs to avoid packing into ILVs through the process named cargo retrieval (Seaman et al., 1997). Complexes such as the retromer and the retriever are required for the recognition of the sorting recycling motifs on the cargo (Cullen & Steinberg, 2018). Once retrieved for recycling, the cargo can undergo two routes. From the early endosome, the cargo can be directly transported to the plasma membrane. This is termed the fast-recycling pathway, which is Rab4 GTPase dependent (Huotari & Helenius, 2011; Maxfield & McGraw, 2004; Sheff et al., 1999; van der Sluijs et al., 1992). Besides Rab4, Rab35 is shown to be another important factor in the fast-recycling process (Kouranti et al., 2006; M. Sato et al., 2008). Proteins not being recycled via the fast-recycling route enter the recycling endosome or endocytic recycling compartments (ERC) for the slow-recycling pathway. The marker for the recycling endosome is Rab11 GTPase. Similarly to the early endosome localization, recycling endosomes in many cells are also tubular membrane-bound compartments located at the cell periphery (Grant & Donaldson, 2009; Maxfield & McGraw, 2004).

Besides Rab11, additional GTPases needed for the transport of cargo from the early to the recycling endosome are Rab22 and Rab10 (Babbey et al., 2006; C. C.-H. Chen et al., 2006; Magadán et al., 2006). The sorting nexins (Snx) are another protein family that serves for the cargo delivery to the recycling endosome (Pelham, 2002; Traer et al., 2007). They are a divergent and conserved protein group that shares the common phospholipid-binding motif termed PX domain. This domain allows Snx proteins to bind membranes enriched in so-called phosphatidylinositol phosphates (PtdInsPs) and thus deliver the cargo in a targeted fashion. PtdInsPs can be found on the cell and endocytic membranes (Worby & Dixon, 2002). Some studies describe members of the sorting nexin family as regulators of E-cadherin transport. Snx1 and Snx5 facilitate E-cadherin recycling and prevent its degradation (Bryant et al., 2007; Schill et al., 2014). The interaction of Rab11 and another sortin nexin, Snx4, with lipid raft protein reggie-1 has also been shown to facilitate E-cadherin sorting and recycling (Solis et al., 2013). A particularly interesting sorting nexin for E-cadherin trafficking is Snx16. Experiments *in vitro* showed that Snx16 depletion results in the reduction of E-cadherin on the cell surface, suggesting that Snx16 regulates E-cadherin recycling in the Rab11-dependent pathway (Jinxin Xu et al., 2017). Further analysis has shown that the PPII/α2 loop of Snx16's PX domain contains two alkaline residues, R170 and K173, that interact with E-cadherin, as R170/K173 double mutant couldn't precipitate together with the E-cadherin (Jinxin Xu et al., 2017). Nevertheless, it is still unclear how Snx16 is recruited for E-cadherin recycling and how it delivers E-cadherin for the subsequent trafficking steps.

Recycling can also occur via the *trans*-Golgi network (TGN), which is termed retrograde transport. Retrograde transport from the endosomes to the Golgi connects the endocytic and the biosynthetic/secretory pathways, and is shown to be crucial for many biological processes such as infection by pathogens (Bärlocher et al., 2017) and sorting of enzymes for the lysosomal degradation (Cheng & Filardo, 2012; Shafaq-Zadah et al., 2016). Such diversity in the recycling routes was shown to be necessary to ensure proper cell polarization and signaling (Cullen & Steinberg, 2018).

1.5.3 Exocyst

The plasma membrane is a dynamic structure that provides a physical barrier between the cytoplasm and the extracellular space, controlling the exchange of biomolecules between the inner and outer cell environment. Transport vesicles carrying cargo between the plasma membrane and membrane-bound compartments as well as between two membrane-bound compartments require proper tethering to the membrane by specialized tethering complexes. The exocyst is a widely studied tethering complex and is conserved from yeast to mammals

(B. He & Guo, 2009; Hsu et al., 1996; TerBush et al., 1996). It localizes to distinct regions of the plasma membrane, where it plays a role in tethering vesicles to the membrane before the SNARE-mediated fusion starts (Grote et al., 2000; Wiederkehr et al., 2004). The exocyst is an octameric complex consisting of subunits Sec3, Sec5, Sec6, Sec8, Sec10, Sec15, Exo70 and Exo84. Studies in yeast cells have shown that it is structurally composed of two sub-complexes: Sec3-Sec5-Sec6-Sec8 and Sec10-Sec15-Exo74-Exo80 (Heider et al., 2016; Katoh et al., 2015). Delivery of the majority of exocyst subunits to the plasma membrane is assisted by actin filaments (Boyd et al., 2004). The exocyst complex has a crucial function in the organism, as all the exocyst subunit null mutants in mammals and *Drosophila* are lethal (Friedrich et al., 1997; Murthy et al., 2003, 2005). *In vivo* and *in vitro* binding assays in mammalian cells reveal that the exocyst subunit Sec15 interacts with the active form of Rab11 GTPase (Zhang et al., 2004). Similarly, a study in *Drosophila* also shows that Sec15 binds to the GTP-bound Rab11 via its C-terminal, as well as to Rab3, Rab8 and Rab27 proteins (S. Wu et al., 2005). Taken together, this hints at Sec15 being an effector of Rab11 GTPase in both *Drosophil*a and mammalian cells. The role of the exocyst in E-cadherin transport has also been demonstrated. Upon the depletion of the exocyst subunit Sec5, both endocytosed E-cadherin and β-catenin accumulate in recycling endosomes that are Rab11 positive (Langevin et al., 2005). Another study in *Drosophila* ovaries suggested that Rab11 may be essential for the recruitment of the exocyst complex in the transport of newly generated E-cadherin as well (Woichansky et al., 2016). Interestingly, the link between the exocyst and E-cadherin is hypothesized to exist via β-catenin, as pull-down assays revealed that β-catenin binds the exocyst subunit Sec10 (Langevin et al., 2005). Sec15 interacts with the MyoV motor, potentially creating a complex with Rab11 GTPase, as previously mentioned (Jin et al., 2011) (see 1.3). Despite extensive research, it is still unclear how exactly DE-cadherin interacts with the exocyst. Additionally, it remains unknown what other components interact with the exocyst in DE-cadherin transport.

2 Aim of my thesis

E-cadherin is an adhesion membrane protein that forms adherens junctions in epithelial cells. Previous studies have shown that E-cadherin passes through the endosomal compartments on its way to the plasma membrane. Additionally, the critical role of Rab11, as an important organizer of E-cadherin transport, as well as the exocyst complex, which is responsible for tethering of E-cadherin to the plasma membrane, have been demonstrated. However, the underlying mechanisms of E-cadherin trafficking remain unknown.

My research aims to elucidate the mechanisms behind the transport of E-cadherin to the plasma membrane in the *Drosophila* follicular epithelium. First, I want to characterize the endosomal compartments through which E-cadherin transverses on the way to the plasma membrane. Further, I would like to investigate the transport of E-cadherin within the endosomal compartments. I am also interested in identifying at which stage does Rab11 play a role in the secretion of E-cadherin. Additionally, I aim to study how are the exocyst subunits recruited for the E-cadherin trafficking steps. Finally, I am particularly interested in identifying motors that deliver E-cadherin to the plasma membrane, as well as the pathways that these motors use to secrete E-cadherin.

3 Materials and Methods

3.1 Fly stocks

Flies were raised at 27°C in incubators with a 12h-light/12h-dark cycle and maintained on an agar medium. 1-3 days after hatching, ovaries were dissected and stained. The only exception are experiments with the dominant-negative *shibire* flies, which were raised at 18°C to avoid lethality (Figure 11b). After hatching flies were kept at 27°C for 24 hours to induce expression and then dissected.

All UAS-transgenes were induced with *traffic jam*-Gal4 with the exceptions of experiments shown in Figures 11a and 18b, where GR1-Gal4 was used to induce UAS-YFP-*Rab11* and UAS-GFP-*Snx1*6.

3.1.1 *Drosophila melanogaster* fly lines

RNAi line	Library	CG Number	Provider	ID Number
RNAi line for Sec15	KK	CG7034	VDRC	105126

Fly line	Reference	Provider	ID
w; *traffic jam*-Gal4	Olivieri et al., 2010	J. Brennecke	N/A
GR1-Gal4/TM3*Ser*	Gupta & Schüpbach, 2003	S. Roth	N/A
UAS-YFP-*Rab11*	Zhang et al., 2007	Bloomington	9790
w[*]; TM3, P{w[+mc]=UAS-*shibire*.K44A}3-10/TM6B, Tb[1]	Srahna et al., 2006	Bloomington	5822
w; FRT40A Rab5^{2}/cyo	Wucherpfennig et al., 2003	A. Guichet	N/A
UAS-HA-*Rab11*	Woichansky et al., 2016	Own lab	N/A
w; y*Rab7*	Dunst et al., 2015	M. Brankatschk	N/A
w;; FRT82B *Rab11*^{dFRT}/TM3Sb	Bogard et al., 2007	R.S. Cohen	N/A
FRT82B *Rab7*$^{Gal4\text{-}knock\text{-}in}$/TM6	Cherry et al., 2013	R. Hiesinger	N/A
UAS-wt*Snx16*-SNAP	Rodal et al., 2011	A.A. Rodal	N/A
UAS-*Snx16*ΔCC-SNAP	Wang et al., 2019	A.A. Rodal	N/A
UAS-GFP-*Snx16*	Wang et al., 2019	A.A. Rodal	N/A

FRT42 *Snx16*$^{\Delta 1}$/cyo	Rodal et al., 2011	A.A. Rodal	N/A
UAS-GFP-*MyoV* full-length (FL)	Krauss et al., 2009	A. Ephrussi	N/A
UAS-GFP-*MyoV*-GT	Krauss et al., 2009	B.J. Thompson	N/A
UAS-*Sec15*-mCherry	Michel et al., 2011	C. Böckel	N/A
UAS-*DE-cadh*ΔCyt/α-cat	Pacquelet et al., 2003	Bloomington	67415
UAS-*DE-cadherin*-$\Delta\beta$-catenin	Pacquelet et al., 2003	Bloomington	58497
UAS-*DE-cadherin*-ΔJM	Pacquelet & Rørth, 2005	Bloomington	58444
UAS-*DE-cadherin*-AAA	Pacquelet et al., 2003	Bloomington	58434
Fas2$^{GFP-397}$	Silies & Klämbt, 2010	C. Klämbt	N/A
w;;sco/Cyo; UAS-*Lifeact*-RFP/TM3 Ser	Riedl et al., 2008	Bloomington	58716

3.2 Detailed experimental genotype

Figure	Genotype	Staining
Figure 7a	hsFLP/w;; FRT82B *Rab11*/FRT82B RFP	DE-cad, RFP
Figure 7b	hsFLP/w; *traffic jam*-Gal4 Sp/UAS-HA-*Rab11*; FRT82B *Rab11*/FRT82B RFP	DE-cad, HA-Rab11, RFP
Figure 7c	w; *traffic jam*-Gal4 Sp/+; UAS-HA-*Rab11*/+	DE-cad, HA-Rab11
Figure 7d	w; *traffic jam*-Gal4 Sp/+; UAS-HA-*Rab11*/+	DE-cad, HA-Rab11
Figure 8a	w; *traffic jam*-Gal4 Sp/+; UAS-YFP-*Rab11*/+	YFP-Rab11, DE-cad
Figure 8c	w; *traffic jam*-Gal4 Sp/+; UAS-YFP-*Rab11*/UAS-HA-*Rab11*	YFP-Rab11, HA-Rab11, DE-cad
Figure 9a	w; *traffic jam*-Gal4 Sp/+; UAS-YFP-*Rab11*/+	YFP-Rab11, Arm, DE-cad
Figure 11a	hsFLP/w; FRT40A *Rab5*^{2}/FRT 40A RFP; UAS-YFP-*Rab11*/GR1-Gal4	YFP-Rab11, RFP, DE-cad
Figure 11b	w; *traffic jam*-Gal4 Sp/+; UAS-YFP-*Rab11*/UAS-DN*shibire*	YFP-Rab11, DE-cad
Figure 12a	w; *traffic jam*-Gal4 Sp/+; UAS-YFP-*Rab11*/+	YFP-Rab11, Golgin-245
Figure 12b	w; *traffic jam*-Gal4 Sp/+; UAS-YFP-*Rab11*/+	YFP-Rab11, Rab7, Rab5
Figure 12c	w; *traffic jam*-Gal4 Sp/+; UAS-YFP-*Rab11*/ UAS-*DE-cadh*ΔCyt/α-cat	YFP-Rab11, DE-cad
Figure 14a	w; *traffic jam*-Gal4 Sp/+; UAS-HA-*Rab11*/y*Rab7*	yRab7, HA-Rab11, DE-cad
Figure 14b	w; *traffic jam*-Gal4 Sp/+; UAS-HA-*Rab11*/y*Rab7*	yRab7, HA-Rab11, aPKC
Figure 15a	hsFLP/w;; FRT82B *Rab11*/FRT82B RFP	DE-cad, Golgin-245, GM130
Figure 15b	hsFLP/w;; FRT82B *Rab11*/FRT82B RFP	DE-cad, Rab7, Rab5

Figure 15c	hsFLP/w;; FRT82B *Rab11*/FRT82B RFP	DE-cad, Rab7, LT/RFP
Figure 16a	hsFLP/w; FRT82B *Rab7*/FRT82B RFP	DE-cad, LT, RFP
Figure 17a	w; *traffic jam*-Gal4 UAS-*Snx16*-SNAP/cyo; Sb/TM3Ser	GM130, Golgin-245, Snx16
Figure 17b	w; *traffic jam*-Gal4 UAS-*Snx16*-SNAP/cyo; Sb/TM3Ser	Rab7, Snx16
Figure 17c	w; *traffic jam*-Gal4 UAS-*Snx16*-SNAP/cyo; UAS-YFP-*Rab11*/TM3Ser	YFP-Rab11, DE-cad, Snx16
Figure 18a	hsFLP/w; FRT42 *Snx16*$^{\Delta 1}$/FRT42 RFP	DE-cad, Rab7, RFP
Figure 18b	hsFLP/w; FRT42 *Snx16*$^{\Delta 1}$/FRT42 RFP; UAS-GFP-*Snx16*/GR1-Gal4	Snx16, DE-cad, RFP
Figure 18c	hsFLP/w; FRT42 *Snx16*$^{\Delta 1}$/FRT42 RFP; FRT82B *Rab7*/FRT82B RFP	DE-cad, RFP
Figure 19a	hsFLP/w; *traffic jam*-Gal4 UAS-wt*Snx16*-SNAP/cyo; FRT82B *Rab7*/FRT82B RFP	DE-cad, Snx16, RFP
Figure 19b	hsFLP/w; *traffic jam*-Gal4 UAS-*Snx16*ΔCC-SNAP/cyo; FRT82B *Rab7*/FRT82B RFP	DE-cad, Snx16, RFP
Figure 20a	hsFLP/w;; FRT82B *Rab11*/FRT82B RFP	Arm, DE-cad, RFP
Figure 20b	hsFLP/w; FRT42 *Snx16*$^{\Delta 1}$/FRT42 RFP	Arm, DE-cad, RFP
Figure 20c	hsFLP/w; FRT82B *Rab7*/FRT82B RFP	Arm, DE-cad, RFP
Figure 21a	w; *traffic jam*-Gal4 Sp/+; UAS-*DE-cadherin*-$\Delta\beta$-catenin/+	KDEL, GM130, DE-cad
Figure 21b	w; *traffic jam*-Gal4 Sp/+; UAS-*DE-cadherin*-$\Delta\beta$-catenin/+	Arm, DE-cad
Figure 21c	w; *traffic jam*-Gal4 Sp/+; UAS-*DE-cadherin*-$\Delta\beta$-catenin/+	Rab5, DE-cad
Figure 21d	w; *traffic jam*-Gal4 Sp/+; UAS-*DE-cadherin*-$\Delta\beta$-catenin/+	Rab7, DE-cad
Figure 22a	w; *traffic jam*-Gal4/cyo, UAS-*Sec15*-mCherry/TM3Ser	DE-cad, Sec15
Figure 22b	w; *traffic jam*-Gal4/+, *Sec15* RNAi/+	DE-cad
Figure 22c	w; *traffic jam*-Gal4/cyo, UAS-*Sec15*-mCherry/*Sec15* RNAi	DE-cad, Sec15
Figure 23a	*Fas2*$^{GFP\text{-}}$397/w; *traffic jam*-Gal4/+, UAS-*Sec15*-mCherry/+	Fas2, Sec15
Figure 23b	*Fas2*$^{GFP\text{-}}$397/w; *traffic jam*-Gal4/+, *Sec15* RNAi/+	Fas2, DE-cad
Figure 24a	w; *traffic jam*-Gal4/cyo, UAS-*Sec15*-mCherry/TM3Ser	DE-cad, Sec15
Figure 24b	w; *traffic jam*-Gal4 Sp/+; UAS-*Sec15*-mCherry/UAS-*DE-cadh*ΔCyt/α-cat	DE-cad, Sec15
Figure 24c	w; *traffic jam*-Gal4 Sp/+; UAS-*Sec15*-mCherry/UAS-*DE-cadherin*-ΔJM	DE-cad, Sec15
Figure 25a	w; *traffic jam*-Gal4 Sp/+; UAS-*Sec15*-mCherry/UAS-*DE-cadherin*-AAA	DE-cad, Sec15

Figure 25b	w; *traffic jam*-Gal4 Sp/+; UAS-YFP-*Rab11*/UAS-*DE-cadherin*-AAA	YFP-Rab11, DE-cad
Figure 26a	w; *traffic jam*-Gal4 Sp/+; UAS-HA-*Rab11*/UAS-*Sec15*-mCherry	HA-Rab11, Sec15, DE-cad
Figure 26b	w; *traffic jam*-Gal4 Sp UAS-HA-*Rab11*/+; UAS-YFP-*Rab11*/UAS-*Sec15*-mCherry	YFP-Rab11, Sec15, HA-Rab11
Figure 27a	w; *traffic jam*-Gal4 UAS-*Snx16*-SNAP/+; UAS-HA-*Rab11*/UAS-*Sec15*-mCherry	HA-Rab11, Sec15, Snx16
Figure 27b	w; *traffic jam*-Gal4 UAS-*Snx16*-SNAP/+; UAS-HA-*Rab11*/UAS-*Sec15*-mCherry	DE-cad, Sec15, Snx16
Figure 28a	w; *traffic jam*-Gal4 Sp/+; UAS-*Sec15*-mCherry UAS-*MyoV-FL*-GFP/UAS-HA-*Rab11*	MyoV, Sec15, HA-Rab11
Figure 28b	w; *traffic jam*-Gal4 Sp/+; UAS-*Sec15*-mCherry UAS-*MyoV-FL*-GFP/UAS-HA-*Rab11*	MyoV, Sec15, DE-cad
Figure 29a	w; *traffic jam*-Gal4 Sp/+; UAS-*MyoV-GT*-GFP/+	MyoV, DE-cad
Figure 29b	w; *traffic jam*-Gal4 Sp/+; UAS-*MyoV-GT*-GFP/UAS-HA-*Rab11*	
Figure 29c	w; *traffic jam*-Gal4 Sp/+; UAS-*MyoV-GT*-GFP/+	MyoV, Rab7, DE-cad
Figure 29e	w; *traffic jam*-Gal4 Sp/+; UAS-*MyoV-FL*-GFP/+	DE-cad
Figure 29f	w; *traffic jam*-Gal4 Sp/+; UAS-*MyoV-GT*-GFP/+	DE-cad
Figure 30c	w; *traffic jam*-Gal4 Sp/+; UAS-HA-*Rab11*/+	DE-cad, Phalloidin, HA-Rab11
Figure 32a	w; *traffic jam*-Gal4 Sp/+; UAS-*MyoV-FL*-GFP/+	MyoV, Phalloidin, DE-cad
Figure 32b	w; *traffic jam*-Gal4 Sp/cyo; UAS-*MyoV-FL*-GFP/UAS-*Lifeact*-RFP	/
Figure 32c	w; *traffic jam*-Gal4 Sp/+; UAS-*Sec15*-mCherry UAS-*MyoV-FL*-GFP/	MyoV, Sec15, Phalloidin
Figure 33b	w; *traffic jam*-Gal4 Sp/+; UAS-*MyoV-FL*-GFP/+	MyoV, Phalloidin, DE-cad
Figure 33c	w; *traffic jam*-Gal4 Sp/+; UAS-*Sec15*-mCherry UAS-*MyoV-FL*-GFP/UAS-HA-*Rab11*	MyoV, Sec15, HA-Rab11
Figure 33d	w; *traffic jam*-Gal4 Sp/+; UAS-*Sec15*-mCherry UAS-*MyoV-FL*-GFP/UAS-HA-*Rab11*	MyoV, Sec15, DE-cad

3.3 Primary antibodies

Antigen (host)	Dilution	Provider	Seller Reference
DE-Cadherin (rat)	1:50	Developmental Studies Hybridoma Bank	DCAD2
RFP (rabbit)	1:200	Rockland	600-401-379
HA (mouse)	1:400	Santa Cruz Biotechnology	11867423001
GFP-FITC (goat)	1:100	Biozol GeneTex	GTX26662-100
Armadillo (mouse)	1:100	Developmental Studies Hybridoma Bank	N2 7A1
Golgi-245 (goat)	1:500	Developmental Studies Hybridoma Bank	Riedel et al., 2016
Rab7 (mouse)	1:20	Developmental Studies Hybridoma Bank	Riedel et al., 2016
Rab5 (rabbit)	1:500	Abcam	ab31261
aPKC (rabbit)	1:200	Santa Cruz Biotechnology	sc-2016
GM130 (rabbit)	1:100	Abcam	ab30637
KDEL (mouse)	1:50	Santa Cruz Biotechnology	sc-58774

3.4 Secondary antibodies

Secondary antibody	Fluorophore	Dilution	Provider	Seller Reference
Alexa goat anti-rabbit	488	1:200	Thermo Fisher Scientific	A11034
	555			A11036
	647			A21244
Alexa goat anti-rat	488	1:200	Thermo Fisher Scientific	A11006
	555			A11077
	647			A21247
Alexa goat anti-mouse	488	1:200	Thermo Fisher Scientific	A11001
	555			A11031
	647			A21235

3.5 Chemicals and drugs

Chemicals/drugs	Provider	Seller Reference	Final concentration
LysoTracker™ Red	Thermo Fisher Scientific	L7528	10 µM
SNAP-Cell TMR-Star	New England BioLabs	S9105S	3 µM
SNAP-Cell 647SiR	New England BioLabs	S9102S	3 µM
Alexa Fluor™ 568 Phalloidin	Thermo Fisher Scientific	A12380	1:100
Alexa Fluor™ 647 Phalloidin	Thermo Fisher Scientific	A22287	1:100
Latrunculin A	Sigma-Aldrich	L5163	20 µM

3.6 Buffers and solutions

Buffers and solutions	Provider	Identifier
Phosphate-Buffered Saline (PBS) tablets	Thermo Fisher Scientific	18912014
Schneiders Medium	Thermo Fisher Scientific	21720024
Triton-X 100	Carl Roth	3051.2
10% Formaldehyde Ultra-pure	PolyScience Europe	04018-1
Vectashield Mounting Medium	Vector Laboratories	VEC-H-1000
Bovine Serum Albumin (BSA)	NEB	B9001 S
Fetal Bovine Serum (FBS)	Thermo Fisher Scientific	10270106
Insulin solution	Sigma	I0516-5ML
Penicillin Streptomycin Solution (Pen/Strep)	Thermo Fisher Scientific	15140122

3.7 Software and algorithms

Software and Algoritmhs	Source	Identifier
FIJI (ImageJ v2.3.2) *Plugins used: Cell Counter*	Schindelin et al., 2012	https://imagej.net/Fiji
GraphPad Prism 9.3.1	GraphPad Software, Inc.	https://www.graphpad.com
Photoshop CS 3.0 and CS 4.0	N/A	https://www.adobe.com/de/products/photoshop.html
Microsoft Excel	N/A	N/A

3.8 RNAi induction, the generation of genetic mosaics and the Rab11^{dFRT} FRT82B recombination

For RNAi knockdown in the follicular epithelium, UAS-inducible *Sec15 RNAi* transgene was driven with *traffic jam*-Gal4.

Heat-shock (hs) inducible Flipase (FLP) was used to generate genetic mosaics were generated using a heat-shock (hs) inducible Flipase (FLP). Heat shocks were used to induce the hs-FLP for the generation of homozygous mutant cell clones by placing the vials in a 37 °C water bath for 1 hour daily until hatching. Females were raised at 27°C and dissected 24 to 48 hours after hatching.

Rab11^{dFRT} was initially on a chromosome containing the FRT site next to the mutation in *Rab11*. I recombined the *Rab11^{dFRT}* allele with the *FRT82B* to use the traditional *FRT82B* for clone induction. This eliminated a mutation that affected the cell cycle in the background.

3.9 Immunohistology

Drosophila ovaries were dissected in Schneider's medium and fixed in 4% formaldehyde in PBS for 10 minutes at room temperature. Ovaries were then washed and permeabilized with 0.1% TritonX-100 in PBS. Further, ovaries were blocked with 0.5% BSA in 0.1% TritonX/PBS containing 0.5 µg/ml DAPI for nucleus staining for 20 minutes. Both primary and secondary antibodies were diluted in 0.1% Triton/PBS and incubated for 3 hours at room temperature. Finally, ovaries were washed and mounted in Vectashield.

3.10 Pulse-chase endoassay

In Schneider's medium, living ovaries were incubated at room temperature in a pulse-chase solution containing α-DE-cadherin antibody (1:25), 10% FCS, and 0,2 mg/ml Insulin. On a rocking platform, the incubation was done for 2 minutes. The ovaries were washed and incubated in Schneider's medium for different intervals in a solution containing only 10% FCS and 0.2% Insulin. The ovaries were then washed and fixed in formaldehyde at a concentration of 4%. The staining was done according to the instructions (see 3.8).

3.11 Live-Imaging

Female flies were kept at 27°C for 1-3 days on fly food with a generous amount of yeast after hatching. They were then dissected, with single ovarioles being transferred to X-well chambers (Sarstedt 94.6190.802) containing 200 µL live-imaging media. Imaging media consists of *Drosophila* Schneider's medium with 15% FCS and 0.2mg/mL insulin. Egg chambers were imaged with 63x/HCX PL APO 1.3 glycerol immersion objective on an inverted Leica LSM SP5 confocal microscope with HyD detectors. Time-lapse videos were taken at a resolution of 512 × 512.

3.12 Lysotracker staining

Ovaries were dissected and incubated at room temperature in Lysotracker solution containing 10 µM Lysotracker, 10% FCS and 0,2 mg/ml Insulin in Schneider's medium. Incubation was performed for 30 minutes on a rocking platform. Ovaries were then washed and fixed in 4% formaldehyde. Staining was carried on as described (see 3.8). All steps were performed protected from light.

3.13 Phalloidin staining

Ovaries were dissected in Schneider's medium and fixed in 4% formaldehyde in PBS for 10 minutes at room temperature. Ovaries were washed and permeabilized with 0.1% TritonX-100 in PBS. Next, ovaries were blocked with 0.5% BSA in 0.1% TritonX/PBS containing 0.5 µg/ml DAPI for nucleus staining for 20 minutes. Additionally, Alexa Fluor™ 568 Phalloidin or Alexa Fluor™ 647 Phalloidin were added into the blocking solution using the concentrations indicated in the table above. Both primary and secondary antibodies were diluted in 0.1% Triton/PBS and incubated for 3 hours at room temperature. When using Alexa Fluor™ 647 Phalloidin, Alexa Fluor™ 647 Phalloidin was added to the solution with primary antibody as well. After incubation with both primary and secondary antibodies, ovaries were washed and mounted in Vectashield.

3.14 SNAP staining

Ovaries were dissected and incubated at room temperature in SNAP solution containing 3 µM SNAP-Cell TMR-Star or SNAP-Cell 647SiR, 10% FCS and 0,2 mg/ml Insulin in Schneider's

medium. Incubation was performed for 30 minutes on a rocking platform. Ovaries were washed and fixed in 4% formaldehyde. Staining was carried on as described (see 3.8). All steps were performed protected from light.

3.15 Latrunculin A treatment

Ovaries were dissected and then incubated with 20 µM Latrunculin A in Schneider`s medium containing 10% FCS and 0.2 mg/mL Insulin for 2 hours at room temperature on a rocking platform. In parallel, another set of ovaries was dissected and then incubated with Schneider`s medium containing 10% FCS and 0.2 mg/mL Insulin and DMSO as a control. Ovaries were then washed and fixed in 4% formaldehyde. Staining was performed as described (see 3.8).

3.16 Imaging

All pictures shown in Figures 6 - 33 are single confocal sections. I usually stained five to eight ovaries in one experiment, and each experiment was repeated at least twice. I used the following method to capture images: at a distance of 0.8 µm, 7-9 images were taken along the apical-basal axis of the epithelium, which were then analyzed for possible defects. The high intensity of the DE-cadherin staining at the plasma membrane helped me identify the zonula adherens as a marker. A second sagittal section was taken to identify the follicle's developmental stage.
Images were acquired using Leica TSC SP5 confocal microscope equipped with HyD detectors using × 63 oil immersion magnification at a resolution of 1,024 × 1,024 then adjusted for gamma, edited and assembled with Adobe Photoshop CS3. Image quantification was performed before “gamma adjustment”. I indicated the cases when maximal projections of z-stacks were used for quantification (see below).

3.17 Quantification and image analysis

3.17.1 Quantification of colocalization between different cell compartments

I selected an area of cells showing the zonula adherens and cropped it for subsequent analysis using the “Polygonal Lasso” tool of Photoshop CS3. I counted the total number of compartments, as well as cases when the colocalization was detected, In ImageJ/FIJI with Plugins>Analyze>Cell counter tool. The ratio of the compartments colocalizing and the total

number of the compartment was then calculated. I performed the analysis with the confocal single sections, except for the Figures 11a, 15a – 15c, 16a and 19b, 20a - 20c where the snapshots of maximal projections of the z-stacks were analyzed. I used Graph Pad Prism Software to analyze and show the data for Figures 9b, 14c, 15d and 20d. This analysis was applied for Figures 7d, 8a, 9a, 11a, 11b, 12b, 13c, 14a, 14b, 15a – 15c, 16a, 17b, 19b, 20a – 20c, 30a and 30c.

3.17.2 Quantification of the size of compartments

I selected and cropped an area of a minimum of 20 cells within a follicle for the analysis. I further selected the compartment of interest using the "Freehand selection" tool in ImageJ/FIJI. Then, I measured the size using the Analyze>Measure tool. The data was saved in ROI manager (Analyze>Tools>ROI manager) and exported to an Excel spreadsheet, where the average compartment size was determined. I used confocal single sections for analysis. Further, I used Graph Pad Prism Software to analyze and show the data for Figures 8d and 26c. This analysis was applied for Figures 8c, 13a, 13b and 26a.

3.17.3 Quantification of the number of DE-cadherin aggregates

I calculated the ratio between the number of cell clones showing the DE-cadherin aggregation and the total cell clones. For analysis and data representation, I used Graph Pad Prism Software data for Figures 18d and 19c. I used snapshots of maximal projections of the z-stacks for analysis. To further analyze and show data in Figures 18d and 19c, I used Graph Pad Prism Software. This analysis was applied for Figures 7b, 16a, 18a – 18c, 19a and 19b.

3.17.4 Quantification of signal intensities at the plasma membrane versus the signal intensity in the cytoplasm

I selected an area with approximately 20 cells showing the zonula adherens using the "Polygonal Lasso" tool. A line was created along the membrane and along the aggregate in the cytoplasm in ImageJ/Fiji using the "Straight line" tool. I used Analyze>Plot Profile tool to acquire the signal intensity values along the membrane and in the cytoplasm. For MyoV-FL-GFP/Sec15-Cherry/HA-Rab11 expressing ovaries, an area with two cells was selected, one with low MyoV expression and one with high MyoV expression. A line was drawn along the membrane in a cell with high MyoV expression and along the aggregate in the cytoplasm in a

cell with low MyoV expression. The average signal intensity values for each membrane and aggregate in the cytoplasm were calculated after the data was exported to an Excel sheet. Finally, for each compartment, the ratio between the intensity values in the cytoplasm/aggregate and on the membrane was calculated. I used single confocal slices for the analysis. I used Graph Pad Prism Software to analyze and represent the data in Figures 8b and 9b. This analysis was applied for Figures 8a and 9a,

3.17.5 Quantification of number of DE-cadherin aggregates with regard to DE-cadherin signal intensity at the plasma membrane in Sec15-Cherry/HA-Rab11 versus MyoV-FL GFP/ Sec15-Cherry/HA-Rab11 expressing epithelia

I selected an area containing a minimum of 20 cells, which show the zonula adherens, and cropped it for further analysis. I used the “Freehand line” tool in ImageJ/FIJI to draw the line along the two faintest membranes. Using Analyze>Plot Profile tool, the plot intensity graph for these two membranes was obtained. I then calculated the signal intensity average from these membranes, which I then used as the reference value for the intensity minimum. This was set in ImageJ/FIJI Image>Adjust>B&C option. DE-cadherin aggregates that remained visible after setting the new reference value for the minimal intensity were counted using Plugins>Analyze>Cell counter tool. Finally, I calculated the number of DE-cadherin aggregates per cell. I used snapshots of maximal projections of the z-stacks for analysis. This analysis was applied for Figure 28b and I used Graph Pad Prism Software to analyze and represent the data in Figure 28c.

3.17.6 Quantification of fragmented membranes in wild type follicles, follicles expressing MyoV-FL-GFP and MyoV-GT-GFP, and follicles treated with Latrunculin A and DMSO

I selected an area of approximately 10 cells showing the zonula adherens and cropped it for further analysis. I used Plugins>Analyze>Cell counter tool in ImageJ/FIJI to count the cells with fragmented zonula adherens as well as the total number of cells. Finally, I calculated the percentage of cells with fragmented zonula adherens. For the analysis and representation of data in Figure 31c, I used Graph Pad Prism Software. I used single confocal slices for the analysis. This analysis was applied for Figures 29d – 29f and 31a – 31b. I used Graph Pad Prism Software to analyze and represent the data in Figure 31c.

3.18 Statistical analysis

Data are shown as mean ± SEM. P values for the two-tailed t-test (equal variance; $\alpha = 0.05$) are as follows: * $p<0.05$; ** $p<0.01$; *** $p<0.001$; **** $p<0.0001$.

4 Results

4.1 Rab11 is a part of the endosomal system where endocytosed and newly synthesized DE-cadherin converge

In epithelial cells, the E-cadherin protein concentrates on the apicolateral membrane and acts as a building block for homophilic cell-cell attachment. As fast changes in the developing organism such as cell division and cell differentiation need rapid turnover, there are two pools of E-cadherin within the cells: newly synthesized E-cadherin and endocytosed E-cadherin. Past studies showed that the transit of E-cadherin through the Rab11 compartment is essential for proper E-cadherin secretion to the plasma membrane (Woichansky et al., 2016; Jiang Xu et al., 2011). However, it remains unclear which of these two E-cadherin pools require Rab11 and at which stage of E-cadherin transport is Rab11 involved.

4.1.1 Endocytosed DE-cadherin localizes to the apical HA-Rab11 compartment

I first wanted to know to which compartment the endocytosed E-cadherin, also known as DE-cadherin in *Drosophila*, localizes within the *Drosophila* follicular epithelium. To answer this question, I performed a DE-cadherin pulse-chase endocytosis experiment. Pulse-chase endocytosis experiment detects DE-cadherin that has been localized to the plasma membrane and then endocytosed. This detection is achieved by incubating the living ovaries for a certain period with an α-DE-cadherin antibody, which binds to the extracellular part of DE-cadherin (Oda et al., 1994). Due to the fact that the plasma membrane is not permeabilized, the antibody will only bind specifically to DE-cadherin present at the plasma membrane, and not to the DE-cadherin within the cell. The ovaries are then washed and incubated with the chase solution for different periods to allow the DE-cadherin internalization. Finally, ovaries are fixed and stained (see also 3.9 in Materials and Methods). For the analysis of DE-cadherin trafficking in the *Drosophila* follicular epithelium, I used follicles in stages 8 and 9.

I first performed the pulse-chase endocytosis experiments with wild type *Drosophila* ovaries. I used the time course of 0 minutes, 10 minutes and 20 minutes. My data revealed that after 0 minutes and 10 minutes of incubation with an α-DE-cadherin antibody, no DE-cadherin spots were detected in the cytoplasm (Figures 6b and 6c). The DE-cadherin was only observed to mildly concentrate to the plasma membrane (compare Figures 6a, 6b and 6c). After 20 minutes, on the other hand, endocytosed DE-cadherin spots were detected in the apical cytoplasm of cells (arrows in Figure 6d). The endocytosed apical DE-cadherin spots detected

after 20 minutes of pulse-chase endocytosis were of an average size of 0.67 μm^2 (± 0.07, n=220 cells from 6 follicles). They most likely represent the cell compartment, to which endocytosed DE-cadherin is transported. This suggests that the DE-cadherin endocytosis and its subsequent transport to the certain cell compartment occurs within 20 minutes in the *Drosophila* follicular epithelium.

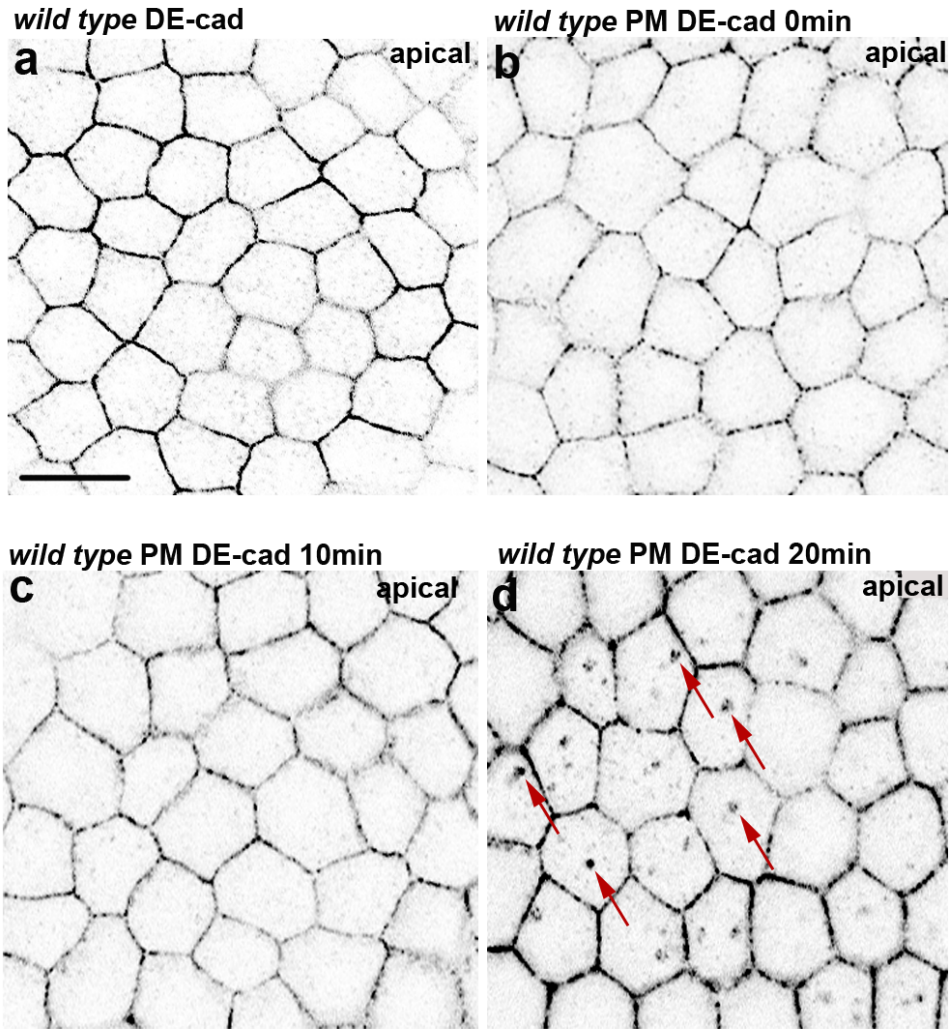

Figure 6. Cytoplasmic endocytosed DE-cadherin detected after 20 minutes of pulse-chase endocytosis. (a-d) Apical confocal optical sections perpendicular to the apical-basal axis of the follicular epithelium. The scale bar represents 10μm. Pulse-chase endocytosis was performed with epithelia shown in (b-d). PM DE-cadherin (plasma membrane DE-cadherin) stands for endocytosed DE-cadherin. (a) Wild type epithelia that is fixed and stained with α-DE-cadherin. (b-c) Wild type epithelia incubated with the α-DE-cadherin antibody for 0 minutes (b) and 10 minutes (c). (d) Wild type epithelia incubated with the α-DE-cadherin antibody for 20 minutes. DE-cadherin spots can be detected in the cytoplasm (red arrows).

Previous studies suggested that the endocytosed E-cadherin passes through the Rab11 compartment (Desclozeaux et al., 2008; Langevin et al., 2005). As it can be seen in Figure 6d, I detected endocytosed DE-cadherin in the cell cytoplasm after 20 minutes of pulse-chase endocytosis. I asked if there is any connection between the Rab11 compartment and endocytosed DE-cadherin spots in the apical area of the cell. To answer this question, I expressed the HA-tagged Rab11 protein in *Drosophila* follicular epithelium using the UAS-HA-Rab11 construct.

For the induction of the overexpression and knockdown of different genes specifically in the cells of the follicular epithelium, I used the Gal4/UAS system (Brand & Perrimon, 1993). The transcription factor Gal4 is encoded by the Gal4 gene and binds to the Upstream Activating Sequence (UAS). The binding of Gal4 to UAS activates the expression of the downstream located gene. Placing the Gal4 gene under the specific promoter allows a controlled gene expression. Since I was interested in investigating the DE-cadherin trafficking in epithelial cells, I used two drivers that specifically induce the expression in the *Drosophila* follicular epithelium. The majority of UAS-transgenes were induced with *traffic jam*-Gal4 driver, which is expressed throughout the whole stages of oogenesis in the *Drosophila* follicular epithelium (Olivieri et al., 2010). In two experiments, the second driver called GR1 is used, which is active from stage 1 of oogenesis in *Drosophila* follicular epithelium (Gupta & Schüpbach, 2003). These two exceptions are emphasized in the experiment explanation.

To test if the HA tag impairs the function of Rab11, I expressed the UAS-HA-Rab11 construct in *Rab11* mutant cells. To generate *Rab11* mutant cell clones, I used $Rab11^{\Delta FRT}$ null allele, in which the promoter and the first two exons are deleted (Bogard et al., 2007). In *Rab11* mutant cell clones, DE-cadherin heavily accumulated in the cytoplasm (Figure 7a). This result is in line with previous findings (Woichansky et al., 2016; Xu et al., 2011). However, the expression of UAS-HA-Rab11 in *Rab11* mutant cells entirely rescued the cytoplasmic DE-cadherin aggregation (100%, n=6 cell clones) (Figure 7b). This suggests that the UAS-HA-Rab11 construct expresses a fully functional Rab11 protein.

Since my data showed that HA-tagged Rab11 protein is functional, I used it as a marker of Rab11 compartments. To investigate the spatial connection between the Rab11 compartments and endocytosed DE-cadherin, I performed the pulse-chase endocytosis experiment with follicles expressing UAS-HA-Rab11. I analyzed the DE-cadherin localization in regard to the HA-Rab11 in the time course of 10 minutes and 20 minutes.

After 10 minutes of the pulse-chase endocytosis, no DE-cadherin endocytic spots were detected (Figure 7c). This is in line with the results obtained after performing pulse-chase endocytosis with wild type *Drosophila* ovaries (Figure 6b). After 20 minutes of pulse-chase endocytosis, the cytoplasmic endocytosed DE-cadherin was detected in the apical area of cells. Overall, 81.84% (± 3.11) of endocytosed DE-cadherin colocalized with HA-Rab11

compartments (n=159 cells from 5 follicles) (arrows in Figure 7d). This suggests that the endocytosed DE-cadherin enters the apical Rab11 compartment.

In summary, my data show that the endocytosed DE-cadherin is detected within the apical area of the cytoplasm after 20 minutes of endocytosis. Moreover, these endocytosed DE-cadherin spots localize to the Rab11 compartment.

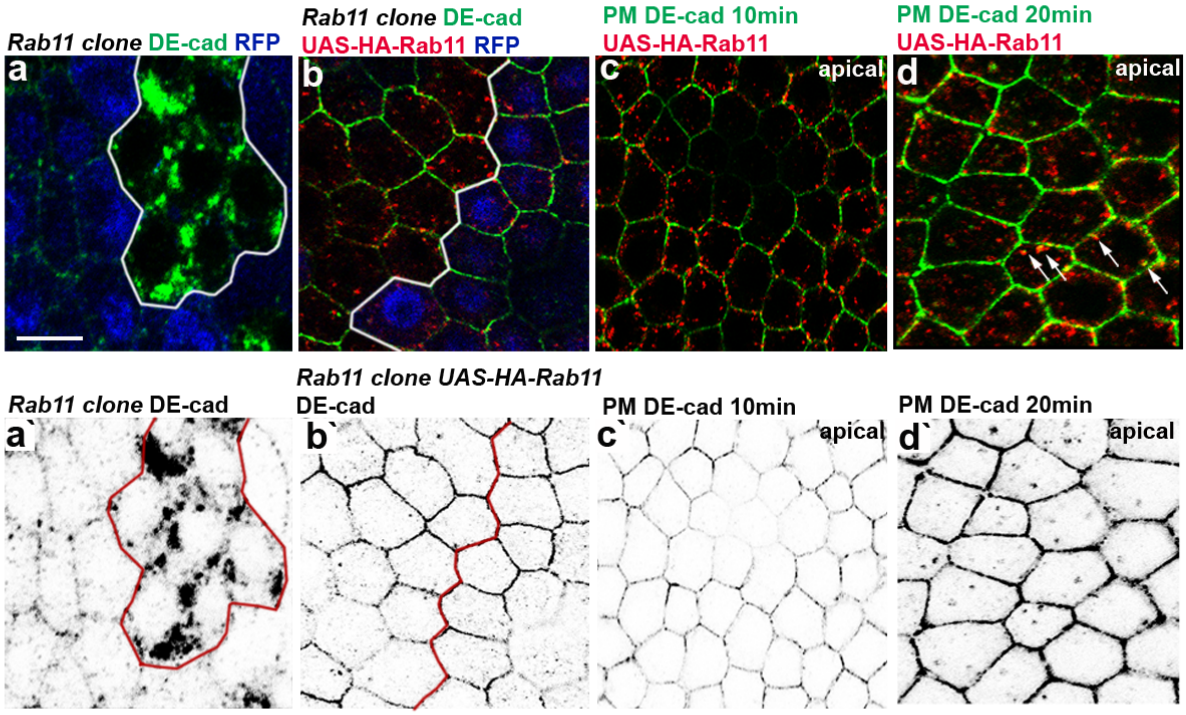

Figure 7. HA-Rab11 colocalizes with endocytosed DE-cadherin. (a-d) Confocal optical sections perpendicular to the apical-basal axis of the follicular epithelium. The scale bar represents 10µm. (a`-d`) show individual DE-cadherin channels. Pulse-chase endocytosis was performed with epithelia shown in (c-d). PM DE-cadherin (plasma membrane DE-cadherin) stands for endocytosed DE-cadherin. (a) *Rab11* clone stained for DE-cadherin (green). Clone cells are indicated by the absence of RFP (blue). The clone border is represented by the white line in (a) and by the red line in (a`). (b) Epithelia expressing UAS-HA-Rab11 (red) and stained with DE-cadherin (green) in *Rab11* clone. Clone cells are indicated by the absence of RFP (blue). The clone border is highlighted by the white line in (b) and by the red line in (b`). (c) Apical epithelia expressing UAS-HA-Rab11 (red) incubated with the α-DE-cadherin antibody (green) for 10 minutes. (d) Apical epithelia expressing UAS-HA-Rab11 (red) incubated with the α-DE-cadherin antibody (green) for 20 minutes. HA-Rab11 colocalizes with the DE-cadherin spots (white arrows).

4.1.2 YFP-Rab11 as a tool for studying DE-cadherin trafficking

My data show that endocytosed DE-cadherin spots localize to the Rab11 compartment. This suggests the role of Rab11 in DE-cadherin trafficking. To further investigate the function of Rab11 in transport of DE-cadherin, I used the UAS-YFP-Rab11 construct. The expression of UAS-YFP-Rab11 construct in *Drosophila* follicular epithelium resulted in prominent Rab11 compartments that are situated in the apical area of the cell (Figure 8a). Such structures were not observed upon the expression of the UAS-HA-Rab11 construct (compare UAS-YFP-Rab11 and UAS-HA-Rab11 in Figure 8c). Surprisingly, these apical YFP-Rab11 compartments accumulated high levels of DE-cadherin (Figure 8a) (100%, n=37 follicles). This suggests that DE-cadherin transport is hindered by the expression of UAS-YFP-Rab11. Nevertheless, DE-cadherin still localized properly at the plasma membrane, as I did not observe any impairment in the formation of the zonula adherens, the apicolateral area of the plasma membrane where DE-cadherin concentrates, or any cell shape distortion (arrows in Figure 8a). This could be explained by the presence of the endogenous Rab11 that is sufficient to support DE-cadherin transport to the plasma membrane in UAS-YFP-Rab11 expressing follicles. This all together suggests that YFP-Rab11 compartments do not completely block DE-cadherin transport, but rather attenuate it.

One of the challenges in studying protein trafficking is the small size of the transport vesicles and the endosomal compartments. This could be overcome with these apical YFP-Rab11 compartments, which could serve as a 'magnifying glass' into the trafficking. The average size of YFP-Rab11 compartments is 1.56 μm^2 (± 0.19, n=176 cells from 5 follicles) and they are significantly bigger than HA-Rab11 structures (Figure 8d). The large apical YFP-Rab11 compartments are thus a convenient tool to investigate DE-cadherin transport within the Rab11 compartment.

The DE-cadherin cytoplasmic accumulation within the YFP-Rab11 compartments suggests that DE-cadherin trafficking in UAS-YFP-Rab11 expressing follicles is attenuated. Namely in wild type epithelia, DE-cadherin is detected only at the membrane and no cytoplasmic DE-cadherin signal can be detected (Figure 6a). To evaluate how much DE-cadherin trafficking is attenuated in UAS-YFP-Rab11 expressing follicles, I compared the signal intensity of DE-cadherin at the plasma membrane and the signal intensity of DE-cadherin aggregating within YFP-Rab11 compartments. I assumed that the more impaired the transport of DE-cadherin is, the less DE-cadherin will be concentrated at the plasma membrane and thus the lower the signal intensity at the plasma membrane will be. To quantify this, I measured the intensities of DE-cadherin signal at the membrane and within YFP-Rab11 compartments using the function Plot Profile in ImageJ/Fiji. The measurement showed 1.65 times higher signal intensity of DE-cadherin within the YFP-Rab11 compartments than at the membrane (Figure 8b). This

suggests that more DE-cadherin is stuck within the YFP-Rab11 compartments than is concentrating at the zonula adherens. This result further confirms that the YFP tag in follicles expressing YFP-Rab11 impairs DE-cadherin transport to the plasma membrane. However, DE-cadherin still reaches the plasma membrane in sufficient amounts, as cell shape and zonula adherens formation were undisturbed.

My previous data show that UAS-HA-Rab11 represents functional Rab11 compartment (Figure 7b). To analyze if functional Rab11 localizes to the YFP-Rab11 apical compartments, I expressed the UAS-HA-Rab11 and the UAS-YFP-Rab11 constructs together in *Drosophila* follicular epithelium. The result revealed that HA-Rab11 punctate compartments were detected at the rims of YFP-Rab11 compartments and close to the plasma membrane (arrows and asterisks in Figure 8c). This suggests that there is a connection between the HA-Rab11 and the YFP-Rab11 compartment, raising the possibility that transport from YFP-Rab11 is possible via the functional Rab11 compartments that are represented by the HA-Rab11.

In summary, my data suggest that the expression of UAS-YFP-Rab11 results in the prominent apical YFP-Rab11 compartments. The DE-cadherin is accumulated within these apical YFP-Rab11 compartments, but the endogenous Rab11 is capable to support the proper DE-cadherin transport to the plasma membrane. Additionally, the functional Rab11 is detected at the edges of the YFP-Rab11 compartments, suggesting that transport from the compartments is possible.

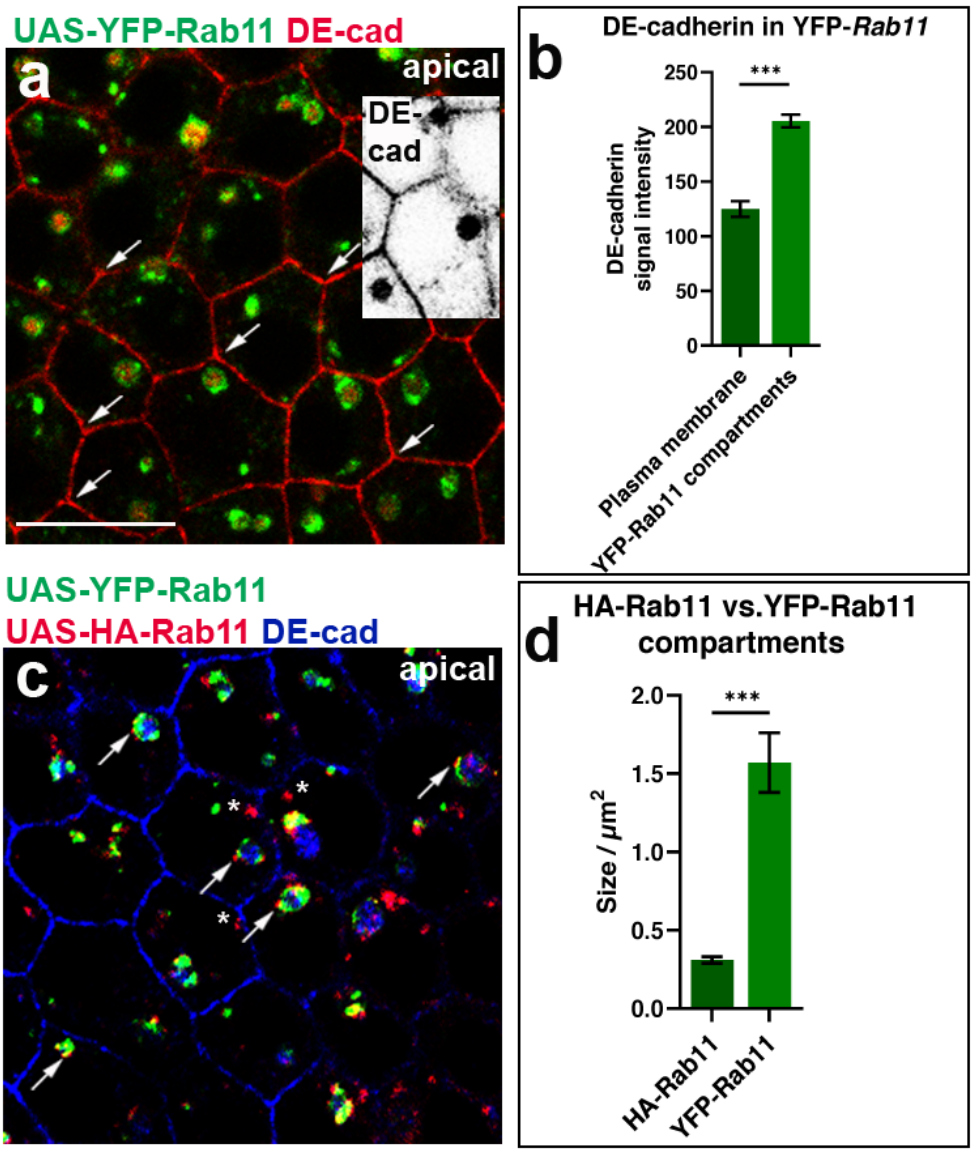

Figure 8. DE-cadherin accumulates within YFP-Rab11 compartments and functional HA-Rab11 localizes at the rims of the YFP-Rab11 compartments. (a) and (c) Apical confocal optical sections perpendicular to the apical-basal axis of the follicular epithelium. The scale bar represents 10µm. (a) DE-cadherin (red) accumulates in YFP-Rab11 GFP compartments (green) in the apical area of the cell. Despite the hindered DE-cadherin transport, zonula adherens forms properly (white arrows). The inset shows the DE-cadherin channel of the designated area alone. (b) Quantification of DE-cadherin signal intensity at the plasma membrane and within the YFP-Rab11 compartments. The representative image is shown in (a). The quantification showed that the DE-cadherin signal intensity within YFP-Rab11 compartments is 1.65 (± 0.08) times higher than the DE-cadherin signal intensity at the membrane (n=8 follicles). Data are shown as mean ± SEM. A two-tailed t-test (equal variance, α=0.05) was performed and p values are presented as ***p < 0.001. (c) Epithelia expressing the UAS-YFP-Rab11 (green) and the UAS-HA-Rab11 (red) is stained with α-DE-cadherin antibody (blue). HA-Rab11 localizes outside of the YFP-Rab11 close to the membrane (white asterisks) as well as on the rims of YFP-Rab11 compartments (white arrows) in the apical area of the cell. (d) Quantification of the size of HA-Rab11 and YFP-Rab11 compartments. The representative image is shown in (c). The average size of HA-

Rab11 compartments is 0.31 µm2 (± 0.02, n=176 cells from 5 follicles), whereas the average size of YFP-Rab11 compartments is 1.56 µm2 (± 0.19, n=153 cells from 5 follicles). Data are shown as mean ± SEM. A two-tailed t-test (equal variance, α=0.05) was performed and p values are presented as ***p < 0.001.

4.1.3 Armadillo mildly accumulates within YFP-Rab11 compartments

My data suggest that DE-cadherin transport is attenuated by the expression of the UAS-YFP-Rab11 compartments (Figure 8a). Since past studies demonstrated that the formation of the complex between E-cadherin and β-catenin is essential for E-cadherin delivery to the plasma membrane (Y. T. Chen et al., 1999; Langevin et al., 2005; Pacquelet et al., 2003), I asked if β-catenin is also hindered by the expression of the UAS-YFP-Rab11 construct.

To answer this question, I analyzed the localization of β-catenin, termed Armadillo in *Drosophila*, in the UAS-YFP-Rab11 expressing follicles. The experiments revealed that at the membrane, especially at the zonula adherens, Armadillo and DE-cadherin colocalized (Figure 9a). This observation is consistent with the previous findings that DE-cadherin and Armadillo are transported in a complex to the zonula adherens (Langevin et al., 2005; Pacquelet et al., 2003). Additionally, I checked for the Armadillo localization within YFP-Rab11 compartments. Surprisingly, the Armadillo signal within YFP-Rab11 vesicles was weaker than the DE-cadherin signal (compare Figures 9a` and 9a``). To confirm my observation, I quantified Armadillo signal intensity within YFP-Rab11 compartments and Armadillo signal intensity at the membrane. The quantification revealed that the Armadillo signal intensity at the membrane was significantly stronger than the Armadillo signal within the YFP-Rab11 compartments (Figure 9b). This implies that more Armadillo concentrated at the membrane than within YFP-Rab11 compartments. Such a result is in contrast to the DE-cadherin localization in UAS-YFP-Rab11 expressing follicles, where more DE-cadherin is concentrated within YFP-Rab11 compartments than at the membrane (compare Figures 8d and 9b). This suggests that the formation of YFP-Rab11 compartments impacts more DE-cadherin localization than Armadillo localization. This further implies that a certain amount of DE-cadherin dissociates from Armadillo and remains trapped within YFP-Rab11 compartments.

Taken together, my data show that Armadillo signal within YFP-Rab11 compartments is weaker than DE-cadherin signal. I speculate that DE-cadherin stuck within YFP-Rab11 compartments dissociated from Armadillo and cannot thus be transported to the plasma membrane.

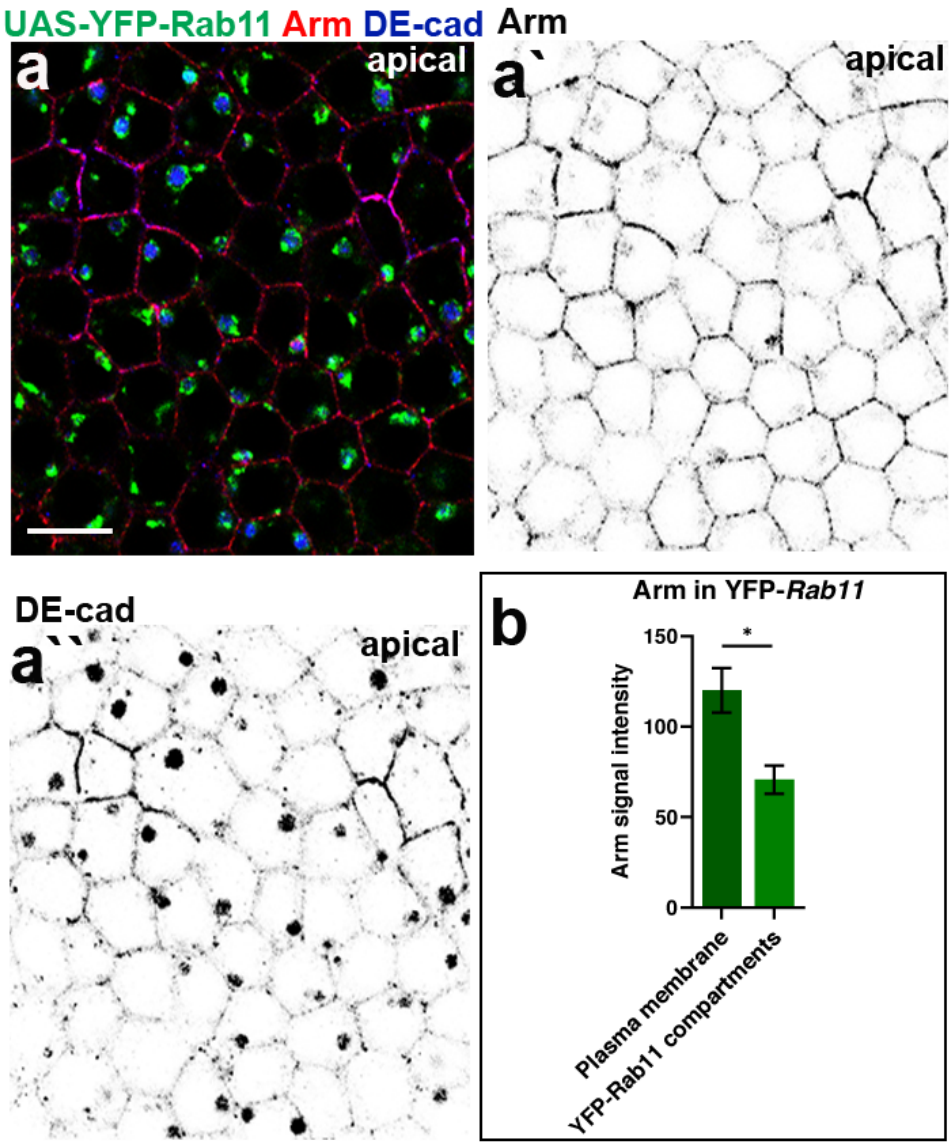

Figure 9. Armadillo mildly accumulates within YFP-Rab11 compartments. (a) Apical confocal optical sections perpendicular to the apical-basal axis of the follicular epithelium. The scale bar represents 10µm. Epithelia expressing YFP-Rab11 (green) and stained for Armadillo (red) and DE-cadherin (blue). (a`) and (a``) show Armadillo and DE-cadherin channels alone respectively. (b) Quantification of Armadillo signal intensity at the plasma membrane and within the YFP-Rab11 compartments. The representative image is shown in (a). The quantification showed that the Armadillo signal intensity at the membrane is 1.70 (± 0.10) times higher than the Armadillo signal intensity within YFP-Rab11 compartments (n=4 follicles). Data are shown as mean ± SEM. A two-tailed t-test (equal variance, α=0.05) was performed and p values are presented as *p < 0.05

4.1.4 Endocytosed DE-cadherin is detected within YFP-Rab11 compartments

My data show that endocytosed DE-cadherin, which can be detected after 20 minutes of endocytosis, localizes to apical HA-Rab11 (Figure 7d). Interestingly, YFP-Rab11 compartments are also observed in the apical cytoplasm (Figure 8a). Because both endocytosed DE-cadherin and YFP-Rab11 compartments are found in the apical cytoplasm, I wondered if there was a possibility of colocalization between endocytosed DE-cadherin and YFP-Rab11 compartments.

To answer this question, I performed a DE-cadherin pulse-chase endocytosis experiment in UAS-YFP-Rab11 expressing follicles. My previous data suggest that the endocytosed DE-cadherin in wild type and in UAS-HA-Rab11 expressing follicles is detected in the apical area of the cell after 20 minutes of endocytosis (Figures 6d and 7d). Interestingly, no endocytosed DE-cadherin was detected after 20 minutes of pulse-chase endocytosis in UAS-YFP-Rab11 expressing follicles (Figure 10a). Only after 30 minutes of pulse-chase endocytosis, I observed mild DE-cadherin aggregation within the YFP-Rab11 compartments (Figure 10b). The slower DE-cadherin transport into the YFP-Rab11 compartments could be attributed to the Rab11 protein's YFP-tag inhibiting DE-cadherin trafficking.

To see if the intensity of DE-cadherin accumulation within YFP-Rab11 compartments will increase over time, I analyzed DE-cadherin localization in UAS-YFP-Rab11 expressing follicles after 6 hours of pulse-chase endocytosis. The accumulation of endocytosed DE-cadherin within apical YFP-Rab11 compartments indeed became more intense after 6 hours of ovary incubation with α-DE-cadherin antibody (compare Figures 10b` and Figure 10c`). This suggests that endocytosed DE-cadherin accumulated over time within YFP-Rab11 compartments. This could be explained by a slower and more hindered process of DE-cadherin transport in *Drosophila* follicles expressing the UAS-YFP-Rab11 construct.

Taken together, my data imply that endocytosed DE-cadherin starts accumulating within YFP-Rab11 compartments after 30 minutes of endocytosis and that this accumulation of endocytosed DE-cadherin increases over time.

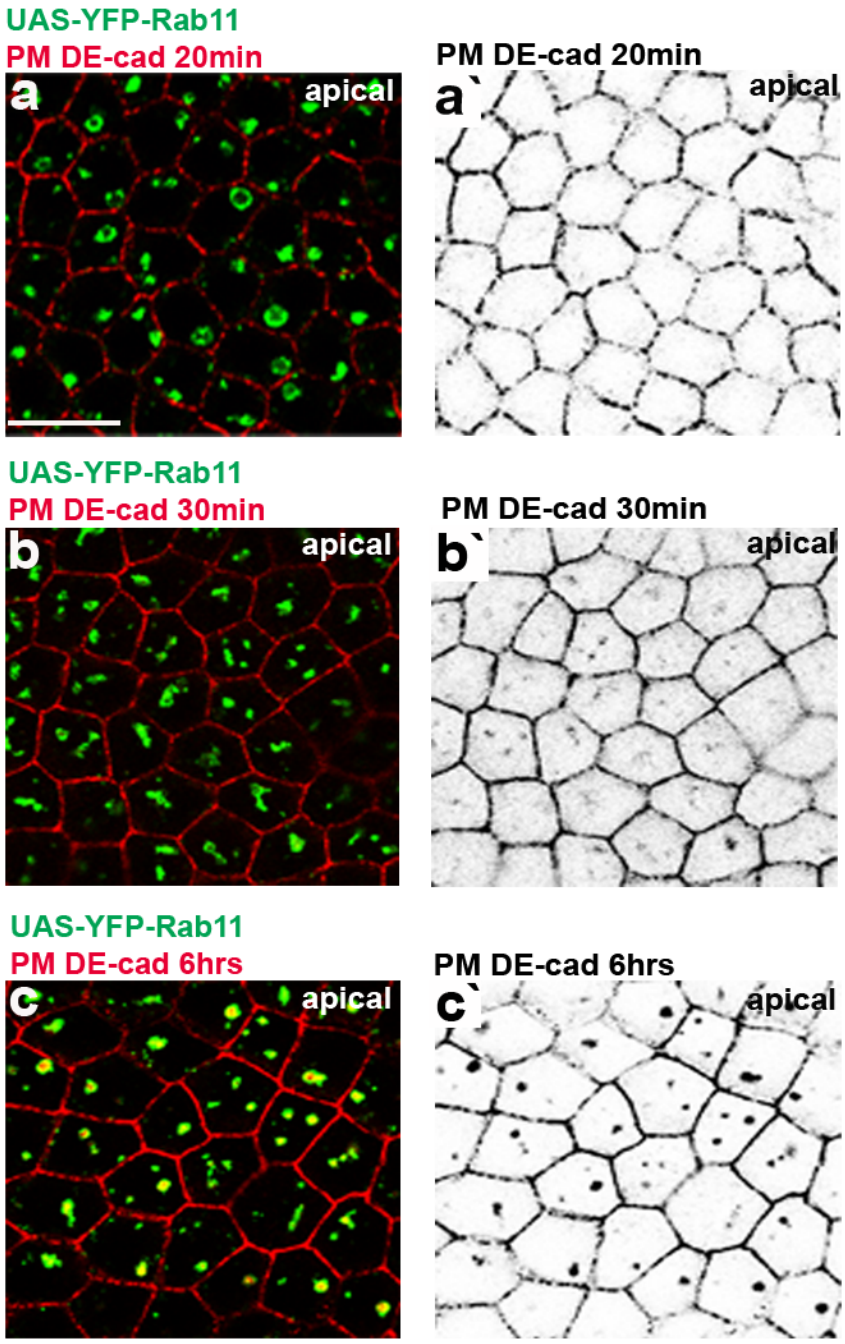

Figure 10. Endocytosed DE-cadherin accumulates within YFP-Rab11 compartments after 30 minutes of endocytosis. (a-c) Apical confocal optical sections perpendicular to the apical-basal axis of the follicular epithelium. The scale bar represents 10µm. Pulse-chase endocytosis with α-DE-cadherin (red) antibody incubated for different periods was performed with all shown epithelia, which express UAS-YFP-Rab11 (green). PM DE-cadherin (plasma membrane DE-cadherin) stands for endocytosed DE-cadherin. (a) shows epithelia incubated for 20 minutes, (b) for 30 minutes and (c) for 6 hours. (a`-c`) show individual DE-cadherin channel.

4.1.5 Newly synthesized and endocytosed DE-cadherin converge in endosomes

My data show that endocytosed DE-cadherin accumulated within YFP-Rab11 compartments (Figure 10). A previous study showed that newly synthesized DE-cadherin also passes through Rab11 compartments (Stow & Lock, 2005). Therefore, I asked whether newly synthesized DE-cadherin accumulates within YFP-Rab11 compartments as well. To answer this question, I blocked the import of endocytosed DE-cadherin to detect only newly synthesized DE-cadherin within the cell. The block of endocytosed DE-cadherin import into early endosomes can be achieved by depleting Rab5 GTPases. Previous studies revealed that Rab5 marks the endocytic vesicle that needs to be fused with the endosomes for proper endocytosis. The binding of Rab5 to the early endosomal antigen 1 (EEA1) leads to membrane curvature and fusion of the endocytic vesicles with the endosomes (Murray et al., 2016). Upon Rab5 depletion, the endocytosis process is inhibited (Zeigerer et al., 2012), thus within the Rab5-depleted cells, only newly synthesized DE-cadherin can be detected.

To test if newly synthesized DE-cadherin accumulates within YFP-Rab11 compartments, I expressed the UAS-YFP-Rab11 construct in *Rab5* mutant cells. For this experiment, I used the FRT/FLP technique, which allows for the generation of mosaic tissues (T. Xu & Rubin, 1993). The FRT/FLP method induces mitotic recombination in proliferating tissues that are heterozygous mutants for a specific gene. The heterozygous follicular epithelium used for analysis has one wild type and one mutant chromosome. The wild type chromosome is GFP/RFP-labelled and is flanked by the specific sequences called 'FRT sites'. The mutant chromosome is also flanked with the FRT sites but has no GFP/RFP label. Finally, the enzyme Flipase, whose expression is induced under the control of a heat-shock promoter, recognizes FRT sites and induces mitotic recombination. As a result, three types of cells are observed in the heterozygous follicular epithelium: homozygous mutant, homozygous wild type and heterozygous mutant. The mutant cells are easily detectable by the absence of GFP/RFP, as wild type chromosome is not labelled by GFP/RFP. Such a system allowed me to directly compare DE-cadherin aggregation in *Rab5* mutant cells expressing UAS-YFP-Rab11 and neighboring cells expressing only UAS-YFP-Rab11.

To eliminate any potential enduring activity of Rab5, I used a $Rab5^2$ allele. $Rab5^2$ allele has a 4-kb deletion of the promoter region, the 5` non-translated leader and the first exon within the open reading frame (ORF) (Wucherpfennig et al., 2003). The deleted exon of the ORF also encodes the guanine base-binding motif of the GTPase domain, and the inability of Rab5 to properly bind to the GTP has been shown to inhibit the early endosome fusion (Olkkonen & Slenmark, 1997). This implies that $Rab5^2$ is a null allele. Additionally, I used cell clones that cover at least one-third of the follicle for the analysis. Such big clones have been induced already in the germarium, and these cell clones have gone through the eight-cell divisions after

the induction, meaning that any residual Rab5 activity is lost (Margolis & Spradling, 1995). For the induction of UAS-YFP-Rab11 construct in *Rab5* clones I used GR1 driver.

The expression of UAS-YFP-Rab11 in *Rab5* clones revealed that DE-cadherin still accumulated in YFP-Rab11 compartments in high levels (Figure 11a) (100%, n=12 cell clones). This suggests that the newly synthesized DE-cadherin could also be detected within YFP-Rab11 compartments. Such a result is consistent with the observation of a study in mammalian cells, where E-cadherin localization was monitored in live cells and detected at the Rab11 positive compartment (Stow & Lock, 2005).

Further, I blocked endocytosis using a different approach to confirm that YFP-Rab11 compartments also accumulated newly synthesized DE-cadherin. I co-overexpressed the YFP-Rab11 construct and the dominant-negative form of shibire. Shibire encodes the *Drosophila* homologue of Dynamin, which plays a crucial role in the scission of endocytic vesicles and late stages of membrane invagination. *In vitro* studies showed that Dynamin binds and hydrolyzes GTP to properly complete its function (Hill et al., 2001). The dominant-negative form of shibire has a mutation in the GTPase binding domain, therefore disabling Dynamin binding of the GTP. This means that the overexpression of the dominant-negative form of shibire restricts the formation of endocytic vesicles and thus blocks the endocytosis. The co-overexpression of the dominant-negative shibire and the YFP-Rab11 construct revealed that the DE-cadherin still accumulates within YFP-Rab11 compartments (Figure 11b). DE-cadherin within YFP-Rab11 compartments was detected in 85.95% of cells (± 3.73, n=207 cells from 6 follicles). Both methods thus confirmed that YFP-Rab11 compartments also consist of newly synthesized DE-cadherin.

Taken together, my data suggest that YFP-Rab11 compartments localize predominantly in the apical area of the cell, and accumulate both endocytosed and newly-synthesized DE-cadherin. This also implicates that biosynthetic and endocytic DE-cadherin pathways converge in the apical Rab11 compartment.

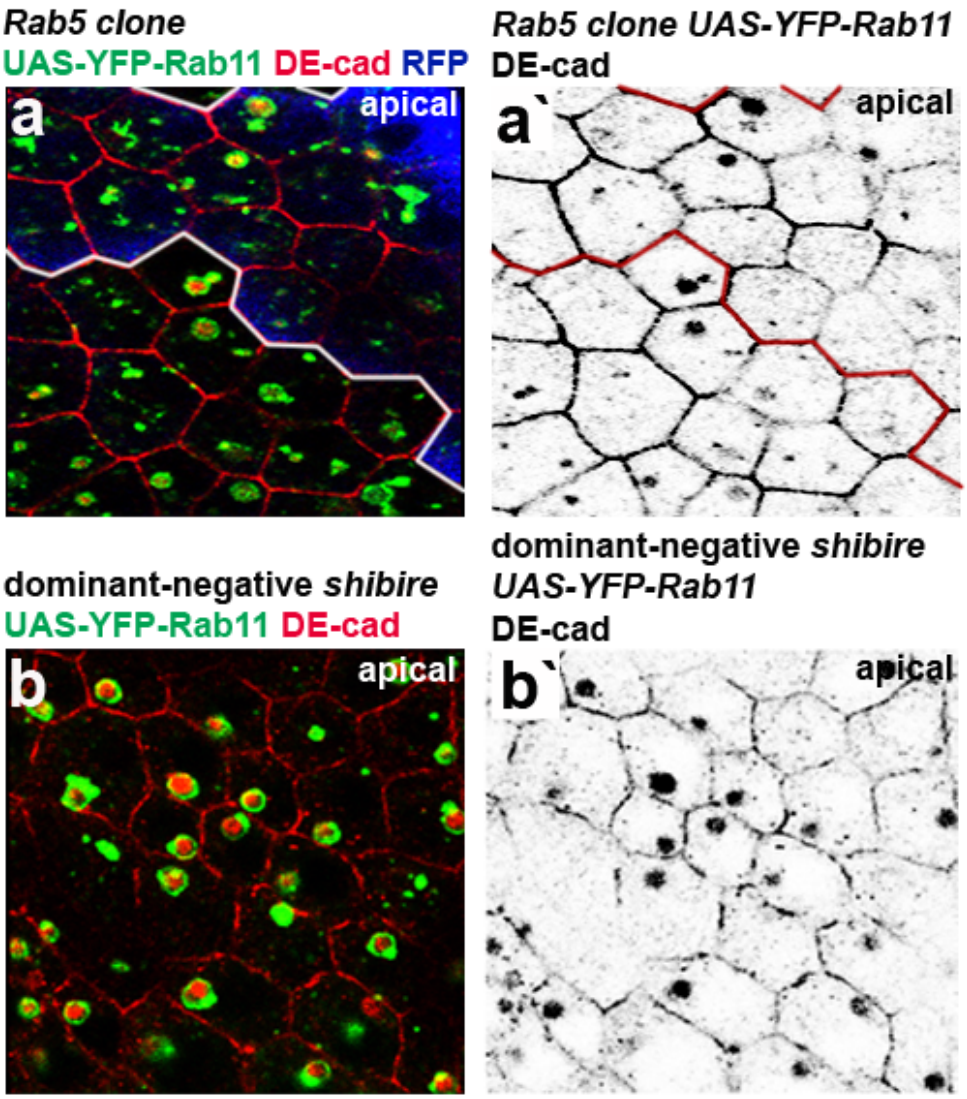

Figure 11. Newly synthesized DE-cadherin accumulates within YFP-Rab11 compartments. (a-b) Apical confocal optical sections perpendicular to the apical-basal axis of the follicular epithelium. The scale bar represents 10µm. (a`) and (b`) show DE-cadherin channel alone. (a) Epithelia expressing YFP-Rab11 (green) and stained for DE-cadherin (red) in *Rab5* clone. Clone cells are indicated by the absence of RFP (blue). The clone border is highlighted by the white line (a) and by the red line (a`). (b) Epithelia co-expressing YFP-Rab11 (green) and a dominant-negative form of shibire and stained for DE-cadherin (red).

4.1.6 YFP-Rab11 is a part of the endosomal system and DE-cadherin cytoplasmic domain is required for the DE-cadherin delivery to the YFP-Rab11 compartments

My data show that apical YFP-Rab11 compartments accumulate endocytosed and newly synthesized DE-cadherin (Figures 10 and 11). I was further interested in the characterization of YFP-Rab11 compartments. To achieve this, I performed co-immunostaining experiments with the UAS-YFP-Rab11 expressing follicles and different cell compartments markers. Since previous studies showed that Rab11 acts at the *trans*-Golgi network (Beronja et al., 2005; Satoh et al., 2005), I first examined if YFP-Rab11 compartments are connected with the *trans*-Golgi network in *Drosophila* follicular epithelium. The Golgi network marker Golgin-245, which is a golgin present on the trans-Golgi network, showed no colocalization with YFP-Rab11 compartments (Figure 12a). By contrast, immunostaining with the endosomal markers Rab5 and Rab7 showed a complete overlap with the YFP-Rab11 structures (Figure 12b) (100%, n=12 follicles). These results suggest that YFP-Rab11 structures are part of the endosomal system and appear not to have a direct connection with the Golgi.

Since my data suggested that YFP-Rab11 compartments are part of the endosomal system, I asked how DE-cadherin reaches endosomes. Specifically, I was interested in the sorting signals found within the E-cadherin domain, which could be responsible for E-cadherin delivery to YFP-Rab11 endosomal compartments. Previous studies showed that the cytoplasmic domain of E-cadherin, highly conserved amongst many species, contains sorting signals (Y. T. Chen et al., 1999; U Tepass et al., 2001). I thus asked if the sorting signals for DE-cadherin transport to the endosomal YFP-Rab11 system could also be located within the DE-cadherin cytoplasmic domain.

To address this question, I used the mutant form of DE-cadherin protein, DE-cadhΔCyt/α-cat, which was previously generated by deleting the whole cytoplasmic domain and replacing it with the coding region of the α-catenin gene (Pacquelet et al., 2003). To test if DE-cadhΔCyt/α-cat reaches the apical YFP-Rab11 compartment, I co-expressed UAS-DE-cadhΔCyt/α-cat and UAS-YFP-Rab11 in the follicular epithelium. The DE-cadherin mutant lacking the cytoplasmic domain wasn't detected within YFP-Rab11 compartments (Figure 12c). This shows that DE-cadherin mutant lacking the cytoplasmic domain cannot be delivered to YFP-Rab11 endosomal compartments. This finding suggests that the sorting signals for DE-cadherin transport to YFP-Rab11 endosomal compartments are located within DE-cadherin cytoplasmic domain.

Taken together, my data show that apical YFP-Rab11 compartments colocalize with the endosomal markers Rab5 and Rab7, suggesting that YFP-Rab11 compartments belong to the endosomal system. Additionally, the cytoplasmic domain of DE-cadherin contains sorting signals that are necessary for the DE-cadherin delivery to YFP-Rab11 endosomal compartments.

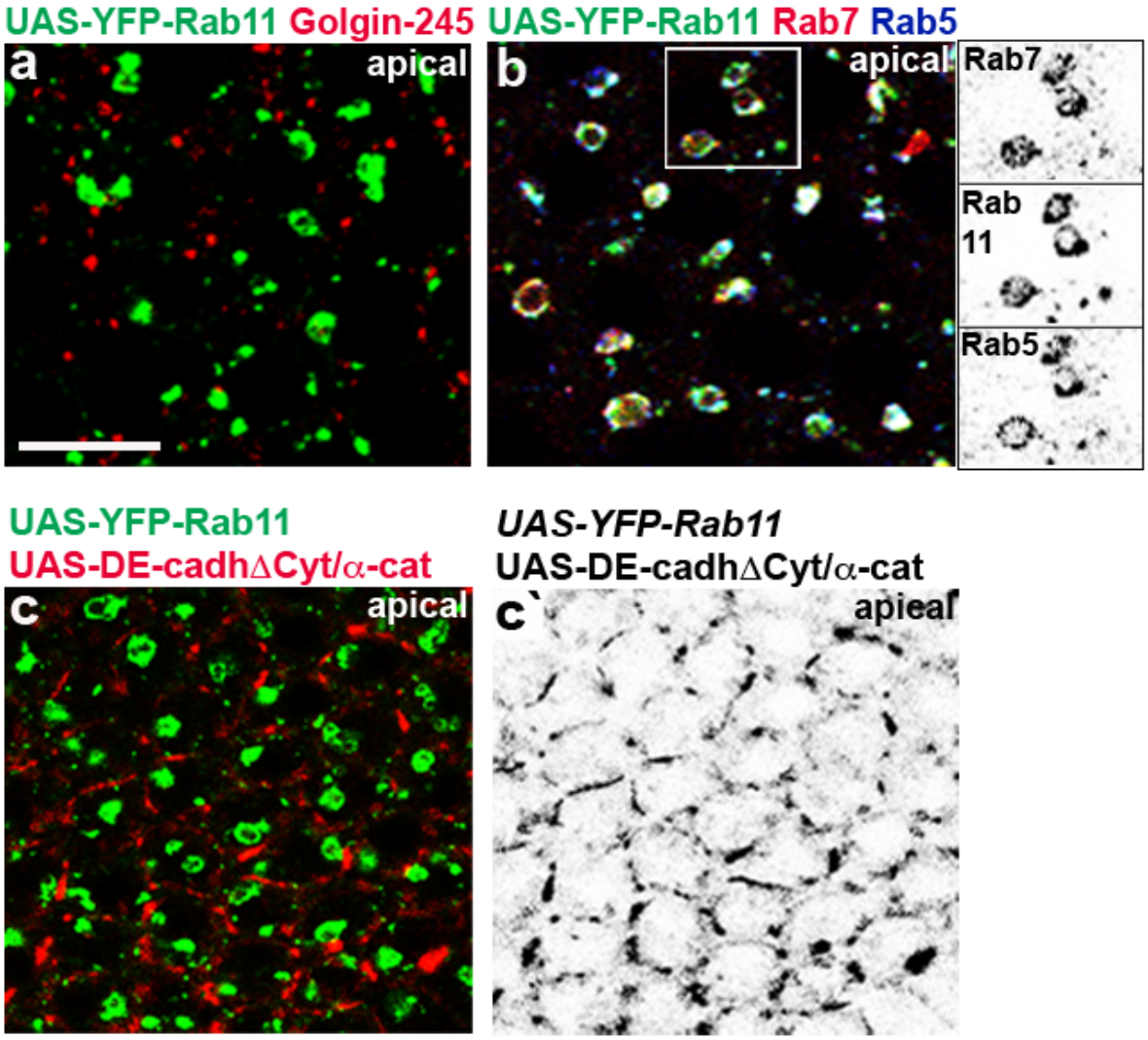

Figure 12. YFP-Rab11 compartments are part of the endosomal system and DE-cadherin cytoplasmic tail is required for the delivery to the YFP-Rab11 compartments. (a-c) Apical confocal optical sections perpendicular to the apical-basal axis of the follicular epithelium. The scale bar represents 10µm. (a) Epithelia expressing UAS-YFP-Rab11 (green) and stained marker Golgin-245 (red). (b) Epithelia expressing UAS-YFP-Rab11 (green) and stained for Rab7 (red) and Rab5 (blue). Insets on the right show the individual Rab7, YFP-Rab11 and Rab5 channels of the marked area. (c) Epithelia co-expressing UAS-YFP-Rab11 (green) and UAS-DE-cadhΔCyt/α-cat, the DE-cadherin mutant protein lacking the cytoplasmic tail (red). (c`) shows the DE-cadherin channel alone.

4.2 Rab7 is involved in DE-cadherin trafficking within the endosome

Endosomes have been described as compartments where the sorting of proteins occurs (McNally & Cullen, 2018; Scott et al., 2014; Simonetti & Cullen, 2019). Proteins are internalized from the plasma membrane via endocytosis and imported into the early endosomal system, where they can either be destined for degradation or recycling. Once the decision has been made, proteins are then sorted into different endosomal tubular extensions (Simonetti & Cullen, 2019). At the end of these branches, tubulo-vesicular carriers are generated, which bud from one compartment and fuse with another, thus facilitating cargo transport (Cullen & Steinberg, 2018; Naslavsky & Caplan, 2018; Simonetti & Cullen, 2019; Weeratunga et al., 2020). My data and previous studies showed that DE-cadherin passes through the endosomes on its route to the plasma membrane (Figure 12) (Zeigerer et al., 2012). Nevertheless, how DE-cadherin moves within the endosomal system for further transport remains unknown.

4.2.1 Rab7 is a part of the apical endosomal system involved in DE-cadherin transport

My results show that YFP-Rab11 compartments are part of the endosomal system where newly synthesized and recycled DE-cadherin accumulate. As I observed that Rab7 colocalized with apical YFP-Rab11 compartments (Figure 12b), I asked what is the role of Rab7 in DE-cadherin transport. On a side note, YFP-Rab11 compartments also colocalized with the endosomal markers Rab5 (Figure 12b). However, I speculate that the colocalization between Rab5 and YFP-Rab11 compartments is due to a well-established route of early endosome fusion with the endosomal system (Naslavsky & Caplan, 2018). The observed overlap between YFP-Rab11 and Rab7 can be more challenging to explain since Rab7 is shown to be involved in both recycling and degradation of proteins (Balderhaar et al., 2010; Bucci et al., 2000; Liu et al., 2012; Priya et al., 2015; Rojas et al., 2008; Seaman, 2004; Seaman et al., 2009).

To investigate the role of Rab7 in the DE-cadherin trafficking pathway, I first analyzed the Rab7 localization in the *Drosophila* wild type follicular epithelium. The immunostaining of wild type *Drosophila* ovaries with α-Rab7 antibody revealed that Rab7 compartments are rather big (0.88 μm^2 ± 0.07, n=120 cells from 7 follicles) and predominantly detected in the apical area of the cell (82% of the total number of Rab7 compartments) (Figures 13a and 13b).

I further analyzed the localization of DE-cadherin in relation to Rab7 compartments in wild type epithelium. My data revealed that DE-cadherin was detected within the apical Rab7 compartments (arrows in Figure 13a). This suggests that DE-cadherin passes through the Rab7 compartment during its transport. Next, I investigated if Rab7 is a part of the apical

compartment where endocytosed DE-cadherin localizes. To do this, I performed pulse-chase endocytosis with the *Drosophila* wild type follicular epithelium and stained the epithelia for Rab7. I observed that endocytosed DE-cadherin colocalized with Rab7 compartments in the apical cytoplasm after 20 minutes of endocytosis (arrows in Figure 13c). Within Rab7 compartments, 89.57% (± 2.26) of endocytosed DE-cadherin spots were detected (n=220 cells from 6 follicles). This suggests that endocytosed DE-cadherin enters the Rab7 compartment after endocytosis. Further, this also implies that Rab7 is part of the apical endosomal system where endocytosed and newly synthesized DE-cadherin accumulates.

Taken together, my data suggest that big Rab7 compartments are predominantly detected in the apical cytoplasm. Furthermore, endocytosed DE-cadherin localizes to apical Rab7 compartments, implying that Rab7 is involved in DE-cadherin transport via the apical endosomal system.

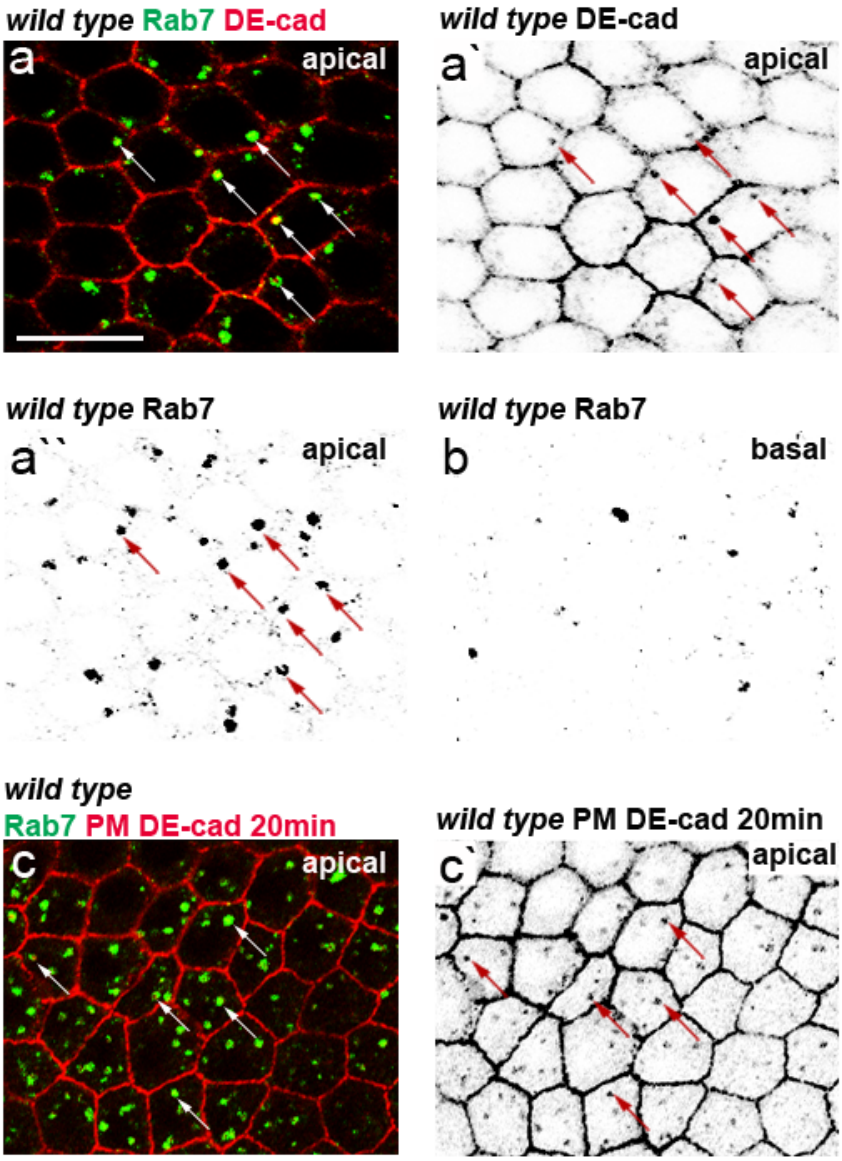

Figure 13. DE-cadherin traffics through the apical endosomal Rab7 compartment. (a-c) Confocal optical sections perpendicular to the apical-basal axis of the follicular epithelium. The scale bar represents 10µm. Experiments shown were performed with wild type epithelia. (a) The apical confocal section of epithelia stained for Rab7 (green) and DE-cadherin (red). (a`) and (a``) show individual DE-cadherin and Rab7 channels respectively. DE-cadherin localizes within Rab7 compartment (white arrows in (a), red arrows in (a`) and (a``)). (b) The basal confocal section of epithelia stained for Rab7. (c) Pulse-chase endocytosis with α-DE-cadherin (red) antibody for 20 minutes and stained for Rab7 (green). PM DE-cadherin (plasma membrane DE-cadherin) stands for endocytosed DE-cadherin. The apical confocal section is shown. (c`) shows the individual DE-cadherin channel. Endocytosed DE-cadherin colocalizes with Rab7 compartments (white arrows in (c) and red arrows in (c`)).

4.2.2 DE-cadherin localizes to Rab7 and functional Rab11 compartment

My data suggest that both YFP-Rab11 and Rab7 are part of the endosomal system, where newly synthesized and endocytosed DE-cadherin accumulate. I further asked if there is an interaction between Rab11 and Rab7 in DE-cadherin transport. For the investigation of the interaction between Rab7 and Rab11 in DE-cadherin trafficking, I aimed to test the localization of Rab7 in regard to the functional Rab11 compartment. For this purpose, I used the UAS-HA-Rab11 construct. As α-Rab7 and α-HA antibodies are generated from the same species, I wasn't able to use them together. To circumvent this problem, I used *Drosophila* follicles expressing yRab7 construct. yRab7 is a construct in which the endogenous Rab7 is tagged with the GFP and can thus be detected with the GFP antibody (Dunst et al., 2015). My data showed that yRab7 and HA-Rab11 were often found either partially colocalizing or nearby (Figure 14a) (77% ± 5.74, n=176 cells from 6 follicles). This implies that Rab11 and Rab7 compartments might be spatially connected.

I also analyzed the localization of DE-cadherin in relation to Rab11 and Rab7 compartments. I observed that DE-cadherin also colocalized with yRab7 and HA-Rab11 (Figure 14a) (63% ± 3, n=324 cells from 6 follicles). This suggests that Rab11 and Rab7 might be interacting in DE-cadherin transport. To evaluate how specific is the DE-cadherin colocalization with HA-Rab11 and yRab7 compartments, I analyzed the localization of atypical protein kinase C (aPKC), the protein unrelated to HA-Rab11 and yRab7. Atypical protein kinase C (aPKC) is a key polarity protein, whose localization in *Drosophila* follicular epithelium doesn't depend on Rab7 and Rab11 but on the apical complex Crb/Sdt and other proteins such as Canoe and the FERM domain protein Willin (Hong, 2018; Hong et al., 2001; Ishiuchi & Takeichi, 2011; Sawyer et al., 2009). In my observation, aPKC colocalized with yRab7 and HA-Rab11 to a significantly lesser extent when compared to DE-cadherin (7% ± 3, n=199 cells from 5 follicles) (Figure 14c). This confirms that the DE-cadherin localization to HA-Rab11 and yRab7 compartments is specific.

In summary, my data show that DE-cadherin localizes to Rab7 and functional Rab11 compartment, suggesting the interaction of Rab7 and Rab11 in DE-cadherin transport.

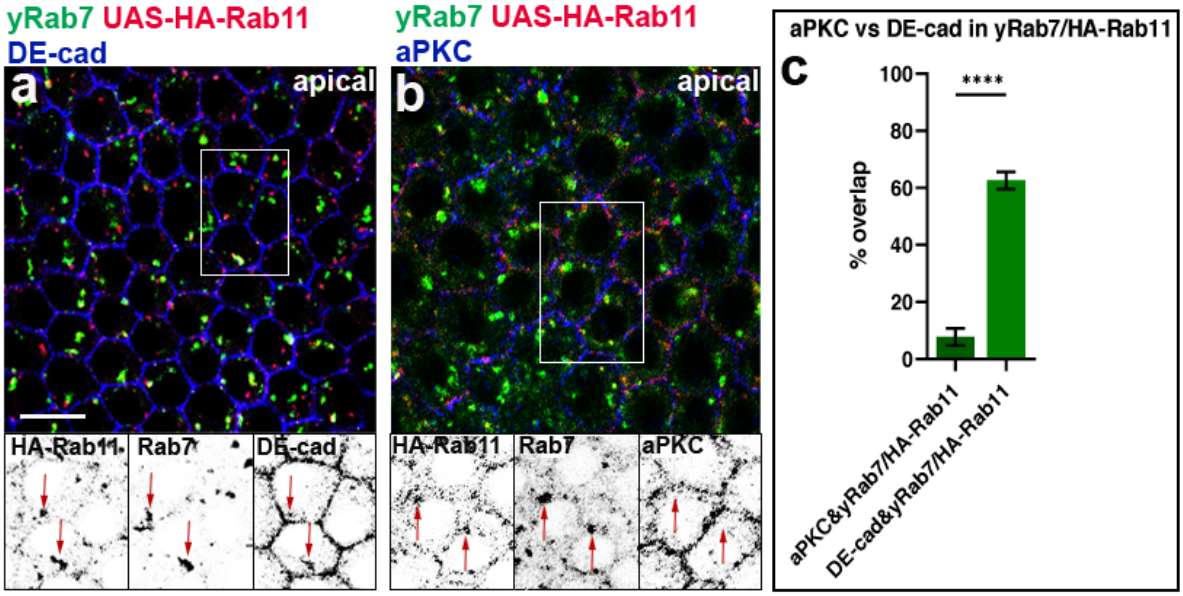

Figure 14. DE-cadherin localizes to Rab7 and Rab11 compartments. (a-b) Apical confocal optical sections perpendicular to the apical-basal axis of the follicular epithelium. The scale bar represents 10µm. (a) Epithelia co-expressing yRab7 (green) and UAS-HA-Ra11 (red) stained for DE-cadherin (blue). Insets below show individual HA-Rab11, Rab7 and DE-cadherin channels of the marked area. HA-Rab11, Rab7 and DE-cadherin colocalize (red arrows). (b) Epithelia co-expressing yRab7 (green) and UAS-HA-Ra11 (red) stained for aPKC (blue). Insets below show individual HA-Rab11, Rab7 and aPKC channels of the marked area. No colocalization is observed between HA-Rab11, Rab7, and aPKC (red arrows). (c) Quantification of the colocalization of the yRab7/HA-Rab11 compartment with aPKC and DE-cadherin. Data are shown as mean ± SEM. Two-tailed t-test (equal variance, α = 0.05) was performed and p values are presented as ****p < 0.0001. The quantification was performed with 5 follicles (n=199 cells) for the aPKC and yRab7/HA-Rab11 and with 6 follicles (n=324 cells) for DE-cadherin and yRab7/HA-Rab11.

4.2.3 DE-cadherin exit from the Rab7 compartment is Rab11 dependent

My data show that DE-cadherin localizes to apical Rab7 and Rab11 compartments (Figure 14a), suggesting the interaction between Rab7 and Rab11 in DE-cadherin transport. I aimed to further study the interaction between Rab7 and Rab11 by characterization of *Rab11* mutants. The *Rab11* mutant cell clones were induced using FRT/FLP technique as previously described (see 4.1.5) (T. Xu & Rubin, 1993).

As shown in Figure 7a and by previous research, DE-cadherin heavily accumulated in *Rab11* clone cells, suggesting the critical role of Rab11 in DE-cadherin transport (Woichansky et al., 2016; Xu et al., 2011). To identify the compartments where DE-cadherin accumulates, I stained

Rab11 mutant cell clones with different markers of cell compartments. I observed that DE-cadherin aggregates weakly colocalized with *trans*-Golgi marker Golgin-245 and almost didn't colocalize at all with *cis*-Golgi marker GM130 in *Rab11* mutants (Figure 15a). This suggests that DE-cadherin aggregates localize outside of the Golgi and are not blocked within the Golgi compartment in the absence of Rab11. I also observed that DE-cadherin aggregates were not colocalizing with Rab5, the marker for early endosome, in *Rab11* mutants (Figure 15b). This further implies that DE-cadherin can leave the early endosome in the absence of Rab11.

Next, I analyzed the localization of DE-cadherin aggregates in *Rab11* cell clones in relation to the lysosome, the degradative cell compartment. The reason for this analysis is that DE-cadherin protein could be destined for degradation after not being delivered to the plasma membrane in the absence of Rab11. For this purpose, I visualized lysosomes using a pH-sensitive dye LysoTracker Red, which is widely used for the detection of lysosomes in many different cells and tissues (Avrahami et al., 2013; Lund et al., 2018; Zhitomirsky et al., 2018). Lysotracker is a weak base that is attached to a fluorophore and accumulates within the organelles with a highly acidic environments (Haller et al., 1996; Johnson et al., 2016). *Drosophila* ovaries are incubated with the lysotracker for 30 minutes at room temperature and the dye accumulates within the low pH compartments. I observed weak colocalization of DE-cadherin aggregates and lysotracker in *Rab11* mutant ovaries (Figure 15c). This result suggests that DE-cadherin is not degraded upon Rab11 depletion.

Finally, I analyzed the localization of DE-cadherin aggregates in *Rab11* clones in relation to the Rab7 endosomal compartment. I observed the extensive overlap of DE-cadherin aggregates with Rab7 compartments upon the Rab11 depletion (Figures 15b and 15c). This result implies that DE-cadherin is blocked and cannot leave the Rab7 compartment in the absence of Rab11. In addition to this, I noticed that Rab7 compartments in *Rab11 mutant* cells were enlarged (Figures 15b and 15c). The finding further suggests that Rab7 compartments in *Rab11* cell clones are enlarged due to the accumulation of DE-cadherin. To confirm the observation that DE-cadherin aggregates are blocked within Rab7 compartments, I quantified the colocalization between DE-cadherin and different cell markers analyzed. The quantification analysis supported the observation that DE-cadherin aggregates extensively localize to Rab7 compartments in *Rab11* mutants (Figure 15d). This further confirms that DE-cadherin aggregates in *Rab11* clones are blocked within the enlarged Rab7 compartment.

Taken together, my data suggest that DE-cadherin can leave the Golgi and early endosome in the absence of Rab11. Furthermore, the DE-cadherin protein accumulating in the cytoplasm is also not sent for degradation upon Rab11 depletion. Instead, DE-cadherin is blocked and unable to leave Rab7 compartments without Rab11, which enlarge as a consequence. This suggests that the DE-cadherin exit from the Rab7 compartment is dependent on the Rab11. Overall, these results further confirm that Rab7 and Rab11 interact in DE-cadherin transport.

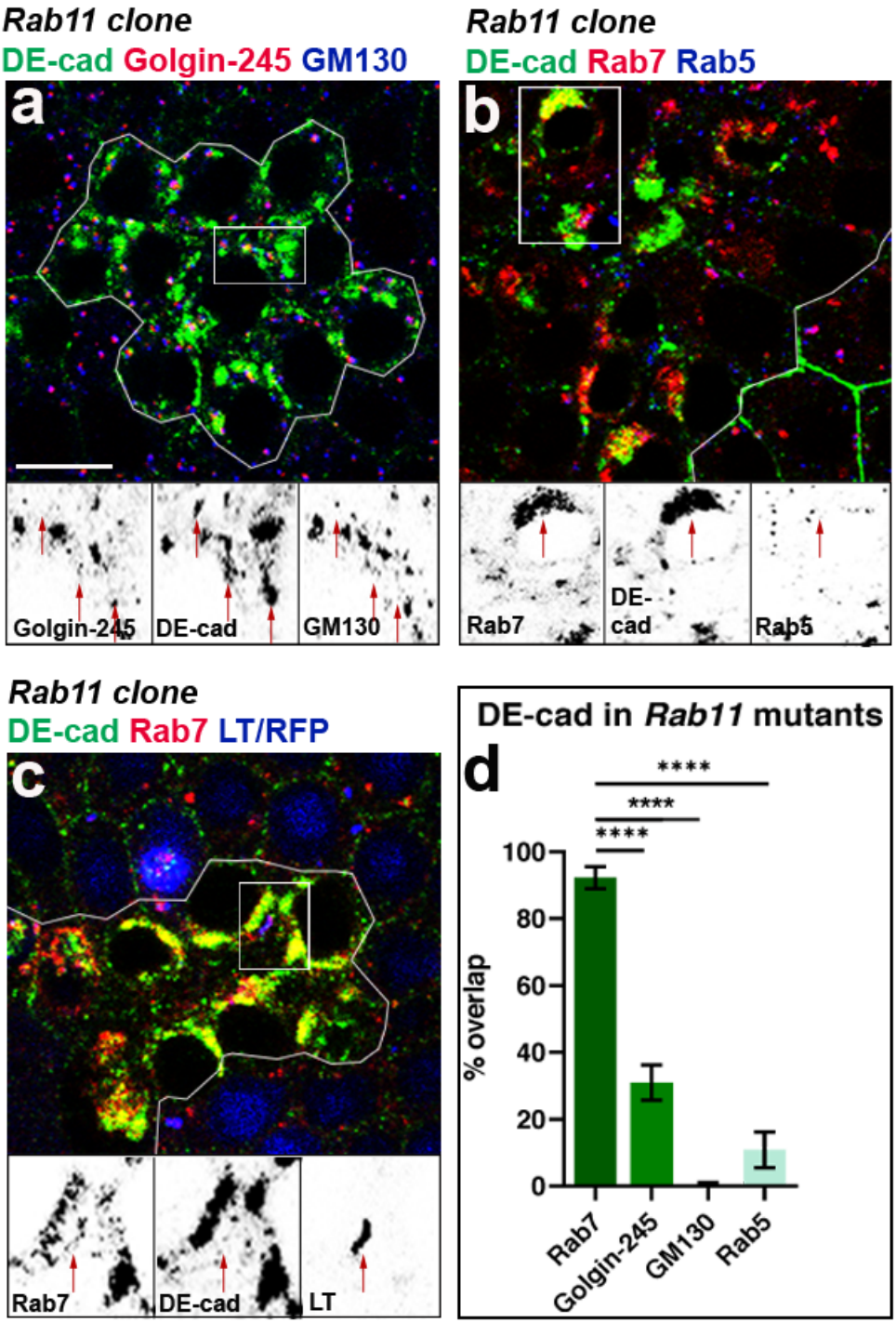

Figure 15. DE-cadherin exit from the Rab7 compartment is Rab11 dependent. (a-c) Confocal optical sections perpendicular to the apical-basal axis of the follicular epithelium. The scale bar represents 10μm. Clone borders are marked by the white line and heavy DE-cadherin (green) accumulation. In (c) clone cells are also recognized by the absence of RFP (blue). (a) *Rab11* clone stained for DE-cadherin (green), Golgin-245 (trans-Golgi) (red) and GM130 (cis-Golgi) (blue). Insets below show individual Golgin-245, DE-cadherin and GM130 channels from the marked area. DE-cadherin aggregates do not colocalize with Golgin-245 and GM130 (red arrows). (b) *Rab11* clone stained for DE-cadherin (green), Rab7 (red) and Rab5 (blue). Insets below show individual Rab7, DE-cadherin and Rab5 channels from the marked area. Rab7 and DE-cadherin aggregates colocalize (red

arrows). (c) *Rab11* clone stained for DE-cadherin (green), Rab7 (red) and lysotracker (LT) (blue). Insets below show individual Rab7, DE-cadherin and LT channels from the marked area. DE-cadherin aggregates do not colocalize with the LT (red arrows). (d) Quantification of the colocalization between DE-cadherin aggregates in *Rab11* mutant cells with Rab7, Golgin-245 (trans-Golgi), GM130 (cis-Golgi) and Rab5. Representative images are shown in (a) and (b). Data are shown as mean ± SEM. Two-tailed t-test (equal variance, α = 0.05) was performed and p values are presented as ****p < 0.0001. The quantification was performed with 10 follicles (n=197 clone cells) for Rab7&DE-cadherin, 14 follicles (n=276 clone cells) for Golgin-245&DE-cadherin, 9 follicles (n=165 clone cells) for GM130&DE-cadherin and 7 follicles (n=122 clone cells) for Rab5&DE-cadherin.

4.2.4 DE-cadherin aggregates in *Rab7* mutants form due to the impaired recycling pathway

My data suggest that DE-cadherin is blocked in Rab7 compartments upon Rab11 depletion (Figure 15). I further asked how is DE-cadherin localized and transported in Rab7 depleted cells. To answer this question, I induced *Rab7* cell clones in *Drosophila* follicular epithelium using the $Rab7^{Gal4\text{-}knock\text{-}in}$ null allele, which was previously generated and published (Cherry et al., 2013). I observed the cytoplasmic DE-cadherin aggregation upon the *Rab7* depletion (Figure 16a). This result implies the requirement of Rab7 in DE-cadherin transport. However, DE-cadherin's proper localization to the plasma membrane revealed that DE-cadherin transport was still possible, suggesting the potential redundant role of Rab7 in DE-cadherin transport.

Next, I asked if DE-cadherin aggregates in *Rab7* clones are resulting from the impaired degradation pathway. I was specifically interested to test whether DE-cadherin aggregates form due to the impairment in the degradation, since previous studies showed that Rab7 plays a role in the degradative pathway of proteins (Bucci et al., 2000; Guerra & Bucci, 2016; Laiouar et al., 2020; Zhang et al., 2009). To answer this question, I analyzed the localization of DE-cadherin aggregates in *Rab7* mutant cells in relation to the lysosomal marker lysotracker. I observed that most DE-cadherin aggregates showed no colocalization with the lysotracker (91% ± 1.93, n=180 clone cells from 4 follicles) (arrows in Figures 16a` and 16a``). This implies that DE-cadherin aggregates in *Rab7* cell clones do not form due to an impairment in the degradative pathway.

Curiously, previous studies demonstrated that Rab7 plays a role not only in the degradation but also in recycling of proteins, suggesting the dual role of Rab7 in endosomes (Balderhaar et al., 2010; Liu et al., 2012; Priya et al., 2015; Rojas et al., 2008; Seaman, 2004; Seaman et al., 2009). Since my data imply that DE-cadherin aggregates in *Rab7* mutants do not result

from the defective degradative pathway, I speculated that they form due to a defective recycling pathway, in which Rab7 also plays a role.

In summary, my data show that DE-cadherin accumulates in the cytoplasm in the absence of Rab7. This suggests the function of Rab7 in DE-cadherin transport. In addition, DE-cadherin localizes properly to the plasma membrane in *Rab7* cell clones, implying that its role in DE-cadherin secretion to the plasma membrane might be redundant. My findings further revealed that DE-cadherin aggregates do not colocalize with lysosomes, implying that DE-cadherin aggregates do not form due to the defective degradation upon Rab7 depletion. I thus propose that DE-cadherin aggregates in *Rab7* mutants result from impaired recycling, suggesting the role of Rab7 in DE-cadherin recycling.

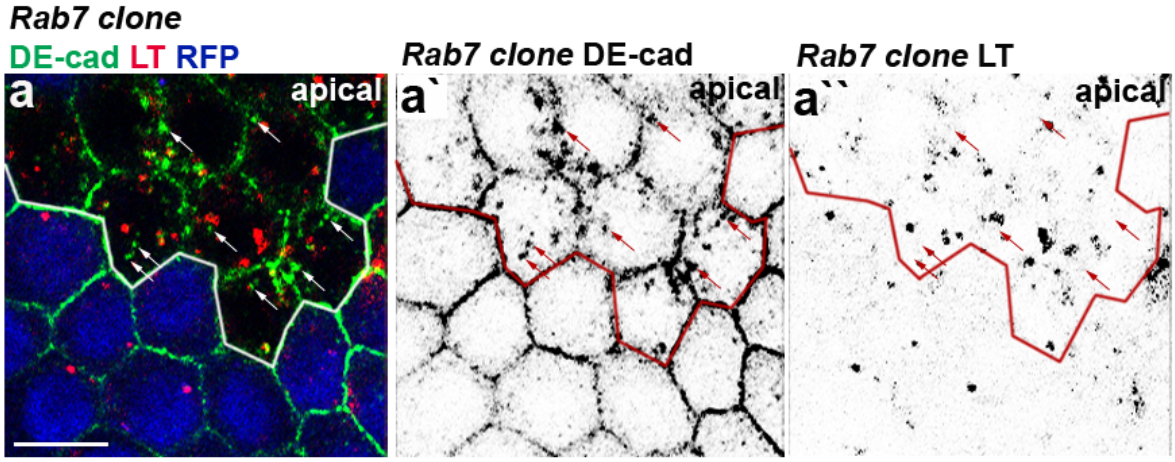

Figure 16. DE-cadherin accumulates in the cytoplasm in *Rab7* clone cells. Apical confocal optical section perpendicular to the apical-basal axis of the follicular epithelium. The scale bar represents 10µm. (a) *Rab7* cell clones stained for DE-cadherin (green) and lysotracker (LT) (red). Clone cells are recognized by the absence of RFP (blue). (a`) and (a``) show individual DE-cadherin and LT channels respectively. The clone border is highlighted by the white line (a) and the red line in (a`) and (a``). DE-cadherin aggregates do not colocalize with the LT (white arrows in (a) and red arrows in (a`) and (a``)).

4.3 Snx16 is recruited by Rab7 for DE-cadherin transport to Rab11 compartments via tubules

Proteins within the endosomal system destined to be recycled are retrieved from degradation. Retrieval complexes recognize cargo and sort it into various endosomal recycling branches, where tubulo-vesicular carriers promote future trafficking (Cullen & Steinberg, 2018; Simonetti & Cullen, 2019; Weeratunga et al., 2020). Despite extensive research and the presence of several promising candidates promoting this process, such as members of the sorting nexin family (Bryant et al., 2007; Solis et al., 2013; Jinxin Xu et al., 2017; Zobel et al., 2015), the mechanism by which DE-cadherin is retrieved from the degradative pathway remains unknown.

4.3.1 Snx16 localizes to Rab7 and Rab11 endosomes

My findings suggest that Rab7 plays a role in DE-cadherin recycling. I further aimed to investigate which factors could interact with Rab7 in this process. Previous studies have shown that Rab7 recruits different effectors to endosomes for the recycling of proteins (Rojas et al., 2008; Seaman et al., 2009). I asked what effectors could be recruited by Rab7 for the DE-cadherin recycling. A very good candidate is a member of the sorting nexin family, sorting nexin 16 (Snx16), since past studies showed that Snx16 localizes to endosomes and directly binds DE-cadherin in the DE-cadherin recycling process (Brankatschk et al., 2011; Jinxin Xu et al., 2017).

To analyze the potential role of Snx16 in DE-cadherin transport, I used *Drosophila* follicles expressing the UAS-Snx16-SNAP construct (Rodal et al., 2011). SNAP-tag is a small polypeptide (19.4kDa) that is a mutant for human DNA repair protein O^6-alkylguanine-DNA-alkyltransferase (hAGT). hAGT reacts fast and specifically with the benzylguanine (BG) derivatives, which results in the covalent labelling of the probe with the SNAP-tag (Keppler et al., 2003, 2004). I first investigated the spatial localization of Snx16 in relation to the different markers for the cell compartments. I observed that Snx16 doesn't colocalize with GM130 (*cis*-Golgi marker) and Golgin-245 (*trans*-Golgi marker), showing the spatial separation of Snx16 from the Golgi network (Figure 17a). This suggests that Snx16 doesn't act in the Golgi compartment.

Next, I observed that Snx16 colocalized with the apical Rab7 compartments (Figure 17b) (88% ± 1.46, n=199 cells from 5 follicles). This suggests that Snx16 acts in the Rab7 endosomal compartment. Such a result is consistent with the previously published finding in cultured cells, which demonstrated that Snx16 localizes to Rab7 endosomes (Brankatschk et al., 2011). I

also investigated the spatial relation between Snx16 and YFP-Rab11 endosomal compartments, to additionally confirm that Snx16 acts at endosomes. To perform this, I co-expressed UAS-Snx16-SNAP and UAS-YFP-Rab11 constructs in *Drosophila* follicles. I observed that Snx16 localizes to apical YFP-Rab11 compartments (Figure 17c). Additionally, I also noticed that Snx16 compartments were enlarged upon UAS-YFP-Rab11 expression. This suggests that the function of Snx16 might be attenuated in follicles expressing the UAS-YFP-Rab11 construct. My previous data show that DE-cadherin accumulates within YFP-Rab11 compartments (Figure 8a), so I further analyzed if DE-cadherin accumulates within YFP-Rab11/Snx16 compartments as well. I indeed observed high levels of DE-cadherin within apical YFP-Rab11/Snx16 compartments (Figure 17c). This suggests that DE-cadherin is blocked within apical YFP-Rab11 compartments that also contain Snx16.

Taken together, my data show that Snx16 localizes to Rab7 and YFP-Rab11 endosomal compartments. These findings suggest a potential function of Snx16 in the apical endosomal system, through which DE-cadherin transits on its way to the plasma membrane.

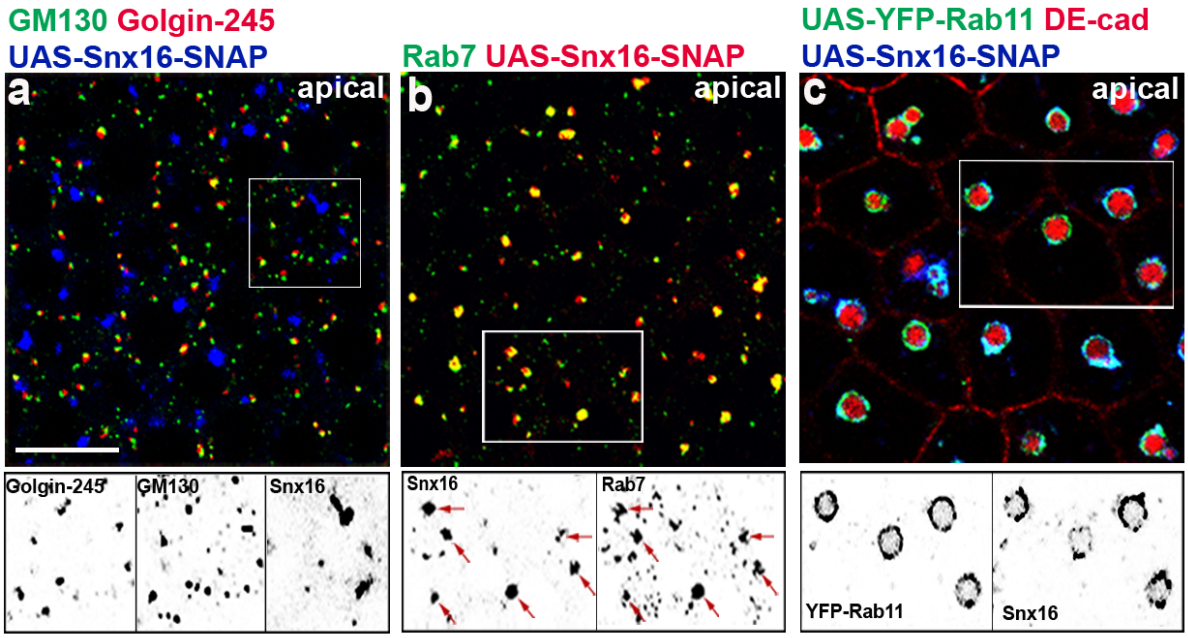

Figure 17. Snx16 localizes to Rab7 and YFP-Rab11 compartments. (a-c) Apical confocal optical sections perpendicular to the apical-basal axis of the follicular epithelium. The scale bar represents 10µm. (a) Epithelia expressing UAS-Snx16-SNAP (blue) and stained for GM130 (green) and Golgin-245 (red). Insets below show individual Golgin-245, GM130 and Snx16 channels of the marked area. (b) Epithelia expressing UAS-Snx16-SNAP (red) and stained for Rab7 (green). Insets below show the individual Snx16 and Rab7 channels of the marked area. Snx16 localizes to Rab7 compartments (red arrows). (c) Epithelia co-expressing UAS-YFP-Rab11 (green) and UAS-Snx16-SNAP (blue) and stained for DE-cadherin (red). Insets below show individual YFP-Rab11 and Snx16 channels of the marked area.

4.3.2 Loss of Snx16 leads to the DE-cadherin aggregation

My data show that Snx16 localizes to Rab7 and YFP-Rab11 compartments that are part of the DE-cadherin transport route. I next asked what role does Snx16 have in DE-cadherin trafficking. To answer this question, I generated *Snx16* clones using an *Snx16*$^{\Delta 1}$ null allele, which has the entire coding region and the part of the neighboring gene removed by imprecise excision (Rodal et al., 2011). I induced *Snx16* cell clones in *Drosophila* follicular epithelium and analyzed the DE-cadherin localization. I observed cytoplasmic DE-cadherin aggregates upon Snx16 depletion (Figure 18a). This implies that Snx16 plays a role in DE-cadherin transport. Nevertheless, DE-cadherin was properly localized to the plasma membrane, which shows that the transport of DE-cadherin still takes place. This suggests that the role of Snx16 in DE-cadherin trafficking might be redundant. Additionally, I noticed that DE-cadherin aggregates in *Snx16* mutants localized within the enlarged Rab7 compartments (arrows in Figures 18a` and 18a``). This suggests that DE-cadherin remains trapped in the Rab7 compartment in the absence of Snx16. I next wanted to confirm that DE-cadherin aggregates in *Snx16* mutants are indeed caused by the absence of Snx16. For this purpose, I used GR1 driver to induce the expression of UAS-GFP-Snx16 construct in *Snx16* mutants. I observed that the overexpression of the GFP-tagged Snx16 protein rescued the DE-cadherin aggregation in *Snx16* mutants (92%, n=12 cell clones) (Figure 18b). This confirms that DE-cadherin aggregates form due to the lack of Snx16.

I noticed similarities in DE-cadherin localization in *Rab7* and *Snx16* mutants. Namely, upon the depletion of Rab7 and Snx16, I observed cytoplasmic DE-cadherin aggregation. Nonetheless, DE-cadherin localized properly to the plasma membrane in both types of mutants (compare Figures 16 and 18a). This suggests that Rab7 and Snx16 might play a redundant role in DE-cadherin transport. I thus asked if Rab7 and Snx16 cooperate in DE-cadherin transport. If Rab7 and Snx16 cooperate in DE-cadherin transport, then the simultaneous depletion of Rab7 and Snx16 would result in a more severe DE-cadherin phenotype. To investigate this hypothesis, I generated *Rab7 Snx16* double cell clones and analyzed DE-cadherin localization. I noticed more cytoplasmic DE-cadherin aggregates in *Rab7 Snx16* double mutants than in individual *Rab7* and *Snx16* mutants (Figure 18c). This observation was confirmed by the quantification of the total number of DE-cadherin aggregates in *Rab7* and *Snx16* single and double mutants (Figure 18d). However, I observed no additional serious cell defects as DE-cadherin was still properly localized to the plasma membrane. This suggests that there might be more factors cooperating with Rab7 and Snx16 in DE-cadherin transport.

In summary, my data reveal that DE-cadherin accumulates in the cytoplasm upon Snx16 depletion. Additionally, these DE-cadherin aggregates localize to enlarged Rab7 compartments. This suggests that Snx16 plays a role in DE-cadherin transport, as well as that

there might be a functional link between Snx16 and Rab7. Nevertheless, the role of Snx16, as well as the role of Rab7, could possibly be redundant and there could be additional factors cooperating with Snx16 and Rab7 in DE-cadherin transport.

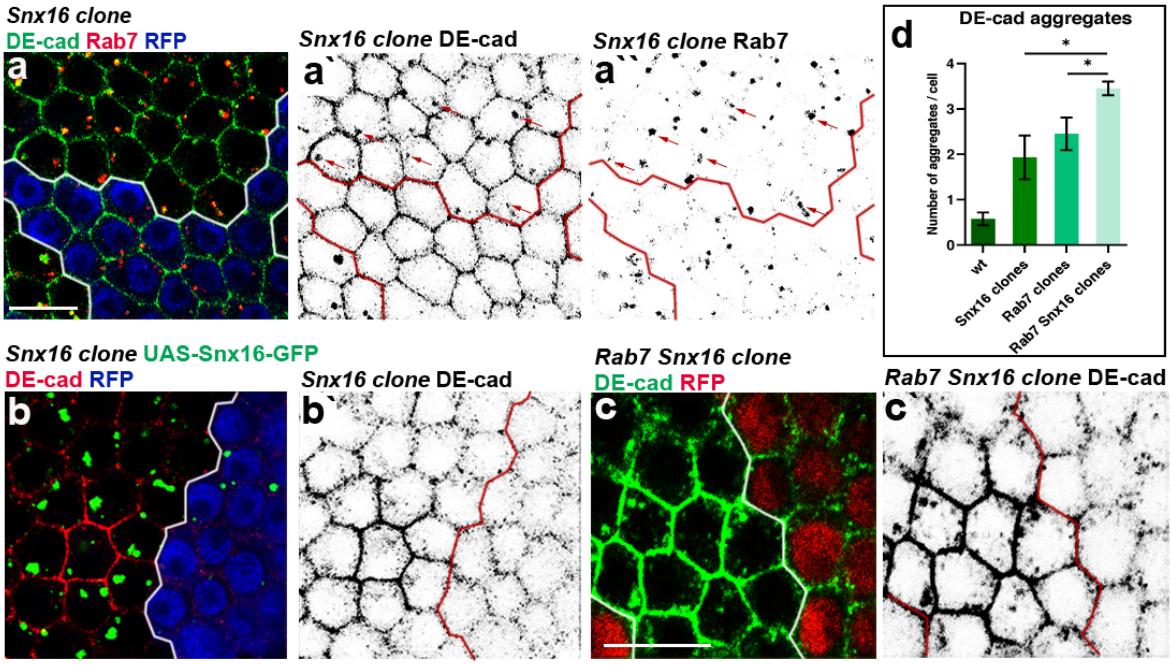

Figure 18. DE-cadherin accumulates in the cytoplasm in *Snx16* clone cells. (a-c) Confocal optical sections perpendicular to the apical-basal axis of the follicular epithelium. Scale bars represent 10µm. The clone border is highlighted by the white line in pictures showing merged channels and by the red line in pictures showing individual channels. Clone cells are additionally indicated by the absence of RFP (blue in (a) and (b) and red in (c)). (a) *Snx16* clone and stained for DE-cadherin (green) and Rab7 (red). (a`) and (a``) show individual DE-cadherin and Rab7 channels respectively. DE-cadherin aggregates localize to Rab7 compartments (red arrows). (b) Epithelia expressing UAS-Snx16-GFP (green) in *Snx16* clone cells stained for DE-cadherin (red). (b`) shows the individual DE-cadherin channel. (c) *Rab7 Snx16* double clone stained for DE-cadherin (green). (c`) shows the individual DE-cadherin channel. (d) Quantification of DE-cadherin aggregates in wild type epithelia, *Rab7* clones, *Snx16* clones and *Rab7 Snx16* double clones. Representative images are shown in (a), (c) and Figure 16a. Data are shown as mean ± SEM. A two-tailed t-test (equal variance, α=0.05) was performed and p values are presented as *p < 0.05. The quantification was performed with 6 follicles (n=161 cells) for wild type, 5 follicles (n=90 clone cells) *Snx16* clones, 6 follicles (n=120 clone cells) for *Rab7* clones and 5 follicles (n=85 clone cells) for *Rab7 Snx16* double clones.

4.3.3 Rab7 recruits Snx16 for subsequent DE-cadherin transport via tubules

My data suggest that Snx16 localizes to Rab7 and YFP-Rab11 endosomes and that it plays a role in DE-cadherin transport (Figures 17 and 18). Furthermore, I aimed to investigate my initial hypothesis that Rab7 recruits Snx16 as an effector molecule in the DE-cadherin recycling pathway (see 4.3.1). To test this hypothesis, I expressed UAS-Snx16-SNAP in *Rab7* cell clones in *Drosophila* follicular epithelium. I anticipated that, if Rab7 is critical for Snx16 recruitment, expressing high levels of Snx16 in cells could overcome its necessity for Rab7 and thus rescue DE-cadherin aggregation. I indeed noticed that the overexpression of Snx16 in *Rab7* mutants rescued cytoplasmic DE-cadherin aggregation (Figure 19a).

A previous study has revealed that the Snx16 protein has a tubulation activity (S. Y. Wang et al., 2019). Tubulation activity of proteins is usually performed via a BAR domain (Peter et al., 2004). Interestingly, Snx16 doesn't have the BAR domain but can still form tubules, which makes it a unique member of the sorting nexin protein family. The tubulation activity of Snx16 depends on the coiled-coil (CC) domain, and mutants lacking the CC domain cannot form tubules (S. Y. Wang et al., 2019). Since my data show that the overexpression of Snx16 in *Rab7* mutants rescued cytoplasmic DE-cadherin aggregation, I asked if the Snx16 ability to rescue DE-cadherin aggregates in *Rab7* cell clones is dependent on the tubulation activity. To test this, I used UAS-Snx16ΔCC-SNAP construct, which lacks the CC domain and cannot thus form tubules (S. Y. Wang et al., 2019). I expressed UAS-Snx16ΔCC-SNAP in *Rab7* mutants and analyzed DE-cadherin localization. Interestingly, I still observed cytoplasmic DE-cadherin aggregation in *Rab7* cell clones overexpressing the Snx16ΔCC construct (Figure 19b). This suggests that the Snx16ΔCC mutant protein cannot rescue DE-cadherin aggregation in *Rab7* mutants. To confirm my observation, I quantified DE-cadherin aggregates in *Rab7* mutants alone as well as in *Rab7* mutants expressing UAS-Snx16-SNAP and UAS-Snx16ΔCC-SNAP. The quantification revealed that DE-cadherin aggregates were present in epithelia expressing UAS-Snx16ΔCC-SNAP in *Rab7* mutants and in *Rab7* mutants alone (Figure 19c). In epithelia expressing UAS-Snx16-SNAP in *Rab7* mutants, on the other hand, a rather low number of DE-cadherin aggregates was detected. This implies that the Snx16 mutant lacking the CC domain cannot rescue DE-cadherin aggregation in *Rab7* mutants. Next, this also suggests that Snx16 rescues DE-cadherin aggregation in *Rab7* mutants via tubulation activity.

Besides the CC domain, the Snx16 protein also has a PX domain. One part of the PX domain (termed PPII/α2 loop) was shown to be critical for binding of Snx16 to E-cadherin (Jinxin Xu et al., 2017). Therefore, I asked if Snx16ΔCC mutant is still able to associate with DE-cadherin via the PX domain, despite lacking the CC domain. To answer this question, I analyzed the DE-cadherin localization in *Rab7* mutants in relation to the Snx16ΔCC mutant protein. I

observed that DE-cadherin aggregates colocalized with Snx16ΔCC (arrows in Figure 19b) (87% clones, n=15). This finding suggests Snx16ΔCC, a mutant lacking CC domain and still harboring PX domain, can associate with DE-cadherin. This further confirms that the PX domain of Snx16 protein is required for the interaction between Snx16 and DE-cadherin.

In summary, my data show that the expression of UAS-Snx16-SNAP rescues DE-cadherin aggregates in *Rab7* clones. The expression of the UAS-Snx16ΔCC-SNAP, the mutant unable to form tubules, cannot rescue DE-cadherin aggregates in Rab7-depleted cells. This overall suggests that Rab7 recruits Snx16 to endosomes and that Snx16 transports DE-cadherin for further trafficking steps via tubulation activity. My data also show that the PX domain within Snx16 is required for Snx16 binding to DE-cadherin.

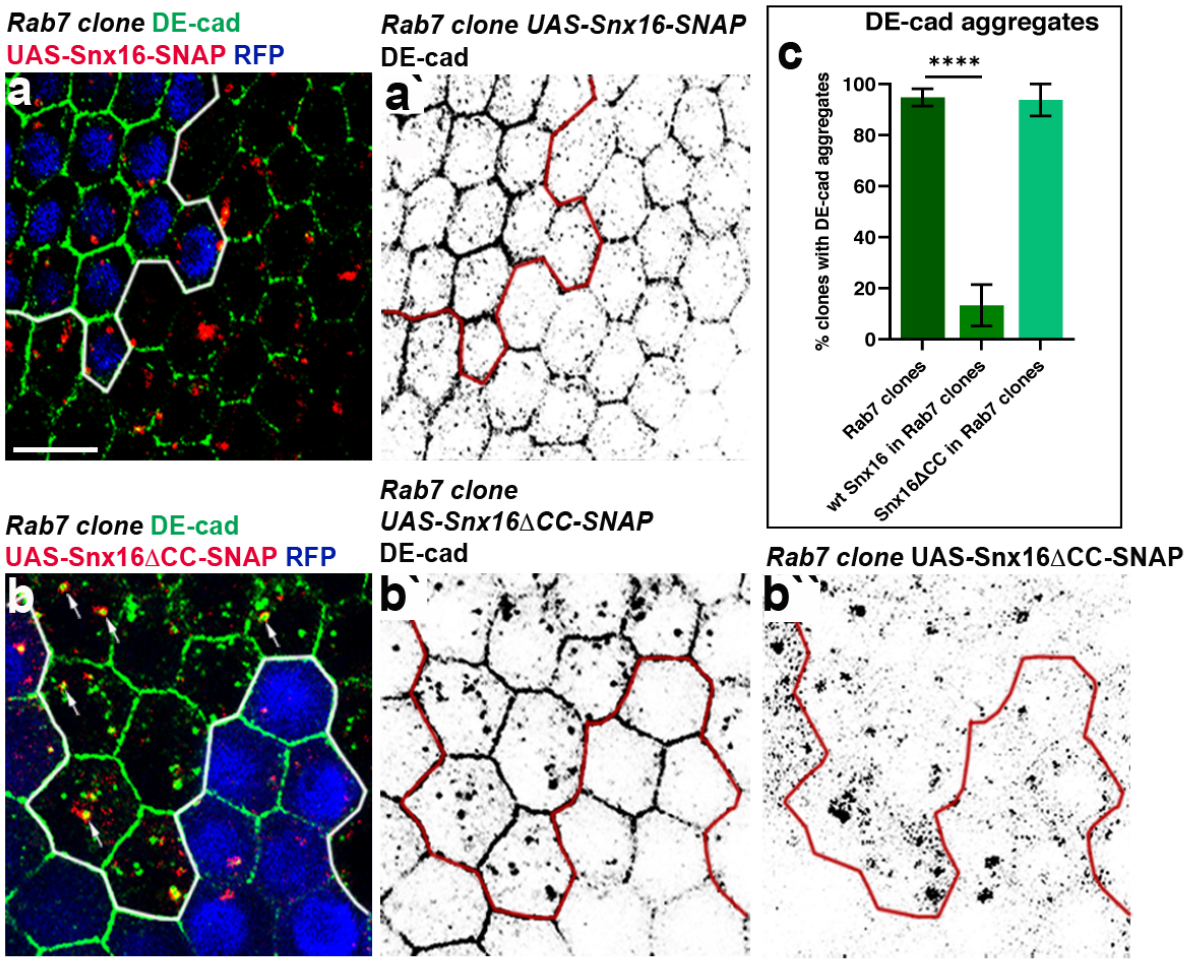

Figure 19. Snx16 overexpression rescues DE-cadherin aggregates in *Rab7* clone cells. (a-b) Confocal optical sections perpendicular to the apical-basal axis of the follicular epithelium. The scale bar represents 10µm. Clone cells are indicated by the absence of RFP (blue). The clone border is highlighted by the white line in pictures showing merged channels and by the red line in pictures showing individual channels. (a) Epithelia expressing UAS-Snx16-SNAP (red) in *Rab7* clone and stained for DE-cadherin (green). (a`) shows the individual DE-cadherin channel. The expression of UAS-Snx16-SNAP rescues cytoplasmic DE-cadherin aggregates (compare to Figure 16). (b) Epithelia expressing UAS-

Snx16ΔCC-SNAP (red) in *Rab7* clone and stained for DE-cadherin (green). DE-cadherin aggregates colocalize with Snx16ΔCC (white arrows). (b`) and (b``) show individual DE-cadherin and Snx16ΔCC-SNAP channels respectively. (c) Quantification of DE-cadherin aggregates in *Rab7* cell clones. Representative images are shown in (a), (b) and Figure 16. Data are shown as mean ± SEM. A two-tailed t-test (equal variance, α=0.05) was performed p values are presented as ****p < 0.0001. The quantification was performed with 30 follicles (n=38 cell clones) for *Rab7* clones, 17 follicles (n=18 cell clones) for UAS-Snx16-SNAP in *Rab7* clones and 5 follicles (n=85 clone cells) for UAS-Snx16ΔCC-SNAP in *Rab7* clones.

4.3.4 Snx16 stabilizes DE-cadherin and Armadillo interaction

My data so far show that DE-cadherin passes through apical Rab11 and Rab7 endosomal compartments to which Snx16 is recruited. In addition, the depletion of Rab11, Rab7 and Snx16 all resulted in cytoplasmic DE-cadherin accumulation (Figures 7a, 16 and 18a). Since previous studies showed that the DE-cadherin/Armadillo complex is essential for efficient DE-cadherin transport (Y. T. Chen et al., 1999; Langevin et al., 2005), I asked how Armadillo localizes upon the depletion of Rab11, Rab7 and Snx16.

To answer this question, I first tested the localization of Armadillo in *Rab11* cell clones. I observed that Armadillo could not localize to the plasma membrane but instead accumulated in the cytoplasm in Rab11-depleted cells (Figure 20a). This suggests that neither DE-cadherin nor Armadillo can be transported to the plasma membrane in the absence of Rab11.

I further asked how Armadillo localizes in *Snx16* cell clones. Surprisingly, despite the cytoplasmic DE-cadherin aggregation in *Snx16* mutants, I observed a low number of Armadillo cytoplasmic aggregates (Figure 20b). This suggests that the Armadillo transport is not impaired upon Snx16 depletion. Since DE-cadherin and Armadillo form the complex for the delivery to the plasma membrane. I speculated that in Snx16-depleted cells, DE-cadherin/Armadillo complex dissociates, resulting only in DE-cadherin cytoplasmic accumulation, while Armadillo is still delivered to the plasma membrane. This hypothesis suggests that Snx16 might be required for the stabilization of the DE-cadherin/Armadillo complex.

I finally tested the localization of Armadillo in *Rab7* cell clones. Comparable to Snx16-depleted cells, very few Armadillo aggregates were detected in cells lacking Rab7 (Figure 20c). This finding suggests that DE-cadherin/Armadillo complex dissociates also in the absence of the Rab7. However, since I speculated that Rab7 is required for Snx16 recruitment (see 4.3.3), I propose that the dissociation of DE-cadherin/Armadillo complex in Rab7-depleted cells is due to the failure of Snx16 recruitment. This result further confirms my hypothesis that Snx16 plays a role in DE-cadherin/Armadillo complex stabilization.

In summary, my data show that DE-cadherin and Armadillo both accumulate in *Rab11* cell clones. This suggests that the Rab11 is required for the delivery of the DE-cadherin/Armadillo complex to the plasma membrane. Further, upon Snx16 and Rab7 depletion, only DE-cadherin accumulates in the cytoplasm, whereas the localization of Armadillo remains undisturbed. I propose that this could be due to the dissociation of the DE-cadherin/Armadillo complex in the absence of Snx16. This suggests that Snx16 might be required for the stabilization of the DE-cadherin/Armadillo complex. The dissociation of the DE-cadherin/Armadillo complex in *Rab7* mutants, on the other hand, is caused by the lack of the Snx16's recruitment.

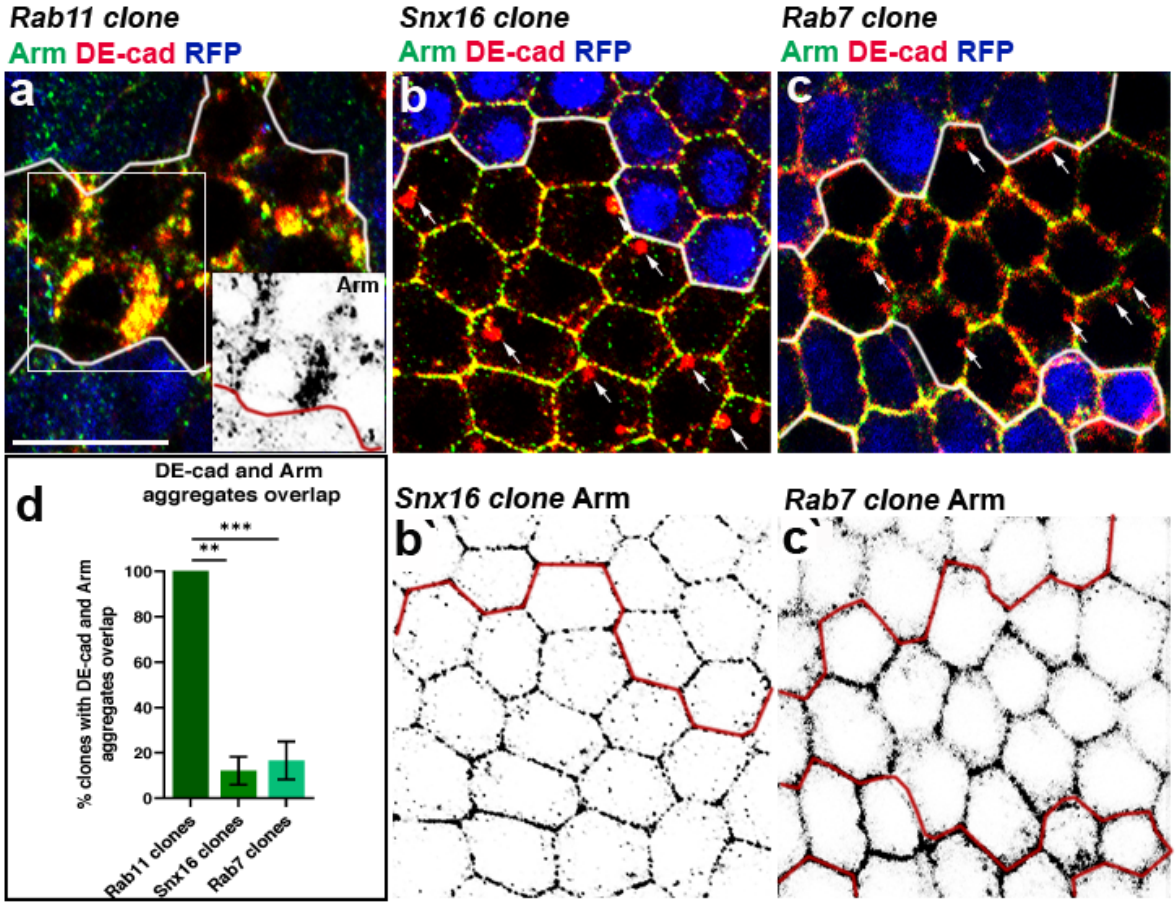

Figure 20. DE-cadherin/Armadillo complex dissociates in *Rab7* and *Snx16* clone cells. (a-c) Confocal optical sections perpendicular to the apical-basal axis of the follicular epithelium. The scale bar represents 10µm. Clone cells are indicated by the absence of RFP (blue). The clone border is highlighted by the white line in pictures showing merged channels and by the red line in pictures showing individual channels. (a) *Rab11* clone stained for Armadillo (green) and DE-cadherin (red). The inset in the lower right corner shows the single Armadillo channel of the marked area. (b) *Snx16* clone stained for Armadillo (green) and DE-cadherin (red). Only DE-cadherin, not Armadillo, aggregates can be observed in the cytoplasm (white arrows). (b`) shows the individual Armadillo channel. (c) *Rab7* clone stained for Armadillo (green) and DE-cadherin (red). Only DE-cadherin, not Armadillo, aggregates can be observed in the cytoplasm (white arrows). (d) Quantification of the colocalization of DE-cadherin and

Armadillo aggregates in *Rab11*, *Snx16* and *Rab7* clones. Representative images are shown in (a), (b) and (c). Data are shown as mean ± SEM. A two-tailed t-test (equal variance, α=0.05) was performed, and p values are presented as **p < 0.01 and ***p < 0.001. The quantification was performed with 23 follicles (n=32 cell clones) for *Rab11* clones, 17 follicles (n=18 cell clones) for *Snx16* clones and 11 follicles (n=12 cell clones) for *Rab7* clones.

4.3.5 DE-cadherin exit from endosomes requires direct association with Armadillo

My data suggest that Snx16 is required for the stabilization of the DE-cadherin/Armadillo complex (Figure 20). This prompted me to further investigate the requirement for the DE-cadherin/Armadillo complex in DE-cadherin secretion to the plasma membrane. To perform this, I used the UAS-DE-cadherin-$\Delta\beta$-catenin construct, which expresses the DE-cadherin mutant unable to bind Armadillo (Pacquelet et al., 2003). I first expressed UAS-DE-cadherin-$\Delta\beta$-catenin in *Drosophila* epithelia and analyzed DE-cadherin localization. I detected cytoplasmic DE-cadherin aggregates in *Drosophila* follicles expressing UAS-DE-cadherin-$\Delta\beta$-catenin construct (Figure 21a). This indicates that transport of DE-cadherin mutant that is unable to bind Armadillo is hampered. Interestingly, I still detected DE-cadherin at the plasma membrane, suggesting that DE-cadherin can reach the plasma membrane without being directly bound to Armadillo. I further analyzed Armadillo localization in UAS-DE-cadherin-$\Delta\beta$-catenin expressing follicles. My finding revealed that Armadillo also aggregates in the cytoplasm upon the expression of the UAS-DE-cadherin-$\Delta\beta$-catenin construct (Figure 21a). Curiously, Armadillo and DE-cadherin aggregates completely colocalized (arrows in Figure 21a). This implies that DE-cadherin and Armadillo might still be transported together towards the plasma membrane even when not directly associated.

I further investigated the spatial relation between the DE-cadherin aggregates in UAS-DE-cadherin-$\Delta\beta$-catenin expressing follicles and different cell markers. My data showed that DE-cadherin aggregates could occasionally be detected in the ER and Golgi as I observed that DE-cadherin aggregates sometimes colocalized with ER marker KDEL and *cis*-Golgi marker GM130 (Figure 21b). This implies that DE-cadherin transport from the ER and Golgi UAS-DE-cadherin-$\Delta\beta$-catenin expressing follicles may be impeded, but can still occur.

I next asked how DE-cadherin aggregates detected in UAS-DE-cadherin-$\Delta\beta$-catenin expressing follicles localize in regard to the Rab5 and Rab7 endosomal markers. I observed the colocalization between DE-cadherin aggregates and Rab5 and Rab7 (Figures 21c and 21d). This suggests that DE-cadherin can reach the endosomal system without physical interaction with the Armadillo. My finding also further implies that the DE-cadherin/Armadillo

complex might be required for the DE-cadherin export from the endosomal compartments, since the DE-cadherin mutant that is unable to bind Armadillo accumulates within endosomes. In summary, my data show that the DE-cadherin can be secreted to the plasma membrane independently of DE-cadherin/Armadillo complex. Nevertheless, the transport route might still be hampered, since DE-cadherin mutant, which cannot bind Armadillo, aggregates in the cytoplasm. Interestingly, Armadillo also aggregates in UAS-DE-cadherin-Δβ-catenin expressing follicles, and these Armadillo aggregates colocalize with DE-cadherin. This suggests that the DE-cadherin and Armadillo might still be transported together even when they are not directly associated. Finally, the DE-cadherin/Armadillo complex might be essential for the export of DE-cadherin from endosomes, as the DE-cadherin mutant protein that cannot bind Armadillo aggregates within endosomes.

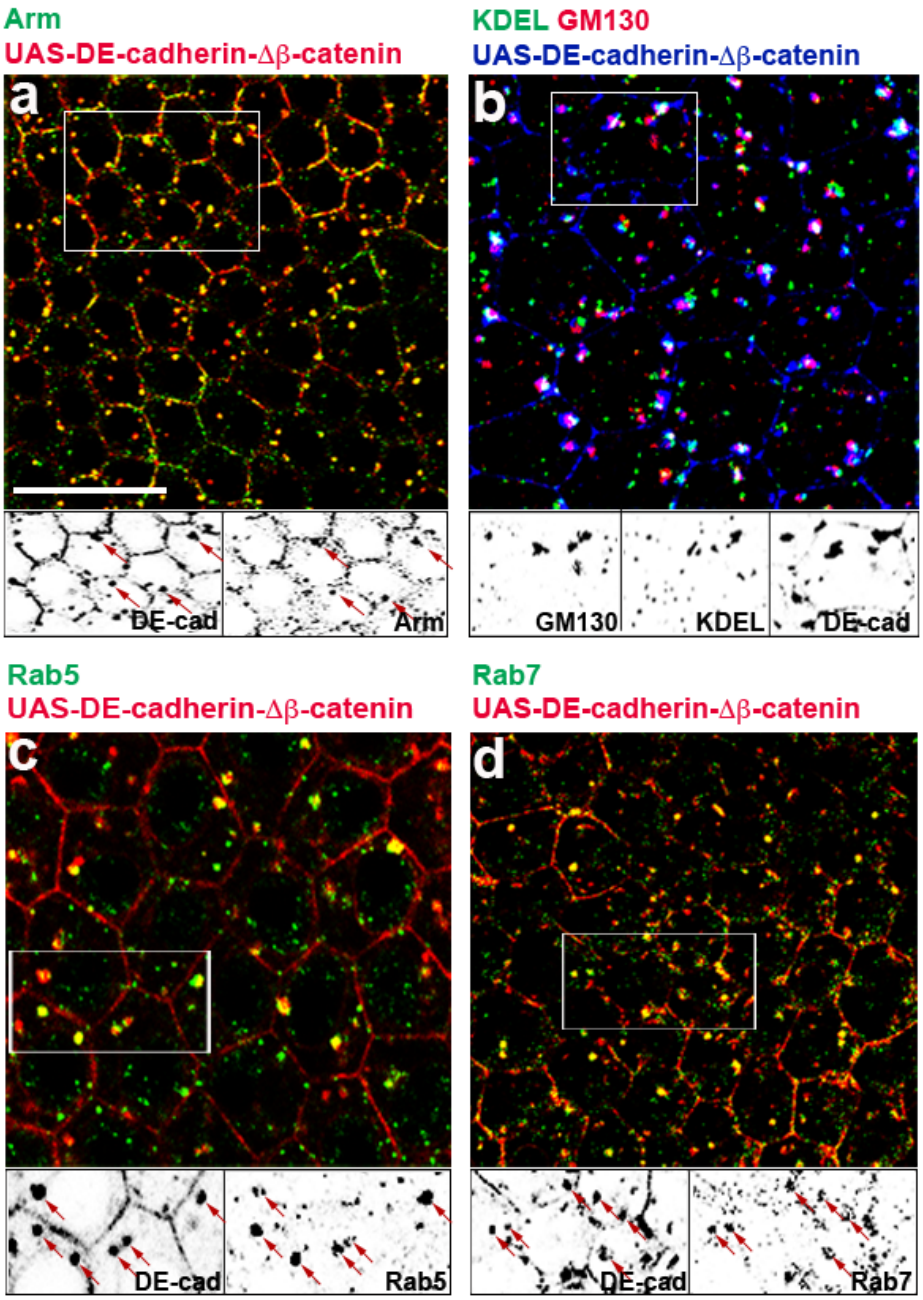

Figure 21. DE-cadherin exit from endosomes requires direct association with Armadillo. (a-d) Confocal optical sections perpendicular to the apical-basal axis of the follicular epithelium. The scale bar represents 10μm. All epithelia shown express UAS-DE-cadherin-Δβ-catenin, the DE-cadherin mutant protein unable to bind Armadillo. Insets below show individual channels of marked areas. DE-cadherin colocalizes with Armadillo (red arrows in (a)), Rab5 (red arrows in (c)) and Rab7 (red arrows in (d)). (a) Epithelia stained for Armadillo (green) and DE-cadherin (red). (b) Epithelia stained for ER marker KDEL (green), Golgi marker GM130 (red) and DE-cadherin (blue). (c) Epithelia stained for Rab5 (green) and DE-cadherin (red). (d) Epithelia stained for Rab7 (green) and DE-cadherin (red).

4.4 The exocyst subunit Sec15 is recruited by Rab11 for DE-cadherin transport

Past studies demonstrated that the exocyst complex is involved in E-cadherin trafficking in both *Drosophila* and cultured cells (Langevin et al., 2005; Xiong et al., 2012; Yeaman et al., 2004). The exocyst complex is a conserved octameric structure that plays a critical role in the tethering of proteins to the plasma membrane (B. He & Guo, 2009). However, mechanisms behind the exocyst recruitment for DE-cadherin transport and for the DE-cadherin secretion to the plasma membrane remain unknown.

4.4.1 The UAS-Sec15-mCherry construct represents functional exocyst subunit Sec15

Previous studies demonstrated that the critical function of Rab11 is the recruitment of its effector Sec15, the exocyst subunit (Prigent et al., 2003; Zhang et al., 2004). Furthermore, a study in *Drosophila* showed that the exocyst components Sec5, Sec6 and Sec15 regulate the DE-cadherin delivery to the plasma membrane (Langevin et al., 2005). I aimed to further investigate the role of the exocyst subunit Sec15 in DE-cadherin transport. For this purpse, I used the UAS-Sec15-mCherry construct, in which the exocyst subunit Sec15 is tagged with mCherry (Michel et al., 2011).

The expression of UAS-Sec15-Cherry in *Drosophila* follicles led to the formation of prominent apical Sec15 compartments (Figure 22a). I analyzed localization of DE-cadherin in regard to Sec15 compartments. Notably, I detected that DE-cadherin localizes within Sec15 compartments (arrows in Figure 22a). This suggests that DE-cadherin interacts with Sec15 during its transport. To test if the UAS-Sec15-mCherry construct is functional, I expressed UAS-Sec15-Cherry in *Drosophila* ovaries in *Sec15* mutants. I generated *Sec15* mutants by inducing Sec15 RNA interference (RNAi). RNA interference (RNAi) is a tool that results in the

specific suppression of gene expression. Using the Gal4/UAS system, the expression of short inverted repeats that bind to each other and form a hairpin RNA (hpRNA) is induced. The hpRNA is complementary to the gene of interest. The enzyme Dicer then cleaves hpRNA into short double-stranded RNA (siRNA) fragments. These siRNAs are then incorporated into the RNA-induced silencing complex (RISC) for the recognition of the complementary mRNA sequence. This leads to the degradation of the mRNA and the gene of interest is silenced (Heigwer et al., 2018).

I first analyzed the DE-cadherin localization in *Drosophila* follicles expressing *Sec15 RNAi*. I observed that DE-cadherin was barely detectable at the plasma membrane, but formed aggregates in the cytoplasm instead. As a result, the cell shape was irregular in the absence of Sec15 (Figure 22b). This observation is in line with the previously published study, where it was shown that DE-cadherin accumulates in the cytoplasm upon Sec15 depletion in *Drosophila* ovaries (Langevin et al., 2005). I then expressed the UAS-Sec15-Cherry in *Sec15 RNAi* to analyze if it can rescue the cytoplasmic DE-cadherin aggregation. I observed that the expression Sec15-Cherry construct indeed resulted in the rescue of irregular cell shape and DE-cadherin cytoplasmic aggregation (92%, n=13 follicles) (Figure 22c). This suggests that the mCherry tag in UAS-Sec15-Cherry construct doesn't impair Sec15 function and that UAS-Sec15-Cherry construct represents functional Sec15 exocyst subunit.

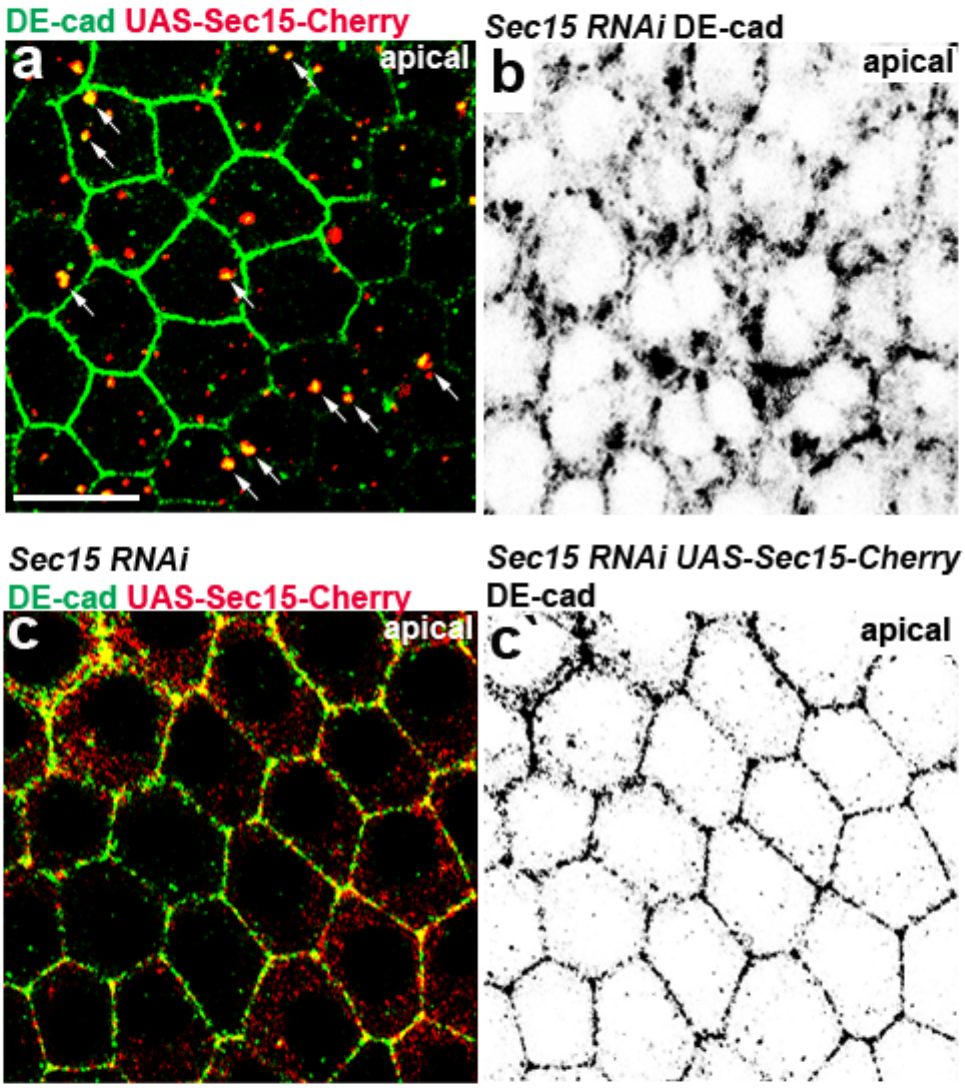

Figure 22. UAS-Sec15-Cherry represents functional exocyst subunit Sec15. (a-c) Apical confocal optical sections perpendicular to the apical-basal axis of the follicular epithelium. The scale bar represents 10µm. (a) Expression of the UAS-Sec15mCherry construct results in the formation of Sec15 compartments (red) to which DE-cadherin (green) localizes (white arrows). (b) Epithelia expressing *Sec15 RNAi* and stained for DE-cadherin. (c) Epithelia expressing UAS-Sec15-mCherry (red) in *Sec15 RNAi* results and stained for DE-cadherin (green). (c`) shows the individual DE-cadherin channel.

I next asked if the lateral protein Fas2 also localizes to the Sec15 compartment. To answer this question, I co-expressed Fas2-GFP and UAS-Sec15-Cherry constructs. My finding showed that Fas2 could not be detected within the cytoplasmic Sec15 compartments (Figure 23a). This suggests that Sec15 is not involved in Fas2 transport towards the plasma membrane. I further analyzed if the absence of Sec15 affects the localization of Fas2. To test this, I expressed Fas2-GFP in *Sec15 RNAi* follicles. Fas2 localized properly to the lateral membrane, suggesting that the downregulation of Sec15 doesn't influence the Fas2 transport (Figure 23b). Overall, this suggests that Sec15 plays a role in the transport of apicolateral

protein, such as DE-cadherin, but is not involved in the transport of proteins localizing to the lateral membrane, such as Fas2. This finding is in line with the previous study, which also demonstrated that upon the depletion of another exocyst unit, Sec5, the localization of the lateral protein Fas3 remains unaffected (Langevin et al., 2005).

In summary, my findings show that the expression of the UAS-Sec15-Cherry construct results in the formation of Sec15 compartments. Within these Sec15 compartments, DE-cadherin is localized. The functionality of the Sec15-Cherry construct was confirmed by the expression of UAS-Sec15-Cherry in *Sec15 RNAi* follicles, which rescued cytoplasmic DE-cadherin aggregation. Further, the localization of the lateral protein Fas2 is not observed within the Sec15 compartment. Fas2 localization was also undisturbed in *Sec15 RNAi* expressing follicles. This suggests that the Sec15, which is a part of the exocyst complex, is involved in the transport of apicolateral protein DE-cadherin, but not in the transport of the lateral protein Fas2.

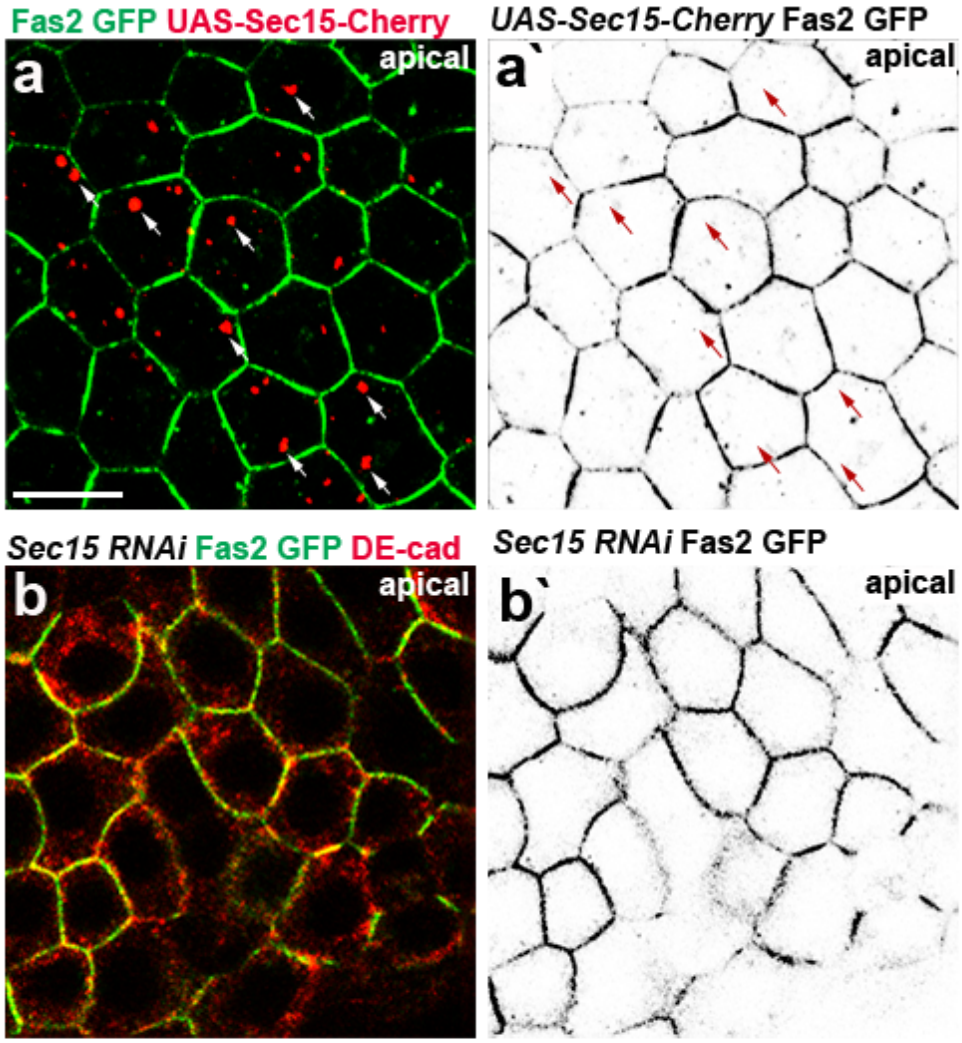

Figure 23. Exocyst subunit Sec15 is not involved in the transport of Fas2. (a-b) Apical confocal optical sections perpendicular to the apical-basal axis of the follicular epithelium. The scale bar represents 10µm. (a) The expression of UAS-Sec15-mCherry (red) and Fas2 GFP (green). (a`) shows the individual Fas2 channel. Fas2 doesn't localize to Sec15 compartments (white arrows in (a) and red arrows in (a`)). (b) Epithelia expressing Sec15 RNAi and Fas2 GFP (green) and stained for DE-cadherin (red). (b`) shows the single Fas2 GFP channel.

4.4.2 The glycine triplet within the DE-cadherin juxtamembrane domain is required for the localization within Sec15 compartments

My data show that DE-cadherin localizes to apical Sec15 compartments (Figure 22a). Since my data previously demonstrated that the DE-cadherin cytoplasmic domain is required for the DE-cadherin delivery to apical endosomes (Figure 12c), I aimed to investigate if the same domain is required for DE-cadherin localization to the Sec15 compartment. To answer this question, I co-expressed UAS-Sec15-Cherry and UAS-DE-cadhΔCyt/α-cat, a mutant lacking the cytoplasmic domain, to see if the DE-cadherin can still localize within Sec15 compartments. My data showed no detectable DE-cadherin mutant protein within Sec15 compartments (compare Figures 24a and 24b). This suggests that the cytoplasmic domain is required for the DE-cadherin localization within the Sec15 compartment.

Previous studies demonstrated that the domain within the DE-cadherin cytoplasmic tail, termed the juxtamembrane domain, is implicated in the regulation of DE-cadherin turnover and degradation (Hartsock & Nelson, 2012; Miyashita & Ozawa, 2007). I next asked if the juxtamembrane domain is required for DE-cadherin localization within Sec15 compartments. To answer this, I co-expressed UAS-Sec15-Cherry and UAS-DE-cadherin-ΔJM construct, a DE-cadherin mutant lacking the 113bp within the juxtamembrane domain (Pacquelet & Rørth, 2005). I observed that the DE-cadherin mutant without the complete juxtamembrane domain didn't localize within Sec15 compartments (compare Figures 24a and 24c). This implies that the juxtamembrane domain is essential for DE-cadherin interaction with Sec15 compartments.

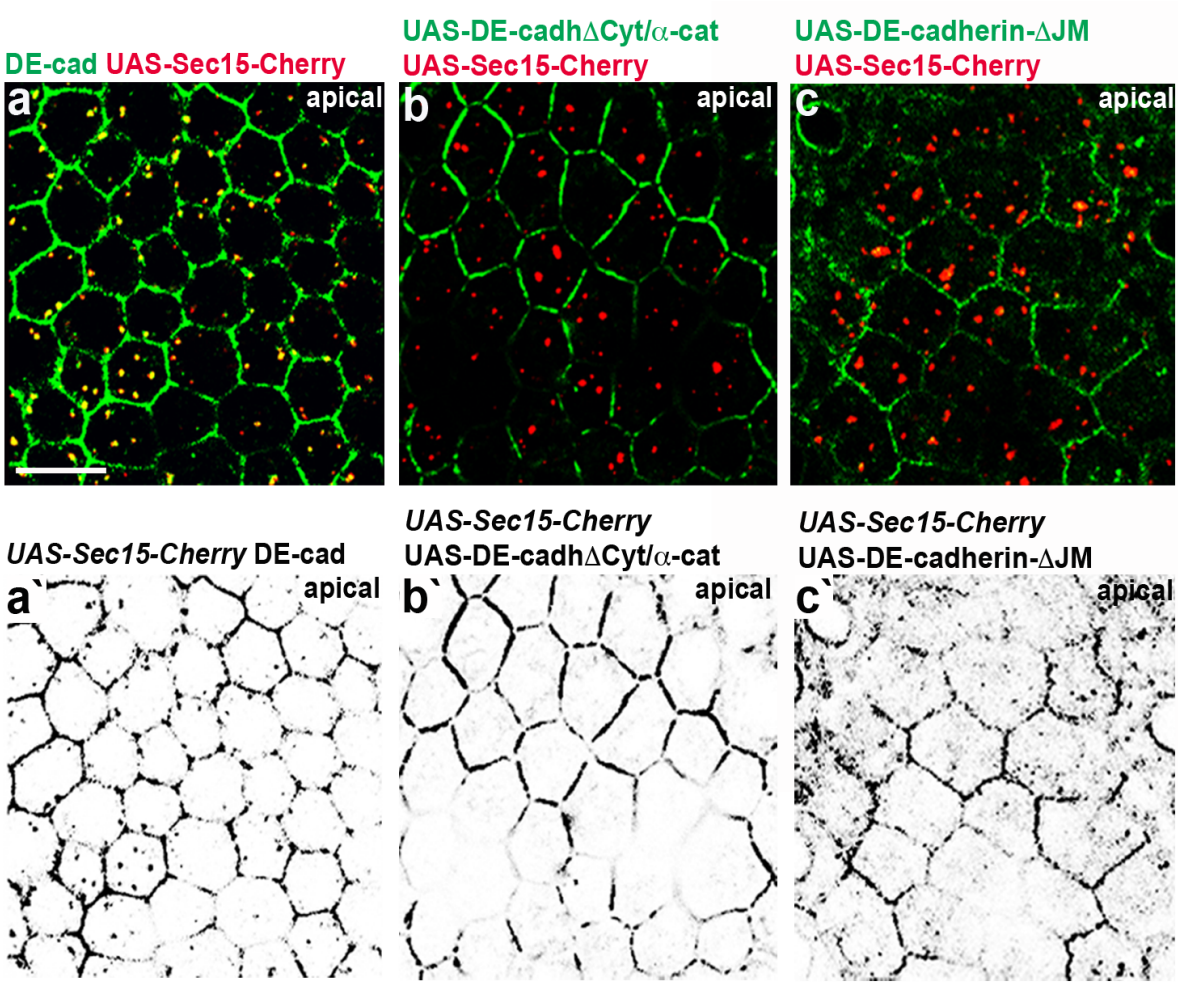

Figure 24. DE-cadherin juxtamembrane domain is required for the localization within Sec15 compartments. (a-c) Apical confocal optical sections perpendicular to the apical-basal axis of the follicular epithelium. The scale bar represents 10µm. (a`-c`) show individual DE-cadherin channels. (a) Epithelia expressing UAS-Sec15-Cherry (red) and stained with DE-cadherin (green). (b) Epithelia co-expressing UAS-DE-cadhΔCyt/α-cat (green), the DE-cadherin mutant protein lacking the cytoplasmic domain, and UAS-Sec15-mCherry (red). (c) Epithelia co-expressing UAS-DE-cadherin-ΔJM (green), the DE-cadherin mutant protein without the complete juxtamembrane domain, and UAS-Sec15-mCherry (red).

After uncovering that the juxtamembrane domain of DE-cadherin is required for DE-cadherin localization within the Sec15 compartment, I asked which part of the juxtamembrane domain could be essential. To answer this question, I used the DE-Cadherin-AAA mutant construct, which yields a mutant protein that has the glycine triplet on the positions 1376-1378 within the juxtamembrane domain replaced by three alanines (Pacquelet et al., 2003). I co-expressed UAS-DE-Cadherin-AAA and UAS-Sec15 Cherry constructs in *Drosophila* follicles and analyzed if the glycine triplet within the juxtamembrane domain is critical for DE-cadherin localization within Sec15 compartments. My results revealed that the DE-cadherin-AAA mutant didn't localize to the Sec15 compartment (Figure 25a). This suggests that the glycine triplet

within the DE-cadherin juxtamembrane domain is required for the localization of DE-cadherin within the Sec15 compartment.

Since my data show that the glycine triplet is essential for DE-cadherin localization within Sec15 compartments, I was curious to study what impact these three glycines have on DE-cadherin localization to endosomes. To answer this question, I co-expressed UAS-DE-Cadherin-AAA and UAS-YFP-Rab11 constructs and analyzed DE-cadherin localization. I used the UAS-YFP-Rab11 construct as a marker for endosomal compartments, as the expression of UAS-YFP-Rab11 in *Drosophila* follicular epithelium results in the formation of prominent apical endosomal structures that can be easily visualized (Figure 8a). My data showed that the DE-cadherin mutant was able to localize to apical YFP-Rab11 endosomal structure (Figure 25b). This finding implies that glycine residues within the juxtamembrane domain are not essential for DE-cadherin delivery to the endosomes.

In summary, my data show that the juxtamembrane domain of the DE-cadherin cytoplasmic tail is required for the DE-cadherin localization within Sec15 compartments. More specifically, the glycine triplet within the DE-cadherin juxtamembrane domain is critical for DE-cadherin localization within Sec15 compartments. Curiously, these glycine residues within the juxtamembrane domain are not required for DE-cadherin localization to the apical endosomal compartment, as DE-cadherin-AAA mutant is still detected within YFP-Rab11 endosomal compartments.

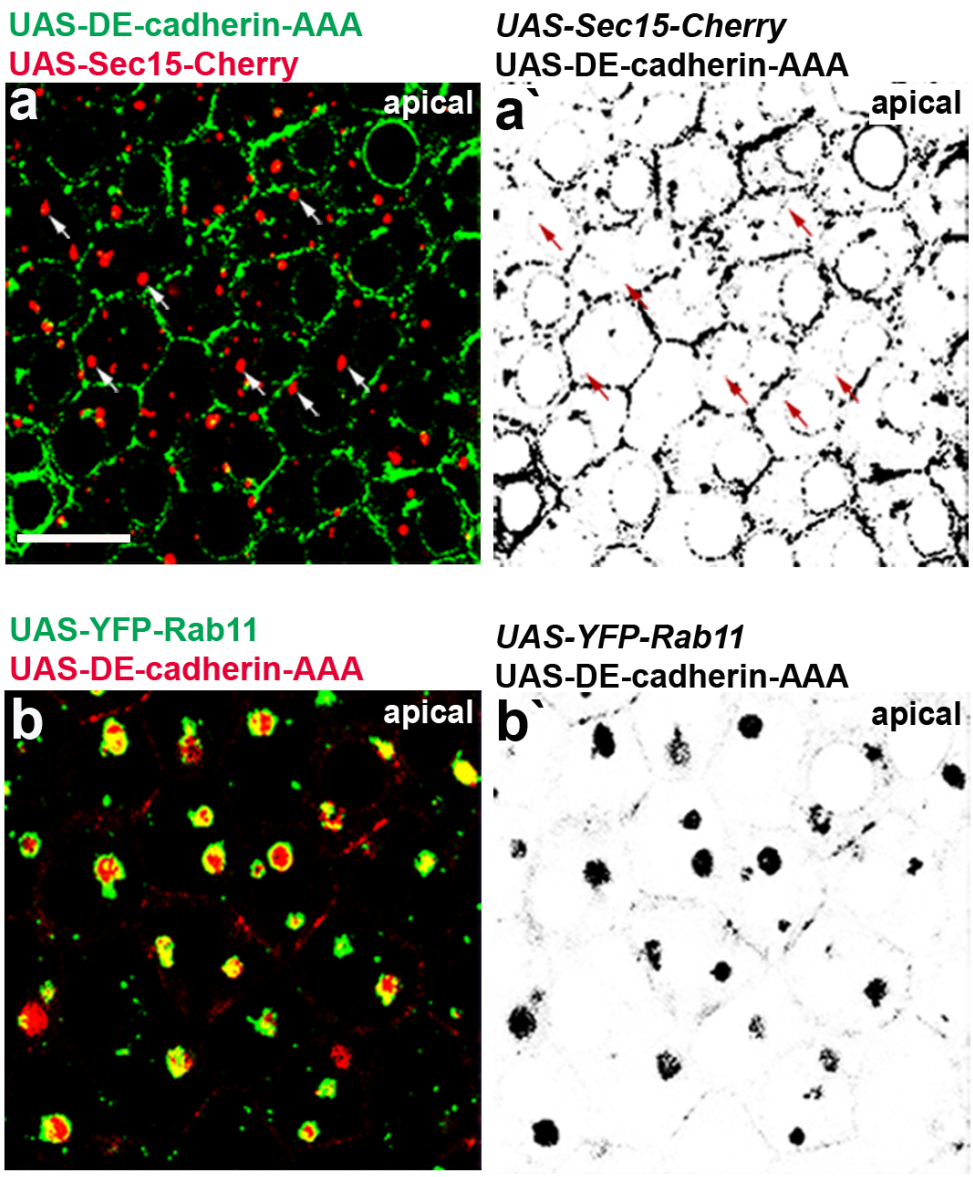

Figure 25. Glycine triplet in the DE-cadherin juxtamembrane domain is required for DE-cadherin localization within Sec15 compartments, but not within YFP-Rab11 compartments. (a-b) Apical confocal optical sections perpendicular to the apical-basal axis of the follicular epithelium. The scale bar represents 10μm. (a) Epithelia co-expressing UAS-DE-cadherin-AAA (green), the DE-cadherin protein with mutated glycine triplet within the juxtamembrane domain, and UAS-Sec15-mCherry (red). (a`) shows the individual DE-cadherin channel. DE-cadherin is not detected within Sec15 compartments (white arrows in (a) and red arrows in (a``)). (c) Epithelia co-expressing UAS-YFP-Rab11 (green) and UAS-DE-cadherin-AAA (red). (b`) shows the individual DE-cadherin channel.

4.4.3 Rab11 recruits the exocyst subunit Sec15 for DE-cadherin transport

Previous research has demonstrated that the exocyst subunit Sec15 is an effector of Rab11 protein (Prigent et al., 2003; Zhang et al., 2004). My data, as well as previous findings, demonstrated that Rab11 plays a critical role in DE-cadherin transport (see 4.1) (Stow & Lock, 2005; Woichansky et al., 2016; Jiang Xu et al., 2011). I thus asked if Sec15 interacts with Rab11 in DE-cadherin transport. To answer this question, I co-expressed UAS-Sec15-Cherry and UAS-HA-Rab11 constructs in *Drosophila* follicular epithelium. The co-overexpression of Sec15-Cherry and HA-Rab11 resulted in the formation of prominent Sec15-Cherry/HA-Rab11 compartments (Figure 26a). These Sec15/Rab11 compartments were enlarged when compared to Sec15-Cherry and HA-Rab11 compartments individually (Figure 26c). In addition, I also observed that DE-cadherin accumulated within these Sec15-Cherry/HA-Rab11 compartments. This suggests that simultaneous high levels of Sec15-Cherry and HA-Rab11 interfere with DE-cadherin transport. Additionally, this also implies possible interaction between Sec15 and Rab11 in DE-cadherin trafficking.

I further aimed to analyze the localization of the Sec15-Cherry/HA-Rab11 compartments in relation to the apical endosomal system represented by YFP-Rab11 compartments. To perform this, I co-expressed UAS-HA-Rab11, UAS-Sec15-Cherry and UAS-YFP-Rab11 constructs in *Drosophila* follicular epithelium. I observed no significant differences in Sec15/Rab11 compartments in presence of YFP-Rab11 compartments when compared to the formation of Sec15-Cherry/HA-Rab11 compartments alone (Figure 26b). Curiously, these enlarged Sec15-Cherry/HA-Rab11 compartments were localized in the close vicinity of the YFP-Rab11 compartments (arrows in Figure 26b). This result shows that Sec15-Cherry/HA-Rab11 compartments and YFP-Rab11 compartments are separated spatially. Further, this data implies that the functional HA-Rab11 protein might recruit Sec15-Cherry protein, but impaired YFP-Rab11 cannot do the same, and that Sec15-Cherry/HA-Rab11 compartment is able to transport DE-cadherin. This is consistent with the previously published data demonstrating that Sec15 is an effector of the Rab11 (Langevin et al., 2005; Zhang et al., 2004).

In summary, my data show that the co-expression of UAS-Sec15-Cherry and UAS-HA-Rab11 results in enlarged Sec15/Rab11 compartments within which DE-cadherin accumulates. These Sec15/Rab11 compartments might represent the functional transport of DE-cadherin from the apical endosomal system. This suggests that Rab11 recruits the exocyst subunit Sec15 for DE-cadherin transport from endosomes to the plasma membrane.

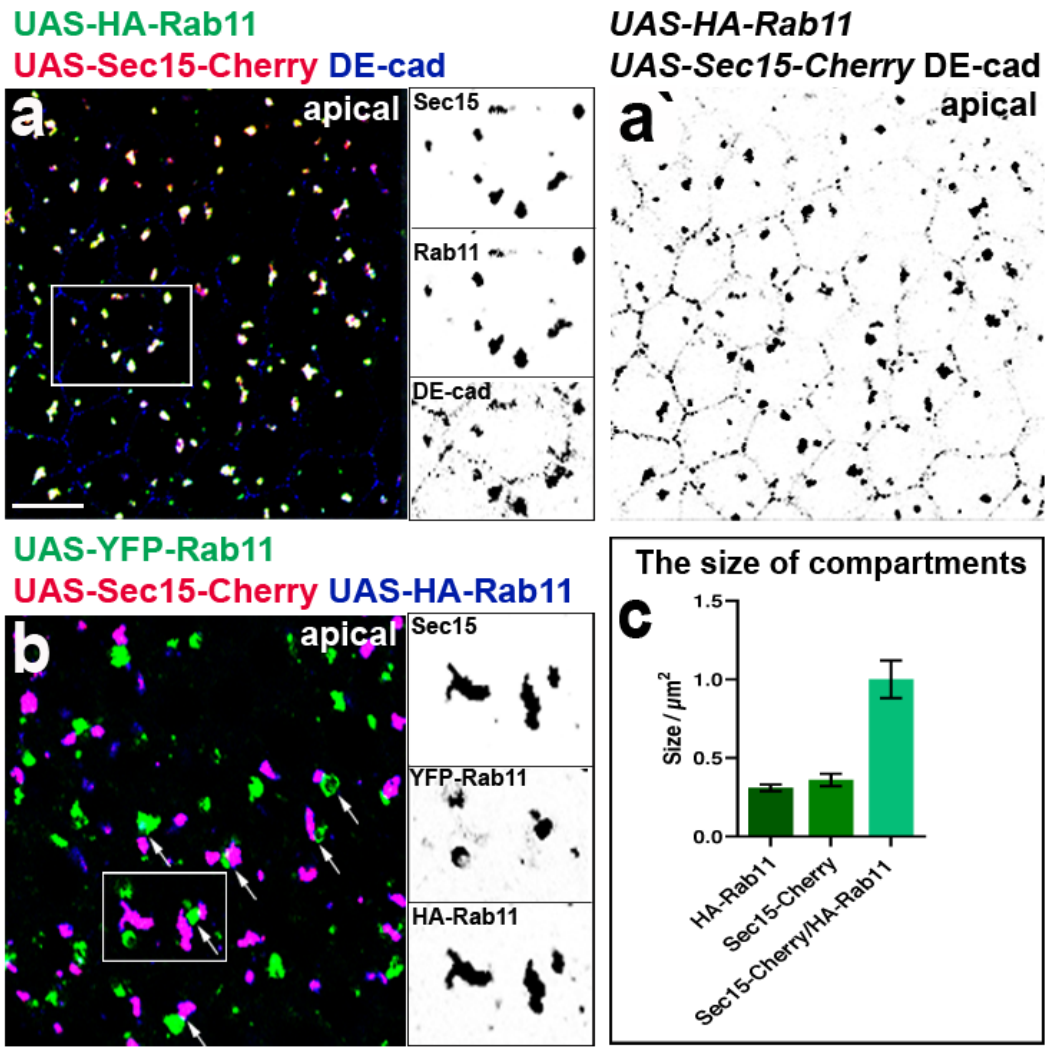

Figure 26. HA-Rab11 recruits Sec15-Cherry in DE-cadherin transport. (a) and (b) Apical confocal optical sections perpendicular to the apical-basal axis of the follicular epithelium. The scale bar represents 10µm. (a) Epithelia co-expressing UAS-HA-Rab11 (green) and UAS-Sec15-mCherry (red) and stained for DE-cadherin (blue). Insets on the right show the individual Sec15, HA-Rab11 and DE-cadherin channels of the marked area. (a`) shows individual DE-cadherin channel. (b) Epithelia co-expressing UAS-YFP-Rab11 (green), UAS-Sec15-mCherry (red) and UAS-HA-Rab11 (blue). Insets on the right show the individual Sec15, YFP-Rab11 and HA-Rab11 channels of the marked area. Sec15-Cherry/HA-Rab11 compartments localize in the vicinity of YFP-Rab11 compartments (white arrows). (c) Quantification of the size of HA-Rab11, Sec15-Cherry and Sec15-Cherry/HA-Rab11 compartments. Representative images are shown in (a), Figure 22a and Figure 7c. Data are shown as mean ± SEM. The quantification was performed with 5 follicles (n=153 cells) for HA-Rab11, and 5 follicles (n=117 cells) for both Sec15-Cherry and Sec15-Cherry/HA-Rab11 compartments.

4.4.4 Snx16 is spatially separated from Sec15/Rab11 compartments

My data show that the co-expression of UAS-Sec15-Cherry and UAS-HA-Rab11 constructs results in the formation of enlarged Sec15-Cherry/HA-Rab11 compartments that accumulate DE-cadherin (Figure 26a). In addition, my data also show that these Sec15-Cherry/HA-Rab11 compartments localize in the vicinity of apical endosomal compartments (Figure 26b). I further asked how do Sec15-Cherry/HA-Rab11 compartments localize in relation to Snx16, another important factor in DE-cadherin transport that I investigated.

To answer this question, I co-expressed UAS-Sec15-Cherry, UAS-HA-Rab11 and UAS-Snx16-SNAP constructs in *Drosophila* follicular epithelium. I observed no significant differences in the formation of Sec15-Cherry/HA-Rab11 compartments in presence of Snx16 when compared to the formation of Sec15-Cherry/HA-Rab11 compartments alone (Figure 27a). In the proximity to Sec15-Cherry/HA-Rab11 compartments, I detected Snx16 (arrows in Figure 27a). This result suggests that there might be a spatial separation between Snx16 and Sec15-Cherry/HA-Rab11 compartments. I speculate that this might be due to Rab11 recruitment of the Sec15 subunit after Rab11 dissociates from Snx16.

I also analyzed the DE-cadherin localization in follicles overexpressing Sec15-Cherry, HA-Rab11 and Snx16-SNAP. I observed that DE-cadherin localizes mostly within Sec15-Cherry/HA-Rab11 compartments and only occasionally colocalizes with Snx16 (Figure 27b). I propose that this is because Sec15-Cherry/HA-Rab11 compartments form a complex with DE-cadherin for the subsequent transport towards the plasma membrane. Snx16, on the other hand, might dissociate from DE-cadherin as soon as it delivers DE-cadherin to the Rab11 compartment.

In summary, my data showed that Snx16 localizes in close proximity to Sec15-Cherry/HA-Rab11 compartments. Further, DE-cadherin was predominantly localized within the Sec15-Cherry/HA-Rab11 compartments. This overall implies that Rab11 recruitment of the Sec15 subunit might occur only after the Rab11 dissociated from the Snx16 compartment.

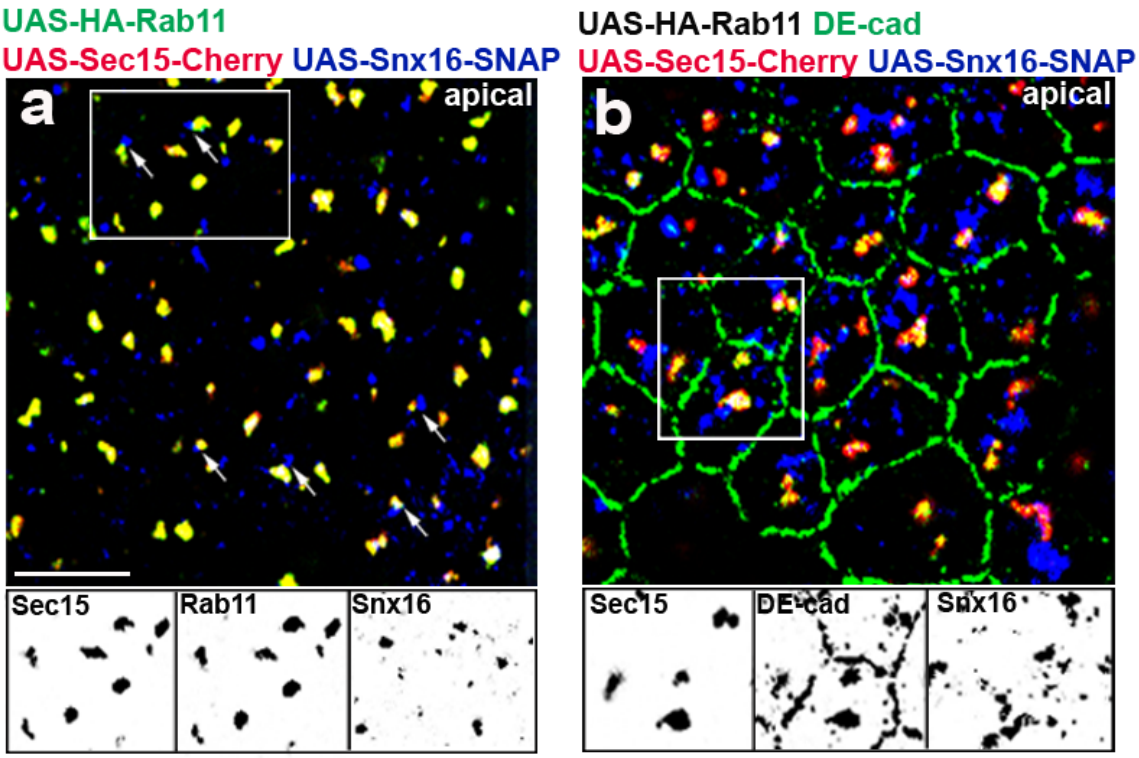

Figure 27. Snx16 localizes in the vicinity of Sec15-Cherry/HA-Rab11 compartments. (a-b) Apical confocal optical sections perpendicular to the apical-basal axis of the follicular epithelium. The scale bar represents 10µm. Insets below show individual channels of the marked area. (a) Epithelia co-expressing UAS-HA-Rab11 (green), UAS-Sec15-mCherry (red) and UAS-Snx16-SNAP (blue). Snx16 localizes in the vicinity of Sec15-Cherry/HA-Rab11 compartments (white arrows). (b) Epithelia co-expressing UAS-HA-Rab11 (not stained), UAS-Sec15-mCherry (red) and UAS-Snx16-SNAP (blue) stained for DE-cadherin (green).

4.5 MyoV is a motor that transports DE-cadherin along the actin filaments in the complex with Sec15 and Rab11

My laboratory has previously suggested the existence of two pathways that deliver DE-cadherin to the plasma membrane: 'apicolateral exocytosis', which transports DE-cadherin to the zonula adherens, and 'lateral exocytosis' which delivers DE-cadherin to the lateral membrane for the formation of punctate adherence junctions (Woichansky et al., 2016). However, it remains unclear which particular motors and cytoskeletal tracks are employed for DE-cadherin delivery from endosomes to the plasma membrane via these different trafficking routes.

4.5.1 MyoV-FL overexpression rescues enlarged Sec15/Rab11 compartments

My data show that the expression of UAS-Sec15-mCherry and UAS-HA-Rab11 constructs results in enlarged Sec15-Cherry/HA-Rab11 compartments (Figure 26a). Studies in yeast cells identified the interaction between Sec15, Rab11 and the actin motor MyosinV (MyoV) (Jin et al., 2011). I thus aimed to investigate if there is an interaction between Sec15, Rab11 and MyoV in DE-cadherin transport in *Drosophila* ovaries. To test this hypothesis, I used the UAS-MyoV-FL-GFP construct, which expresses the full-length MyoV protein tagged with GFP. I co-expressed UAS-MyoV-FL-GFP, UAS-Sec15-mCherry and UAS-HA-Rab11 in *Drosophila* follicular epithelium.

The expression of UAS-MyoV-FL-GFP in *Drosophila* follicles resulted in variable expression in epithelial cells. This inconstancy in the expression may be due to the Gal4/UAS system, and this observation has been previously reported (Skora & Spradling, 2010). A study in *Drosophila* ovaries demonstrated that variation in the Gal4/UAS expression results from unstable epigenetic inheritance (Skora & Spradling, 2010). As a result of this variable epithelial MyoV-FL-GFP expression, I was able to compare cells with high and low MyoV-FL-GFP expression in *Drosophila* follicles co-expressing UAS-MyoV-FL-GFP, UAS-Sec15-Cherry and UAS-HA-Rab11 constructs. In Figures 28a and 28b, low MyoV-FL-GFP expression cells are marked with asterisks while high MyoV-FL-GFP expression cells lack asterisks.

Cells with low levels of MyoV-FL-GFP expression showed enlarged Sec15-Cherry/HA-Rab11 compartments. These enlarged Sec15-Cherry/HA-Rab11 compartments were similar to Sec15-Cherry/HA-Rab11 compartments detected in follicles not expressing MyoV-FL-GFP (Figure 26a). Additionally, I observed that MyoV-FL-GFP localized to these Sec15-Cherry/HA-Rab11 compartments. Curiously, cells with high levels of MyoV-FL-GFP expression showed no detectable Sec15-Cherry/HA-Rab11 compartments. This suggests that MyoV-FL-GFP is able to rescue the enlarged Sec15-Cherry/HA-Rab11 compartments. In addition, I also observed colocalization of MyoV-FL-GFP, Sec15-Cherry and HA-Rab11 at the plasma membrane in cells with high levels of MyoV-FL-GFP expression. This implies that high levels of MyoV could rescue the enlarged Sec15-Cherry/HA-Rab11 compartments by delivering them to the plasma membrane.

In parallel, I also analyzed the effect of co-expression of UAS-HA-Rab11, UAS-Sec15-mCherry and UAS-MyoV-FL-GFP on DE-cadherin localization. My data previously showed that the co-expression of UAS-Sec15-mCherry and UAS-HA-Rab11 resulted in enlarged Sec15-Cherry/HA-Rab11 compartments that also accumulated DE-cadherin (Figure 26a). I observed that the co-expression of UAS-MyoV-FL-GFP, UAS-Sec15-mCherry and UAS-HA-Rab11 resulted in different intensities of DE-cadherin aggregation. In the case of cells with high MyoV-FL-GFP expression, I observed almost no DE-cadherin aggregates (Figure 28b), as no

enlarged Sec15-Cherry/HA-Rab11 compartments were detected either. Similarly, in cells expressing low levels of MyoV-FL-GFP, I observed DE-cadherin aggregates within enlarged Sec15-Cherry/HA-Rab11 compartments (Figure 28b). This data suggests that the overexpression of MyoV-FL-GFP rescues DE-cadherin aggregation within Sec15-Cherry/HA-Rab11 compartments.

To confirm my observation, I quantified the DE-cadherin signal intensity in cytoplasmic aggregates with respect to the plasma membrane. In the first case, I quantified the DE-cadherin signal in cells expressing UAS-MyoV-FL-GFP (high levels), UAS-Sec15-Cherry and UAS-HA-Rab11, and in the latter case, the DE-cadherin signal in cells expressing only UAS-Sec15-Cherry and UAS-HA-Rab11 (see also 3.16.5 in Materials and Methods). The quantification has revealed a tenfold reduction in the number of DE-cadherin aggregates in cells expressing MyoV-FL (Figure 28c). This result further confirms that the expression of UAS-MyoV-FL-GFP suppresses the DE-cadherin aggregation which is induced by the expression of UAS-Sec15-mCherry and UAS-HA-Rab11.

Taken together, my data suggest that the UAS-MyoV-FL-GFP expression rescues the formation of enlarged Sec15-Cherry/HA-Rab11 compartments. Similarly, MyoV-FL-GFP overexpression also rescues DE-cadherin aggregates. This suggests that MyoV plays a crucial role in DE-cadherin transport towards the plasma membrane via Sec15/Rab11 compartments.

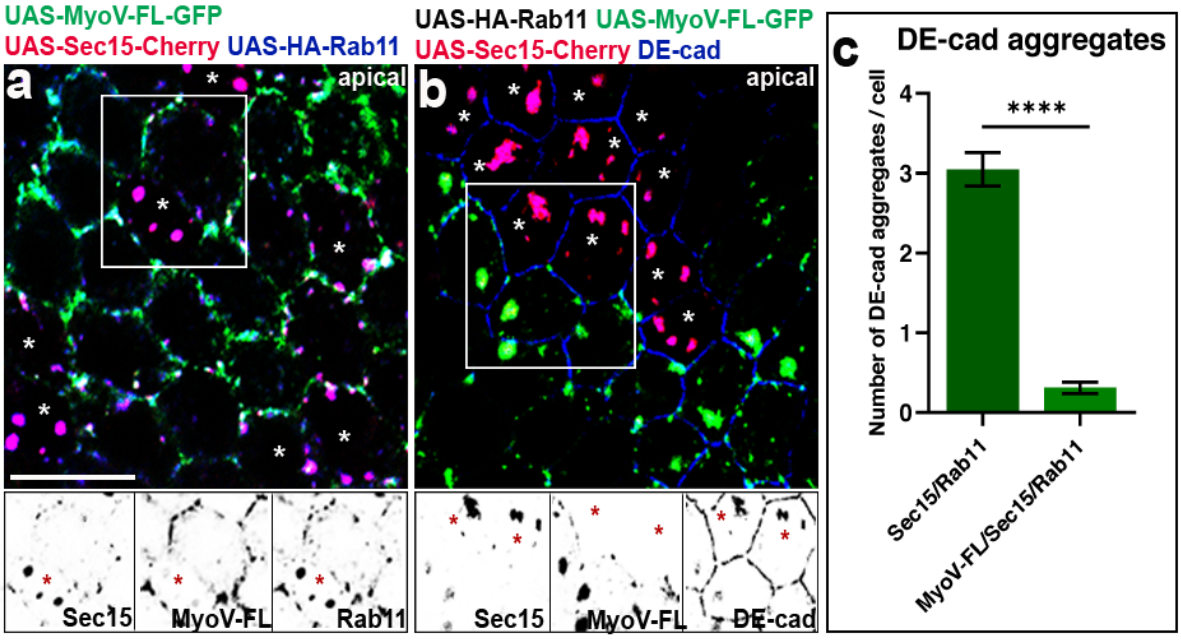

Figure 28. MyoV-FL overexpression rescues DE-cadherin aggregates within Sec15-Cherry/HA-Rab11 compartments. (a-b) Apical confocal optical sections perpendicular to the apical-basal axis of the follicular epithelium. The scale bar represents 10µm. (a) Epithelia co-expressing UAS-MyoV-FL-GFP (green), UAS-Sec15-mCherry (red) and UAS-HA-Rab11 (blue). Insets below show individual Sec15, MyoV-FL and Rab11 channels of the marked area. Asterisks mark cells with low levels of MyoV-

FL-GFP expression. (b) Epithelia co-expressing UAS-HA-Rab11 (not stained), UAS-MyoV-FL-GFP (green) and UAS-Sec15-mCherry (red) and stained for DE-cadherin (blue). Insets below show individual Sec15, MyoV-FL and DE-cadherin channels of the marked area. Asterisks mark cells with low levels of MyoV-FL-GFP expression. (c) Quantification of the number of DE-cadherin aggregates in regard to DE-cadherin membrane signal in UAS-MyoV-FL-GFP/UAS-Sec15-Cherry/UAS-HA-Rab11 expressing follicles vs. UAS-Sec15-Cherry/UAS-HA-Rab11 expressing follicles. Data are shown as mean ± SEM. Two-tailed t-test (equal variance, $\alpha = 0.05$) was performed and p values are presented as ****$p < 0.0001$. The quantification was performed with 10 follicles (n=300 cells) for the UAS-Sec15-Cherry/UAS-HA-Rab11 and with 9 follicles (n=249 cells) for UAS-MyoV-FL-GFP/UAS-Sec15-Cherry/UAS-HA-Rab11.

4.5.2 Dominant-negative form of MyoV results in DE-cadherin aggregation and zonula adherens fragmentation

My data show that MyoV-FL-GFP interacts with the Sec15-Cherry/HA-Rab11 compartment in transport of DE-cadherin to the plasma membrane (Figure 28). I further aimed to investigate how the reduced activity of the MyoV motor influences DE-cadherin transport. To answer this question, I used the dominant-negative form of the MyoV motor, UAS-MyoV-GT-GFP construct. UAS-MyoV-GT-GFP has a mutation in a globular domain, which is crucial for cargo binding (Krauss et al., 2009; X. Wu et al., 1998). I expressed the dominant-negative form of MyoV, UAS-MyoV-GT-GFP, in *Drosophila* follicles, which resulted in the formation of enlarged cytoplasmic compartments (Figure 29a). This phenotype is in line with the result of a previous study in *Drosophila* ovaries, where they also observed enlarged MyoV compartments upon expression of the dominant-negative MyoV-GT-GFP construct (Aguilar-Aragon et al., 2020). I further analyzed DE-cadherin localization in *Drosophila* follicles expressing UAS-MyoV-GT-GFP. I detected DE-cadherin aggregates within these MyoV-GT-GFP compartments, which suggests that DE-cadherin transport is hindered (Figure 29a). This finding implies that the dominant-negative form of MyoV hinders DE-cadherin transport towards the plasma membrane. Such a result suggests that the functional MyoV motor plays a critical role in DE-cadherin transport.

I next asked if the dominant-negative form of MyoV affects the formation of the zonula adherens, the plasma membrane's apical-most region that is built by DE-cadherin. To investigate this, I analyzed DE-cadherin localization at the zonula adherens in wild type epithelia, in epithelia overexpressing full-length MyoV-FL-GFP and in epithelia overexpressing dominant-negative MyoV-GT-GFP. Zonula adherens in wild type epithelia as well as in epithelia overexpressing MyoV-FL-GFP was intact, which suggests that DE-cadherin transport was not affected (Figures 29d and 29e). Zonula adherens in epithelia overexpressing the dominant-negative MyoV-GT-GFP form, on the other hand, was not continuously formed but

fragmented instead (Figure 29f). Such a phenotype could be due to the nonfunctional MyoV motor being unable to deliver DE-cadherin to the plasma membrane. This suggests that the functional MyoV motor is required for DE-cadherin transport to the plasma membrane and proper zonula adherens formation.

I further wanted to characterize the inactive MyoV-GT-GFP compartments that form in epithelia expressing the dominant-negative form of MyoV. To perform this, I co-expressed UAS-HA-Rab11 and UAS-MyoV-GT-GFP constructs in *Drosophila* epithelia. My data showed that HA-Rab11 and MyoV-GT-GFP colocalized together (Figure 29b). Additionally, I also observed that DE-cadherin accumulated within these HA-Rab11/MyoV-GT-GFP compartments. This suggests that if the MyoV motor is not active, this leads to the entrapment of DE-cadherin within the endosomal compartment represented by HA-Rab11. Next, I also analyzed the localization of additional endosomal marker Rab7 in epithelia expressing the dominant-negative form of MyoV. I observed that Rab7 also completely colocalized with MyoV-GT-GFP compartments, similar to HA-Rab11 colocalization with MyoV-GT-GFP compartments (Figure 29c). This further confirms that DE-cadherin requires the activity of the MyoV motor to leave endosomal Rab7 and Rab11 compartments.

Taken together, my data show that the expression of the dominant-negative form UAS-MyoV-GT-GFP results in enlarged MyoV compartments that accumulate DE-cadherin. Additionally, I observed fragmented zonula adherens in cells expressing UAS-MyoV-GT-GFP. This suggests that the activity of MyoV is required for efficient DE-cadherin delivery to the plasma membrane as well as for zonula adherens formation.Further, MyoV-GT compartments colocalize with Rab7 and HA-Rab11, suggesting that DE-cadherin is blocked within HA-Rab11 and Rab7 endosomes upon the reduced activity of MyoV motor. This implies that the functional MyoV motor is required for DE-cadherin transport from the apical endosomal system.

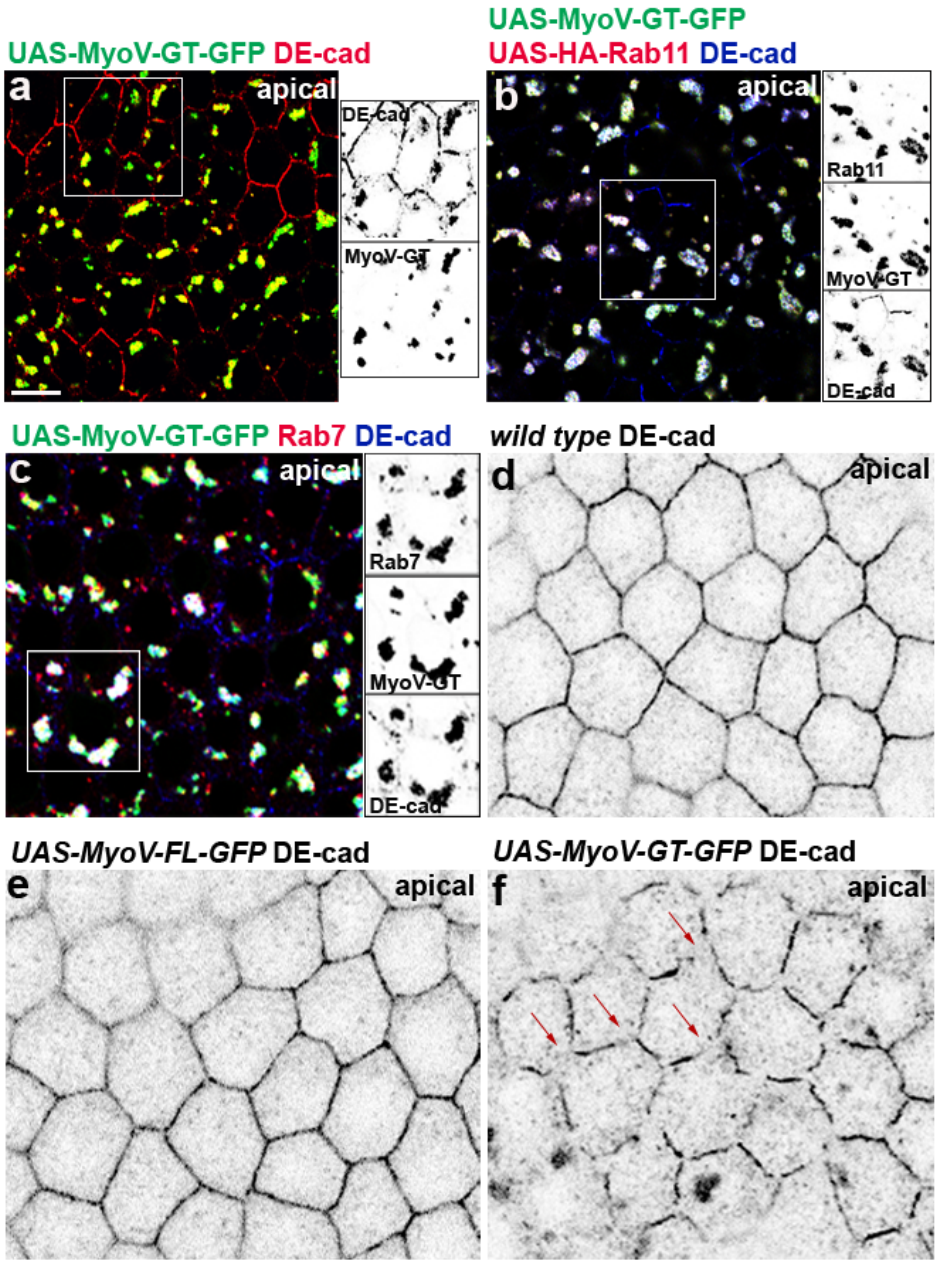

Figure 29. Expression of dominant-negative MyoV results in cytoplasmic DE-cadherin aggregation and zonula adherens fragmentation. (a-f) Apical confocal optical sections perpendicular to the apical-basal axis of the follicular epithelium. The scale bar represents 10μm. (a) Epithelia expressing UAS-MyoV-GT-GFP (green) and stained for DE-cadherin (red). Insets on the right show individual DE-cadherin and MyoV-GT-GFP channels of the marked area. (b) Epithelia co-expressing UAS-MyoV-GT-GFP (green) and UAS-HA-Rab11 (red) and stained for DE-cadherin (blue). Insets on the right show individual Rab11, DE-cadherin and MyoV-GT-GFP channels of the marked area (c) Epithelia expressing UAS-MyoV-GT-GFP (green) and stained for Rab7 (red) and DE-cadherin (blue). Insets on the right show individual Rab7, DE-cadherin and MyoV-GT-GFP of the marked area. (d) The apical section of wild type epithelia stained for DE-cadherin. (c) The apical section of epithelia expressing UAS-MyoV-FL-GFP and stained for DE-cadherin. (d) The apical section of epithelia expressing UAS-MyoV-GT-GFP and stained for DE-cadherin. Zonula adherens is fragmented and ruptured (red arrows).

4.5.3 Endocytosed DE-cadherin localizes to endosomes within the apical actin network

My data show the functional role of the MyoV motor in the transport of DE-cadherin from apical endosomal compartments towards the zonula adherens. Since it is well-established that MyoV is a motor that uses the actin cytoskeleton to transport any cargo within the cell (Kodera & Ando, 2014; Langford, 2002; Mehta A.D. et al., 1999), I asked if the actin cytoskeleton may be used by the MyoV motor in DE-cadherin exit from endosomes. To answer this question, I visualized the actin cytoskeleton using a specific fluorescently labelled phallotoxin termed Phalloidin, which forms tight complexes with F actin (Cooper, 1987; Melak et al., 2017; Wulf et al., 1979). Phalloidin staining revealed that the apical actin network is concentrated at adherens junction (arrows in Figures 30a and 30a`). Structurally, apical actin cables are arranged in an irregular pattern, which spreads in random directions (Figures 30a and 30a`). In addition to this, I analyzed the localization of endocytosed DE-cadherin spots along the actin cables that were visualized with Phalloidin. For this purpose, I used the pulse-chase endocytosis experiment. After 20 minutes of endocytosis, I observed that endocytosed DE-cadherin spots were detected either near actin or colocalized with actin (total 96.67% ± 0.20, n=176 cells from 4 follicles) (Figure 30a). This implies that the endocytosed DE-cadherin uses the actin cables during transport.

Additionally, I also analyzed the localization of endosomal compartments within the apical actin network. I tested the localization of Rab7 and HA-Rab11 compartments in relation to the actin network. My data showed that Rab7 was present within actin the network (Figure 30b). Similar findings were noticeable in the case of HA-Rab11 (Figure 30c). I specifically quantified the colocalization between HA-Rab11, endocytosed DE-cadherin and actin fluorescence signals in the cytoplasm. The quantification revealed the colocalization of all three proteins (81.84% ± 3.11, n=159 cells from 5 follicles). This data suggests that actin cables are the path that the DE-cadherin uses for transportation from the endosomes.

In summary, my data show that endocytosed DE-cadherin localizes to the apical actin network. Furthermore, endosomal Rab7 and HA-Rab11 compartments that colocalize with endocytosed DE-cadherin were also found within the actin network. This suggests that the DE-cadherin uses the actin network for the transport from the apical endosomal system.

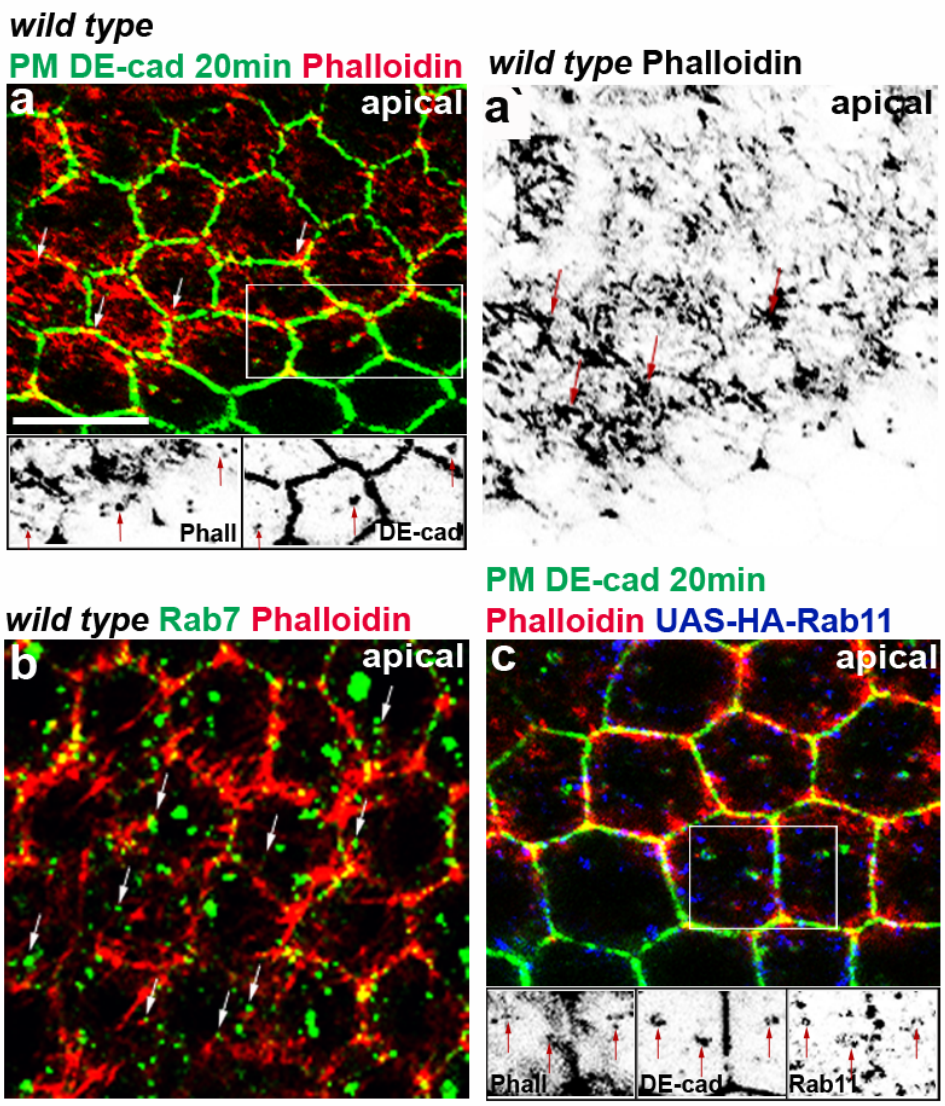

Figure 30. Endocytosed DE-cadherin is transported from apical endosomal compartments via the actin network. (a-c) Apical confocal optical sections perpendicular to the apical-basal axis of the follicular epithelium. The scale bar represents 10µm. Pulse-chase endocytosis was performed with epithelia shown in (a) and (c). PM DE-cadherin (plasma membrane DE-cadherin) stands for endocytosed DE-cadherin. (a) Wild type epithelia stained for actin filaments (red) and incubated with the α-DE-cadherin antibody (green) for 20 minutes. (a`) shows the individual actin channel. Actin cables are concentrated at zonula adherens (white arrows in (a) and red arrows in (a`)). Insets below show the actin and DE-cadherin channels of the marked area individually. Red arrows in insets point to the colocalization between actin and endocytosed DE-cadherin. (b) Wild type epithelia stained for actin filaments (red) and Rab7 (green). Rab7 localizes within the actin network (white arrows). (c) Epithelia expressing UAS-HA-Rab11 (blue) stained for actin network (red) and incubated with the α-DE-cadherin antibody (green) for 20 minutes. Insets below show the actin, DE-cadherin and Rab11 channels of the marked area individually. HA-Rab11, DE-cadherin and actin spots colocalize (red arrows).

4.5.4 Disruption of the actin network leads to the zonula adherens fragmentation

My data show that DE-cadherin exits endosomal compartments towards the plasma membrane via apical actin tracks. To provide additional support for this finding, I disrupted the actin network and analyzed DE-cadherin localization. I presumed that the disruption of the actin will affect the DE-cadherin delivery to the plasma membrane, specifically to the zonula adherens, where DE-cadherin is mostly concentrated. To test this, I treated *Drosophila* ovaries with Latrunculin A, a marine toxin that inhibits actin polymerization. The role of latrunculin A is well-known for increasing the hydrolysis rate of the ATP at the actin ends, which eventually results in the actin depolymerization (Coue et al., 1987; Fujiwara et al., 2018; Spector et al., 1983).

I compared the zonula adherens in *Drosophila* ovaries in Latrunculin A versus the dimethyl sulfoxide (DMSO) control group. Treatment with Latrunculin A resulted in fragmented zonula adherens and complete disruption of the apical actin network (Figure 31a). In the case of the DMSO control group, DE-cadherin at membranes formed intact zonula adherens (Figure 31b). To confirm my observation, I quantified the number of cells with the fragmented zonula adherens in both Latrunculin A and DMSO groups. Quantification revealed that 82.38% (± 3.63) of cells treated with Latrunculin A had a fragmented zonula adherens. In contrast, only 2.55% (± 1.05) of cells in the DMSO control group showed a fragmented zonula adherens (Figure 31c). This implies that disruption of the actin network impairs DE-cadherin transport to the zonula adherens. This observation was similar to the effect of the expression of the dominant-negative form of MyoV, UAS-MyoV-GT-GFP, in *Drosophila* follicular epithelium, which also resulted in fragmented zonula adherens (Figure 29f).

In summary, my data show that the disruption of the actin cytoskeleton results in the fragmented zonula adherens. A possible reason for the fragmented zonula adherens could be the disruption of tracks that DE-cadherin uses for reaching the plasma membrane This suggests that the actin network is essential for the delivery of DE-cadherin to the plasma membrane where it forms continuous zonula adherens.

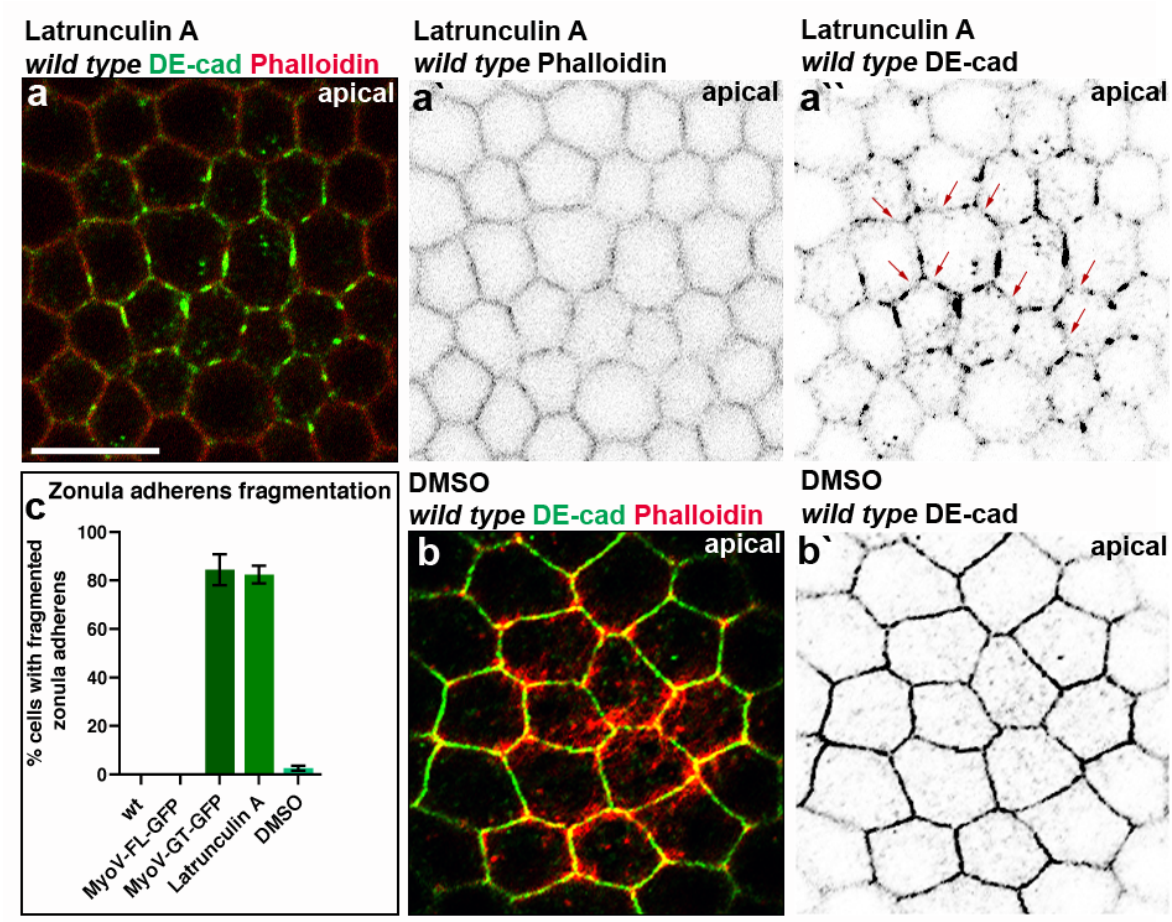

Figure 31. Disruption of actin filaments results in zonula adherens fragmentation. (a-b) Apical confocal optical sections perpendicular to the apical-basal axis of the follicular epithelium. The scale bar represents 10μm. (a) Wild type epithelia treated with 20μM Latrunculin A for 2 hours and stained for DE-cadherin (green) and actin (red). (a`) and (a``) show individual actin and DE-cadherin channels respectively. Zonula adherens is fragmented and ruptured (red arrows). (b) Control wild type epithelia for (a) treated with DMSO for 2 hours and stained for DE-cadherin (green) and actin (red). (b`) shows the individual DE-cadherin channel. (c) Quantification of zonula adherens fragmentation shown in (a), (b) and in Figures 29d-29f. Data are shown as mean ± SEM. The quantification was performed with 5 follicles (n=138 cells) for wild type, 5 follicles (n=131 cells) for MyoV-FL-GFP, 4 follicles (n=85 cells) for MyoV-GT-GFP, 6 follicles (n=152 cells) for ovaries treated with Latrunculin A and 9 follicles (n=287 cells) for ovaries treated with DMSO.

4.5.5 The MyoV-FL-GFP/Sec15-Cherry/HA-Rab11 compartment functions in apical DE-cadherin transport

My data show that DE-cadherin uses the actin network to leave endosomes and reach zonula adherens (Figures 30 and 31). I further analyzed if MyoV-FL-GFP/Sec15-Cherry/HA-Rab11 compartments are involved in DE-cadherin transport along the actin cytoskeleton. To answer this question, I first expressed the UAS-MyoV-FL-GFP construct in *Drosophila* ovaries and visualized the actin network with Phalloidin. I observed that MyoV-FL localized to the apical actin network (arrows in Figure 32a). I additionally performed live imaging experiment with *Drosophila* ovaries to see if MyoV-FL vesicles indeed move along the actin network. For this purpose, I expressed the UAS-Lifeact-RFP construct in *Drosophila* follicular epithelium, which is a protein that binds filamentous actin and can thus be used for visualization of actin dynamics (Riedl et al., 2008). I was able to monitor the movement of MyoV-FL vesicles along the actin filaments (arrows in Figure 32b), which confirmed that MyoV-FL is using the actin cytoskeleton for movement within the cell.

I further asked if MyoV-FL-GFP/Sec15-Cherry/HA-Rab11 compartment can also be detected within the actin cytoskeleton. To answer this question, I co-expressed UAS-MyoV-FL-GFP and UAS-Sec15-Cherry in *Drosophila* follicle cells and visualized the actin network with Phalloidin. My data revealed that Sec15-Cherry localized to the actin network (Figure 32c). Since my previous results showed that Sec15-Cherry and HA-Rab11 compartments completely colocalize (Figure 26a), as well as that HA-Rab11 localizes within the apical actin network (Figure 30c), this suggests that HA-Rab11 probably also colocalizes with Sec15-mCherry to the apical actin network. This overall implies that MyoV-FL-GFP/Sec15-Cherry/HA-Rab11 complex utilizes the actin network for DE-cadherin transport.

In summary, my data show that MyoV-FL vesicles are detected within the apical actin network. Further, Sec15-Cherry also localize within the actin network. This implies that MyoV, Sec15 and Rab11 act together in DE-cadherin transport via apical actin tracks. This pathway correlates to what my lab previously termed ‘apicolateral exocytosis’ (Woichansky et al., 2016).

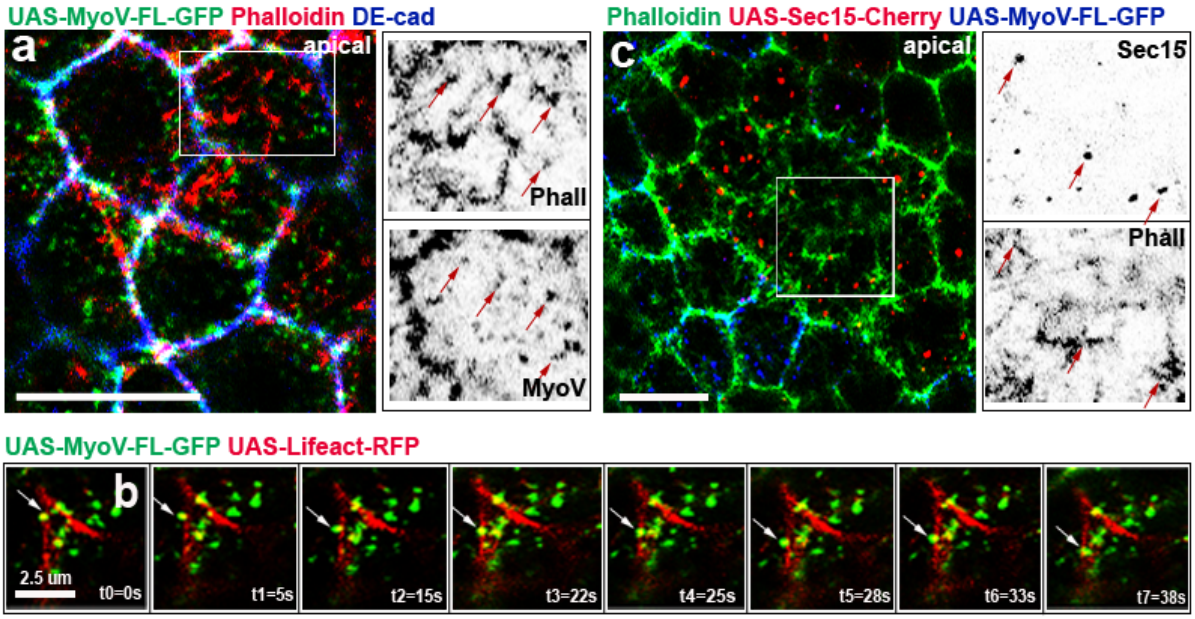

Figure 32. MyoV-FL-GFP/Sec15-Cherry/HA-Rab11 compartment localizes within apical actin filaments. (a) and (c) Apical confocal optical sections perpendicular to the apical-basal axis of the follicular epithelium. Scale bars in (a) and (c) represent 10µm. (a) Epithelia expressing UAS-MyoV-FL-GFP (green) and stained for actin (red) and DE-cadherin (blue). Insets on the right show the individual actin and MyoV-FL channels of the marked area. MyoV-FL localizes within the apical actin network (red arrows). (b) Montage of a live imaging movie showing the follicular epithelium in an apical view. Eight images of the movie are shown. The scale bar represents 2.5µm. White arrows point to the moving MyoV-FL (green) vesicle along the actin filament (red). (c) Epithelia co-expressing UAS-MyoV-FL-GFP (blue) and UAS-Sec15-Cherry (red) and stained for actin (green). Insets on the right show the individual Sec15 and actin channels of the marked area. Sec15 localizes within the apical actin network (red arrows). The detection of Sec15 compartments is only possible in the cells which show low MyoV-FL expression (see 4.5.1).

4.5.6 MyoV-FL-GFP/Sec15-Cherry/HA-Rab11 compartment in basal DE-cadherin transport

My data suggest that MyoV-FL/Sec15/Rab11 compartment utilizes the apical actin network to deliver the DE-cadherin to the zonula adherens. In parallel, I also investigated the possibility of DE-cadherin transport in a basal area of the cells. For this purpose, I visualized the basal actin cytoskeleton with Phalloidin in wild type epithelia. My data showed that the basal actin filaments are organized in parallel structures (Figure 33a). This observation is in line with a previous study in *Drosophila* ovaries (Baum & Perrimon, 2001). However, the parallel basal actin structures are in contrast to the apical actin cytoskeleton, which revealed an irregular disorganized network (compare Figures 30a` and 33a`).

I further asked whether the MyoV motor also uses basal actin filaments for DE-cadherin transport. To answer this question, I checked for the basal localization of MyoV-FL-GFP vesicles. I expressed the UAS-MyoV-FL-GFP construct in ovaries and stained them with Phalloidin for actin network visualization. Notably, I detected MyoV-FL-GFP vesicles along basal actin filaments as well (white arrows in Figure 33b). This suggests that MyoV also uses a basal actin network for cargo transport. I next asked if the MyoV motor uses basal actin filaments in the complex with Sec15-Cherry/HA-Rab11 for DE-cadherin transport. To answer this question, I co-expressed UAS-MyoV-FL-GFP with the UAS-Sec15-Cherry and UAS-HA-Rab11 and analyzed the localization of these compartments in the basal area of the cell. In the case of low MyoV-FL-GFP expressing cells, Sec15-Cherry, HA-Rab11 and MyoV-FL-GFP indeed formed a compartment in the basal cytoplasm (arrows in Figure 33c). In addition, I also analyzed DE-cadherin localization in the basal cytoplasm in follicles co-expressing UAS-MyoV-FL-GFP, UAS-Sec15-Cherry and UAS-HA-Rab11 constructs. As shown in Figure 33d, DE-cadherin was also localized to the MyoV-FL-GFP/Sec15-Cherry/HA-Rab11 compartments in the basal area (Figure 33d). This finding suggests the existence of a basal DE-cadherin transport pathway involving the MyoV-FL-GFP/Sec15-Cherry/HA-Rab11 compartment along the organized basal actin network. Such a route corresponds to what my lab previously termed ‘lateral exocytosis’ (Woichansky et al., 2016). Lateral exocytosis could be a source for the DE-cadherin puncta concentrated along the lateral membrane. DE-cadherin within these puncta could also be fed into the zonula adherens by an apical membrane transport termed ‘cadherin flow’. Cadherin flow is a pathway initially reported in mammalian cells (Kametani & Takeichi, 2007), but has also been confirmed in *Drosophila* follicular epithelium by my lab (Woichansky et al., 2016).

Taken together, my data show that the MyoV motor transports DE-cadherin in the complex with the Sec15-Cherry/HA-Rab11 compartment along the actin filaments in both apical and basal areas of the cell. The transport via apical actin filament is organized in irregular patterns and provides DE-cadherin for zonula adherens formation, corresponding to apicolateral exocytosis. Transport via basal cables organized in regular patterns might, on the other hand, represent the lateral exocytosis pathway and act together with cadherin flow to contribute to DE-cadherin localization at the lateral membrane. Additionally, it can also serve as an alternative route for supplying DE-cadherin to the zonula adherens.

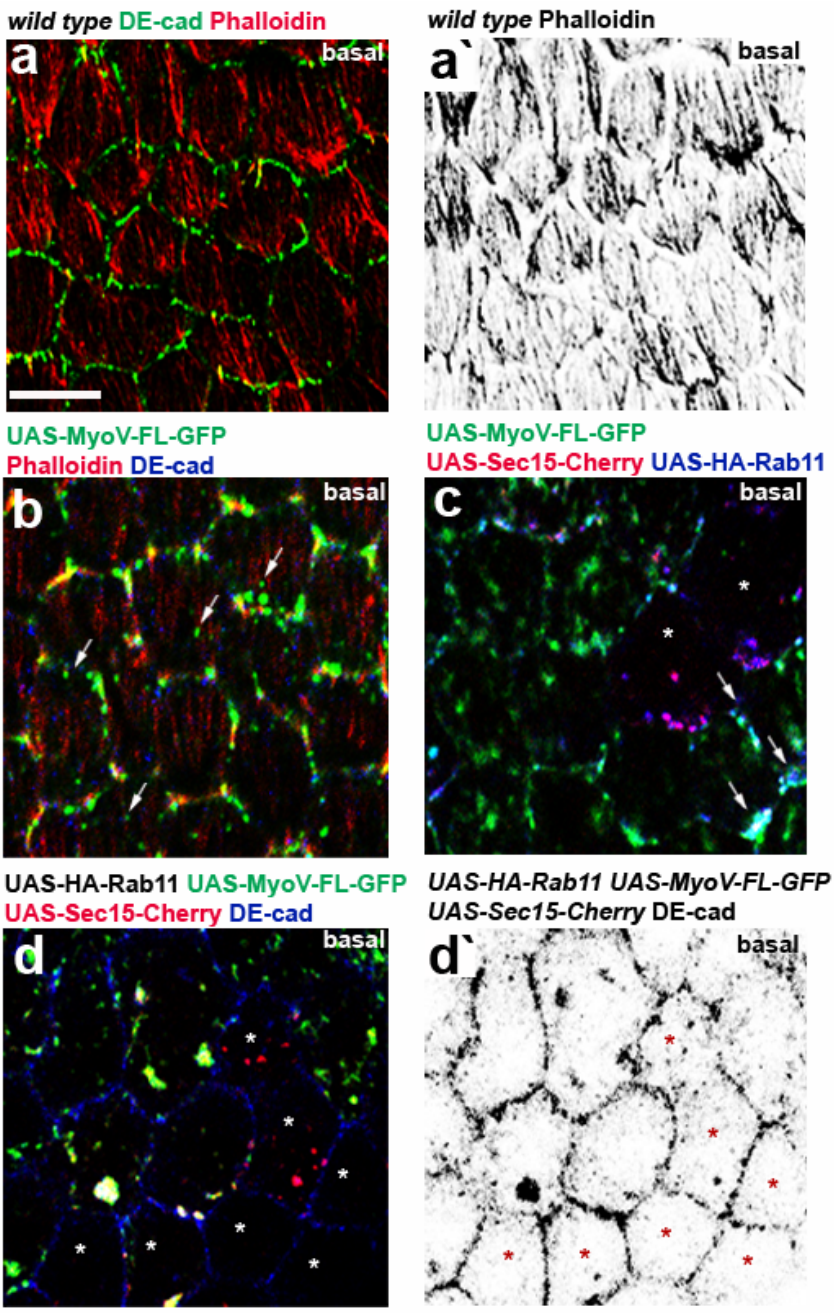

Figure 33. MyoV-FL-GFP/Sec15-Cherry/HA-Rab11 compartment uses basal actin filaments for DE-cadherin transport. (a-d) Basal confocal optical sections perpendicular to the apical-basal axis of the follicular epithelium. The scale bar represents 10µm. (a) Basal section of wild type epithelia stained for DE-cadherin (green) and actin (red). (a`) shows the individual actin channel. (b) Basal section of epithelia expressing UAS-MyoV-FL-GFP (green) and stained for actin (red) and DE-cadherin (blue). MyoV-FL, DE-cadherin and actin colocalize (white arrows). (c) Basal section of epithelia co-expressing UAS-MyoV-FL-GFP (green), UAS-Sec15-Cherry (red) and UAS-HA-Rab11 (blue). Asterisks mark cells with low levels of MyoV-FL-GFP expression. MyoV-FL-GFP, Sec15-Cherry and HA-Rab11 colocalize in the basal area of the cell (white arrows). (d) Basal section of epithelia co-expressing UAS-MyoV-FL-GFP (green), UAS-Sec15-Cherry (red) and UAS-HA-Rab11 (not stained), and stained for DE-cadherin (blue). (d`) shows the individual DE-cadherin channel. Asterisks mark cells with low levels of MyoV-FL-GFP expression.

5 Discussion & Outlook

5.1 Model for DE-cadherin transport in *Drosophila* follicular epithelium

I aimed to investigate the mechanism behind DE-cadherin secretion to the plasma membrane in the epithelial cells of the *Drosophila* ovary. My data suggest the following model for the DE-cadherin transport (Figure 34). After endocytosis from the plasma membrane (A in Figure 34), DE-cadherin enters the apical endosomal compartment, where newly synthesized DE-cadherin is also transported (B in Figure 34). Rab7 recruits Snx16 to these compartments, which then transports DE-cadherin to the Rab11 compartment via tubulation activity (C in Figure 34). Eventually, Rab11 recruits Sec15 and MyoV (D in Figure 34). MyoV is a motor that uses actin cytoskeleton for cargo transport within the cell (E in Figure 34), while the subunit Sec15 of the exocyst complex recruits the exocyst's other components, which are necessary for the fusion of the DE-cadherin vesicle with the plasma membrane (F in Figure 34). Hence, MyoV/Sec15/Rab11 complex transports DE-cadherin towards the plasma membrane along the actin cables in the apical area of the cell (so-called 'apicolateral exocytosis') and in the basal area of the cell ('lateral exocytosis').

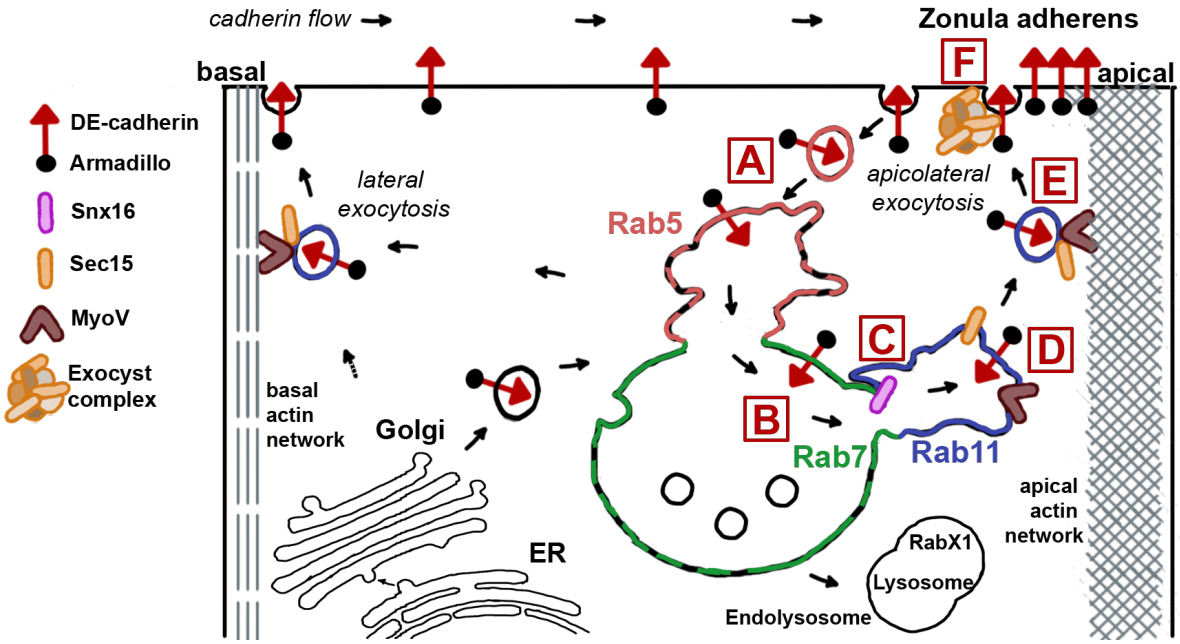

Figure 34. Model for DE-cadherin transport in *Drosophila* follicular epithelium. DE-cadherin (red arrow), in the complex with Armadillo (black circle), is endocytosed (A) via Rab5 (pale red) and delivered to endosomes, where it meets newly synthesized DE-cadherin (B). From the Rab7 (green) within the endosome, DE-cadherin is transported via the tubulation activity of Snx16 (pink oval rectangle) to Rab11 (blue) (C). Rab11 then recruits the MyoV motor (brown 'reversed V') and the exocyst subunit Sec15 (orange oval rectangle) for the subsequent trafficking steps (D). MyoV forms a complex with Sec15 and Rab11 and then transports DE-cadherin along the apical actin network (E). This process is termed 'apicolateral exocytosis'. Once the complex reaches the zonula adherens, Sec15 recruits other exocyst subunits for the fusion of DE-cadherin with the membrane (F). In parallel, the MyoV/Sec15/Rab11 also transports DE-cadherin along the basal actin network in a process termed 'lateral exocytosis'.

5.2 Apical endosomal compartments as sorting stations for recycling and degradation

At the beginning of my investigation, I first analyzed the localization of endocytosed DE-cadherin. My data showed that endocytosed DE-cadherin spots were detected in the cytoplasm after 20 minutes of endocytosis (Figure 6d). Similarly, in the case of cultured mammalian cells, endocytosed intracellular E-cadherin was observed after 5 minutes (Le et al., 1999). The delayed endocytosis observed in my experiments may be due to fixed intact tissues being investigated, whereas in the mentioned study they have used cultured mammalian cells. The experimental evidence provided by using *in vitro* studies do not consider the physiological levels of proteins, and the complexity of the living tissues could impact the duration of endocytosis (Weigert, 2014).

My data showed that newly synthesized and endocytosed DE-cadherin converge in one endosomal compartment located in the apical cytoplasm (B in Figure 34). Furthermore, my results also showed that Rab7 and Rab11 domains appear to be present within these endosomes (Figure 12b). It is thus tempting to suggest that the apical endosomal system serves as a sorting station for the subsequent DE-cadherin transport steps. The existence of such endosomal apical compartments decorated by Rab proteins has already been suggested (Hoekstra et al., 2004).

Namely, the DE-cadherin protein in the cell can have two fates: either be recycled back to the plasma membrane or degraded (Brüser & Bogdan, 2017). The apical endosomes that accumulate newly synthesized and endocytosed DE-cadherin could be a site where the decision is made. The more DE-cadherin is sorted for recycling, the more DE-cadherin will be present at the membrane, which could eventually result in stronger adherence. As suggested by Nanes and colleagues, this more solid cell-cell adhesion could be essential during cell proliferation (Nanes & Kowalczyk, 2012). On the other hand, the more DE-cadherin is destined for degradation, the less is available for building the zonula adherence at the plasma membrane. This could result in weaker adherence between the cells, which is favorable during dynamic and rapid changes such as cell differentiation and the growth of the oocyte (Brüser & Bogdan, 2017; Nanes & Kowalczyk, 2012). The apical endosome would thus be able to finetune the intensity of cell-cell adhesion by dictating the rate of recycling and degradation. Since the evaluation of the ratio between the recycled and degraded DE-cadherin would be an interesting point, I attempted to address this issue in preliminary research. For this purpose, I have used the UAS-HA-Rab11 construct as a marker for a recycling compartment and the UAS-RabX1-GFP construct as a marker for a degradative compartment. Rab11 has traditionally been considered a marker for the recycling endosomes (Zerial & McBride, 2001). An earlier study from my lab proposed the role of RabX1 in DE-cadherin recycling (Woichansky et al., 2016). However, a later study also from my laboratory showed that RabX1 actually coordinates the endosomal degradative branch (Laiouar et al., 2020). I thus proposed that DE-cadherin destined for degradation enters the RabX1 endosomal domain. For this reason, I used RabX1-GFP as a marker for the degradative compartment. I performed pulse-chase endocytosis experiments with *Drosophila* follicles co-expressing UAS-HA-Rab11 and UAS-RabX1-GFP and tried to quantify the amount of DE-cadherin localized within these compartments. The idea behind this was to compare the amount of DE-cadherin in the recycling compartment and in the degradative compartment, and thus estimate the ratio between recycled and degraded DE-cadherin. Unfortunately, the HA-Rab11 and RabX1-GFP compartments are located in very close proximity to one other, which makes it rather hard to distinguish between them. Hence better experimental approaches are required to estimate the ratio between recycled and degraded DE-cadherin.

One way could be blocking degradation by proteasomal inhibition and thus quantifying the total amount of DE-cadherin detected in the cell. This amount should then be compared with the amount of DE-cadherin detected when degradation takes place. However, impaired degradation could also result in enhanced autophagy (Low et al., 2013), thus the way of blocking degradation should be carefully selected.

5.3 Endosomal compartments can be transported to the apical cytoplasm

Rab11 and Rab7 compartments, in which newly synthesized and endocytosed DE-cadherin converge, are noticeable larger in the apical area of the cell in comparison to compartments found in the basal area of the cell (Figures 8a and 13a). I speculated that the reason for the increase in the size of apical endosomes is due to the accumulation of DE-cadherin protein.
To confirm this hypothesis, I suggest investigating where endosomes start collecting the protein cargo. One possibility is that cargo accumulation occurs in the apical cytoplasm, where endosomes are detected. Another possibility is that endosomes start accumulating cargo elsewhere, such as in the basal cytoplasm. Endosomes then increase in size due to the collection of proteins which they then transport to the apical part of the cell. If endosomes start accumulating DE-cadherin prior to apical transport, this suggests that the synthesis of DE-cadherin and its endocytosis occur somewhere other than the cytoplasm's apical region. Directed transport of cargo from the basal to the apical area has already been described in a past study that investigated the transport of the transmembrane protein Crumbs (Crb) in *Drosophila* ovaries (Aguilar-Aragon et al., 2020). Namely, Crb protein normally localizes to the apical domain of the plasma membrane. However, downregulation of the microtubular motor Dynein led to the accumulation of Crb in Rab11 compartments specifically at the basal area of the cytoplasm. This suggests that the directed motor transport of Rab11 endosomes towards the apical area of cells is required for proper Crb localization (Aguilar-Aragon et al., 2020). This study prompted me to speculate that apical endosomal compartments, which I found to collect endocytosed and newly synthesized DE-cadherin, are also transported via motor dynein to the apical cytoplasm. One way to test this is to express *Dynein RNAi* construct and to analyze whether Rab7 and Rab11 compartments remain apically localized. Another approach could be to destabilize microtubules either by low temperature or by different microtubule inhibitors like vinblastine and nocodazole (Laisne et al., 2021). However, interfering with dynein-mediated transport could lead to disruption of other organelles and could affect polarity markers. This makes it difficult to evaluate if the possible effect observed is direct or indirect. Hence additional fine approaches and the utilization of appropriate controls are required.

If endosomal compartments containing newly synthesized DE-cadherin are transported to the cell's apical area, it is likely that they were initially near the DE-cadherin translation site. Firstly, detecting the place of the local DE-cadherin translation could thus help to address the question of whether endosomes themselves are being transported apically. Secondly, blocking the local translation of proteins could reveal where DE-cadherin is synthesized. Protein translation can be blocked using drugs such as thapsigargin, cycloheximide and lactimidomycin, and this approach has been widely applied (Jaskulska et al., 2021; Schneider-Poetsch et al., 2010). If DE-cadherin accumulates in the basal cytoplasm after the inhibition of protein synthesis, this would suggest that endosomal compartments could be transferred from the basal area of the cell, where the protein synthesis takes place, to the apical area of the cell. Endosomes would accumulate both newly created and endocytosed DE-cadherin during transport in this scenario, resulting in enlarged apical endosomal compartments.

5.4 Rab7 and Snx16 redundancy in DE-cadherin transport

My data showed that the member of sorting nexin family 16 (Snx16) localizes to Rab7 and Rab11 endosomes, within which newly synthesized and endocytosed DE-cadherin aggregates (Figure 17b). Furthermore, my findings revealed that DE-cadherin aggregates in the cytoplasm upon the Snx16 depletion (Figure 18a). Curiously, Rab7 likely recruits Snx16 for the DE-cadherin recycling (Figure 19a). This overall suggests the interaction between Rab7 and Snx16 in the DE-cadherin transport process.

Despite DE-cadherin cytoplasmic accumulation in *Rab7* and *Snx16* cell clones, I observed no severe defects in the cell shape or zonula adherens formation (Figures 16a and 18a). This suggests that DE-cadherin secretion to the plasma membrane is still possible. Mild DE-cadherin phenotype in *Rab7* and *Snx16* cell clones might be due to a Rab7 and Snx16 redundancy. Redundant mechanisms that control DE-cadherin transport have already been reported (Zobel et al., 2015). A previous study showed that the simultaneous depletion of two BAR proteins, Cip4 and Nostrin, resulted in the reduction of DE-cadherin turnover and in DE-cadherin intracellular accumulation (Zobel et al., 2015). DE-cadherin also accumulates in the cytoplasm in *Cip4* single mutants, but to a significantly lesser extent. *Nostrin* single mutants, on the other hand, do not result in DE-cadherin aggregation in the cytoplasm. Taken together, this suggests that Cip4 and Nostrin work together to regulate DE-cadherin transport (Zobel et al., 2015). This research prompted me to test whether the simultaneous depletion of Rab7 and Snx16 could also result in a more severe phenotype. My data revealed that the cell shape and the zonula adherens formation in *Rab7 Snx16* double mutants were intact (Figure 18c). Nevertheless, I did observe an increased number of cytoplasmic DE-cadherin aggregates

(Figure 18d). This suggests that Rab7 and Snx16 are involved in the same DE-cadherin transport route, but that there could also be an additional factor involved in the regulation of DE-cadherin trafficking. An interesting candidate is a member of the sorting nexin family 1 (Snx1). A study in cultured cells showed that the endocytosed E-cadherin accumulates in the cytoplasm upon Snx1 depletion (Bryant et al., 2007). It would thus be interesting to investigate the simultaneous knockdown of Rab7, Snx16 and Snx1 in *Drosophila* and analyze DE-cadherin localization and the formation of zonula adherens.

Further studies are necessary to identify other factors possibly interacting with Rab7 and Snx16 in DE-cadherin transport. This could be done by the purification of Rab7 and Snx16 interactors by affinity chromatography and by subsequent mass spectrometry analysis. This would yield the list of candidates, which could be tested in *Drosophila* ovaries using different RNAi strains and null mutants.

Rab7 recruits Snx16 to endosomes for further DE-cadherin transport stages, as previously indicated (Figure 19a). The precise mechanism by which this is accomplished is another intriguing topic that needs to be investigated. Recruitment to the endosomal membrane and tubule formation of another member of the sorting nexin family 5 (Snx5), is thought to be dependent on the microtubule network, according to a previous study (Kerr et al., 2006). It would be interesting to see if Snx16 recruitment to Rab7 endosomes is likewise influenced by the microtubule integrity.

5.5 Snx16 stabilizes the DE-cadherin/Armadillo complex

Previous studies have shown that DE-cadherin and Armadillo, the *Drosophila* homolog of β-catenin, are secreted together to the plasma membrane in a complex that is formed soon after DE-cadherin synthesis (Y. T. Chen et al., 1999; Langevin et al., 2005; Stow & Lock, 2005). Hence the finding that, when Snx16 and Rab7 are depleted, only DE-cadherin – but not Armadillo – accumulates in the cytoplasm was unexpected (Figures 20b and 20c). I speculated that the DE-cadherin/Armadillo complex dissociates in the absence of Snx16 and Rab7. Since my data suggest that Rab7 recruits Snx16 (Figure 19a), I proposed that Snx16 is required for the stabilization of DE-cadherin/Armadillo complex. The absence of Armadillo accumulation in *Rab7* mutants is an indirect effect due to a failure to recruit Snx16.

Both Armadillo and Snx16 bind DE-cadherin directly (Aberle et al., 1994; Jinxin Xu et al., 2017). An earlier study showed that β-catenin binds newly synthesized E-cadherin in the ER (Y. T. Chen et al., 1999). Since a previous study suggested that the Snx16 is recruited to endosomes (Brankatschk et al., 2011), I proposed that the E-cadherin is most likely bound to Snx16 at endosomes. This binding could further stabilize the DE-cadherin/Armadillo complex.

My other results are additionally also strengthening the hypothesis that Snx16 stabilizes DE-cadherin/Armadillo complex. My data showed that Armadillo only mildly accumulates in YFP-Rab11 compartments, in contrast to heavy DE-cadherin accumulation within YFP-Rab11 compartments (Figures 8 and 9). I speculated that this is due to the dissociation of the DE-cadherin/Armadillo complex within YFP-Rab11 compartments. As a consequence, a certain amount of DE-cadherin remains trapped within YFP-Rab11 compartments. This speculation is in line with the hypothesis that Snx16 stabilizes DE-cadherin/Armadillo complex at endosomes. The stabile DE-cadherin/Armadillo complex might be required for efficient DE-cadherin transport from endosomes. Since the stability of the complex is critical for successful transport, another protein on endosomes helps to keep the complex stable. My data suggest that this protein could be Snx16.

My findings further add to conflicting studies regarding the requirement of DE-cadherin/Armadillo complex for DE-cadherin delivery to the plasma membrane. An early study in cultured cells has shown that E-cadherin that is incapable of binding β-catenin remains in the ER (Y. T. Chen et al., 1999). Notably, some later studies have demonstrated that E-cadherin can not only leave ER without being bound to β-catenin, but is also capable to localize to the membrane independently (Miranda et al., 2001; Pacquelet & Rørth, 2005). Despite this, β-catenin remains the main regulator of E-cadherin transport. In the absence of β-catenin, E-cadherin accumulates in the cytoplasm (Drees et al., 2005). Additionally, upon the depletion of β-catenin, E-cadherin is not capable to bind another regulator, α-catenin, which mediates the link of E-cadherin to the actin cytoskeleton (Drees et al., 2005). My findings also point to the need for the DE-cadherin/Armadillo complex, but only in the endosome-to-plasma membrane path of DE-cadherin transport. It, therefore, remains to be further investigated how crucial DE-cadherin/Armadillo complex is for DE-cadherin secretion and at what stages it might be redundant.

5.6 The glycine triplet within the DE-cadherin cytoplasmic tail is important for the interaction with the exocyst

A previous study demonstrated that both Armadillo and mammalian homolog β-catenin form a complex with exocyst components (Langevin et al., 2005). More precisely, immunoprecipitation experiments revealed that the exocyst subunit Sec10 is capable of precipitating Armadillo, suggesting a direct association between Sec10 and Armadillo. The same study also performed immunoprecipitation experiments with mammalian β-catenin. Interestingly, Armadillo and mammalian homolog β-catenin seem to be interacting with different exocyst subunits, as β-catenin immunoprecipitated Sec5 and Sec8 (Langevin et al.,

2005). This result is even more surprising since these exocyst subunits belong to different exocyst subcomplexes. Namely, Sec5 and Sec8, which interact with β-catenin, belong to the exocyst subcomplex I, whereas Sec10, which interacts with Armadillo, belongs to the subcomplex II. This suggests certain differences in the regulation of the exocyst in *Drosophila* and mammalian cells.

Additionally, these results also point at β-catenin mediating the interaction between E-cadherin and the exocyst complex. Therefore, I was surprised by the result that the mutation of the glycine triplet within the DE-cadherin cytoplasmic domain prevents DE-cadherin localization within Sec15 compartments (Figure 25a). This result implies that these glycine residues might be required for the interaction of DE-cadherin with the exocyst complex. Curiously, these glycine residues in human E-cadherin represent the binding site for p120, catenin that is involved in the regulation of cell-cell adhesion and endocytosis (Bulgakova & Brown, 2016; K. Sato et al., 2011; Thoreson et al., 2000). It is thus tempting to speculate that DE-cadherin might be associated with the exocyst complex via p120 protein.

Despite the research, no direct association between the exocyst and DE-cadherin has been demonstrated so far. It is thus unclear what role the glycine triplet plays in the E-cadherin-exocyst complex relationship. One possibility could be that it mediates the direct interaction between the E-cadherin and one of the exocyst subunits. Another possibility could be that E-cadherin interacts via glycine residues with another component (which is not β-catenin) and which then, in turn, makes a complex with the exocyst as well. As suggested above, this component could be p120 protein.

Curiously, a study in *Drosophila* ovaries showed that DE-cadherin accumulates in the cytoplasm in *Armadillo* mutants (Langevin et al., 2005; Pacquelet et al., 2003). If DE-cadherin interacts with the exocyst via Armadillo, this DE-cadherin cytoplasmic aggregation may be a result of the inability of the exocyst complex to be recruited to the DE-cadherin vesicles in the absence of Armadillo. The cytoplasmic aggregation of DE-cadherin seen in *Rab11* cell clones could be due to the same cause – a failure to recruit the exocyst complex.

5.7 The exocyst complex is involved in the transport of the apical proteins

My results suggest that the lateral protein Fas2 doesn't localize within the Sec15 compartment (Figure 23a). Additionally, the expression of the *Sec15 RNAi* construct also doesn't influence the localization of Fas2, as it is the case with the DE-cadherin (Figure 23b). This suggests that the transport of the lateral protein Fas2 is not dependent on the function of the exocyst subunit Sec15. This finding is consistent with a previous study in *Drosophila,* where it was shown that the localization of another lateral protein, Fas3, remains unaffected upon the depletion of the

exocyst subunit Sec5 (Langevin et al., 2005). Overall, this implies that the transport of proteins localizing to the basolateral membrane such as Fas2 and Fas3 does not involve the exocyst complex. More research is required on other transport mechanisms that may exist for delivering proteins localizing to the other area of the plasma membrane. It also remains to be investigated if newly translated or endocytosed Fas2 and Fas3 are delivered to endosomes.
The localization of apical protein Crb, on the other hand, seems to be dependent on the exocyst complex. One study suggests that exocyst subunits Sec5 and Sec15, together with Rab11 and MyoV motor, facilitate Crb localization to the apicolateral plasma membrane (Aguilar-Aragon et al., 2020). In the context of my results, these findings suggest that the exocyst complex is involved in the transport of apical proteins such as DE-cadherin and Crb (Aguilar-Aragon et al., 2020). However, there must be some differences in the way these two proteins are being sorted for subsequent secretion processes. As previously stated, DE-cadherin might interact with the exocyst via Armadillo (Langevin et al., 2005). On the other hand, Crb's association with Armadillo is unlikely, which raises the question of how Crb interacts with the exocyst complex. Furthermore, DE-cadherin uses both apical and basal actin tracks, whereas Crb is not detected at the basolateral membrane (Ulrich Tepass et al., 1990). As a result, there must be a way to prevent Crb from localizing to the basolateral membrane. Crb and DE-cadherin trafficking routes from the endosome to the plasma membrane also differ because Crb is recycled via the retromer complex (Pocha et al., 2011). It would thus be interesting to investigate the differences in pathways of various cargos and mechanisms used for sorting cargos along these distinct routes.

5.8 The existence and the activation of different DE-cadherin routes to the plasma membrane

My data showed that the simultaneous overexpression of Sec15 and Rab11 results in enlarged Sec15-Cherry/HA-Rab11 compartments that accumulate DE-cadherin (Figure 26a). Further, the simultaneous expression of UAS-MyoV-FL-GFP, UAS-Sec15-Cherry and UAS-HA-Rab11 constructs in *Drosophila* follicles rescued the formation of Sec15-Cherry/HA-Rab11 compartments and DE-cadherin aggregation (Figures 28a and 28b). This suggests that MyoV interacts with the Sec15 and Rab11 in DE-cadherin transport. Additionally, the expression of the dominant-negative form of MyoV resulted in the fragmented zonula adherens (Figure 29f). This further confirms the role of the MyoV in DE-cadherin delivery to the zonula adherens. My data also revealed that the disruption of the actin cytoskeleton leads to the same phenotype as observed after the expression of the dominant-negative form of MyoV - zonula adherens

fragmentation (Figure 31a). This implies that the MyoV motor, together with the Sec15 and Rab11, delivers DE-cadherin along the actin filaments to the zonula adherens.

Furthermore, the transport of DE-cadherin via the MyoV, Sec15 and Rab11 is performed along the apical and basal actin network (Figures 32 and 33). Apical actin tracks deliver DE-cadherin directly to the apical-most area of the plasma membrane, where the zonula adherens is formed. Basal actin tracks, on the other hand, suggest the existence of DE-cadherin transport routes in the basal region of the epithelium, for which the interaction between MyoV, Sec15 and Rab11 compartments is also employed. However, it is unclear if MyoV-FL-GFP/Sec15-Cherry/HA-Rab11 compartments that are detected within the basal actin network transport newly synthesized DE-cadherin, endocytosed DE-cadherin, or both. This basal pathway could represent a possible route that my laboratory previously termed 'lateral exocytosis' (Woichansky et al., 2016). I speculated that lateral exocytosis supplies the DE-cadherin that forms a punctate-like adherens junction, which is observed below the zonula adherens and along the lateral membrane. After reaching the basal membrane, DE-cadherin could be distributed along the lateral membrane via the so-called 'cadherin flow' (Figure 34). Cadherin flow has already been described for vascular endothelial cadherin (VE-cadherin) in mammalian cells (Kametani & Takeichi, 2007). VE-cadherin moves from the basal to the apical area of the membrane via actin filaments. The actin motor myosin II transports the VE-cadherin, as the inhibition of the myosin II function as well as the disruption of the actin filaments leads to the block of the cadherin flow. The cadherin flow could also be used as an alternative source of DE-cadherin, to be fed into the zonula adherence. This speculation has been confirmed by the study from my laboratory, which showed that upon blocking of the cadherin flow, DE-cadherin is detected along the lateral membrane but not concentrated at the zonula adherens (Woichansky et al., 2016). Furthermore, the block of the cadherin flow is achieved by inhibition of the actin polymerization, suggesting that in *Drosophila,* similar to mammalian cells, cadherin flow depends on the actin filaments. It would, therefore, be interesting to test whether myosin II also transports DE-cadherin along the membrane in *Drosophila*.

As previously mentioned, my findings imply that Rab11 recruits the exocyst complex for DE-cadherin trafficking in both apical and basal regions of the cell. However, how Rab11 is activated for the recruitment of the exocyst protein Sec15 remains unknown. Rab11 activation could be regulated by the interaction of 'transport protein particle II' (TRAPPII) complex and Parcas, which enhances the GDP-GTP exchange (Riedel et al., 2018). Another open question is how Sec15 vesicles, which transport DE-cadherin, build within the Rab11 endosomal compartment. A recent study in *C. elegans* and mammalian cells identified so-called 'factors for endosome recycling and Rab interactions' (FERARI) (Solinger et al., 2020). FERARI is a multiprotein tethering complex that recruits Rab11 to endosomes and provides a link between Rab11 and the Rab11 effector Rab11FIP5. Live imaging experiments showed that FERARI is

required for Rab11 fusion and fission at sorting endosomes, where it picks up proteins similarly to the kiss-and-run mechanism.

Furthermore, it is unknown when the other exocyst subunits are recruited for the fusion of vesicles carrying DE-cadherin with the plasma membrane. One possibility could be that it happens already at endosomes, as soon as Sec15 is recruited. However, one study in cultured cells used live imaging to demonstrate that the exocyst sub-complexes meet at the plasma membrane, which they reach at similar times (Ahmed et al., 2018a). This finding suggests that the remaining exocyst subunits are recruited directly at the plasma membrane after the complex reaches the zonula adherens. This implies that, in the case of DE-cadherin transport, MyoV/Sec15/Rab11 compartment might reach the plasma membrane independently of the remaining exocyst subunits, which would only then be recruited for the fusion of the complex with the plasma membrane.

Another interesting point to be discussed is how exactly DE-cadherin is fused with and precisely targeted to the plasma membrane. A study in cultured mammalian cells revealed that Par3 protein serves as an anchor for the exocyst complex (Ahmed & Macara, 2017), which localizes to the zonula adherens in *Drosophila* follicular epithelium (Franz & Riechmann, 2010). A *Drosophila* homolog of the Par3 gene, Bazooka (Baz), is thus a great candidate for the precise targeting of the MyoV/Sec15/Rab11 compartment that delivers DE-cadherin to the zonula adherens. Furthermore, another study in cultured mammalian cells showed that aquaporin3 (AQP3) localizes to zonula adherens at the plasma membrane, suggesting that it can also be a landmark for the targeted delivery of DE-cadherin and its transport complex (Nejsum & Nelson, 2007). However, no *Drosophila* homolog of AQP3 has yet been found. Finding the crucial E-cadherin anchor and the factors involved in the precise delivery may be of therapeutical significance, as the restoration of E-cadherin targeted secretion in leukemia cells resulted in the enhancement of E-cadherin adhesion (Shaaban & Mohammed, 2021). Therefore, it would be beneficial to elucidate the exact mechanism behind DE-cadherin delivery to the plasma membrane and its anchor. However, additional research is needed to investigate the precise mechanisms for the recruitment of Sec15 and the motor MyoV to the endosomes, as well as to tether DE-cadherin vesicles to the membrane. Live imaging experiments have already been employed to elucidate mechanisms behind the exocyst dynamics (Ahmed et al., 2018b). The same approach might therefore be useful to monitor the association of DE-cadherin with the complex consisting of MyoV, Sec15 and Rab11, as well as the fusion of DE-cadherin vesicles with the plasma membrane. Another useful technique that could be used for elucidating the trafficking of DE-cadherin vesicles is ‘retention using selective hooks’ (RUSH) system. This method allows the monitoring of cargo transport in a timely controlled manner and has already been used in cultured cells (Boncompain et al., 2012).

5.9 Rab11 compartments transporting DE-cadherin via MyoV motor as a part of the actin nucleation center

My data showed that endocytosed DE-cadherin was detected within the apical actin network (Figure 30a). Additionally, I have observed that HA-Rab11 compartments also colocalize with endocytosed DE-cadherin within the apical actin network (Figure 30c). Curiously, these endocytosed DE-cadherin spots, as well as HA-Rab11 compartments, localize to the actin 'clumps' (Figure 30c). I speculated that these actin clumps represent the actin nucleation centers.

Nucleation, or the catalysis of new actin filaments, is usually the first step in constructing the actin network. Previous studies have pointed to the importance of the interaction between actin nucleators, motors and proteins to be transported (J. Cheng et al., 2012; Schuh, 2011; Sirotkin et al., 2005; Sun et al., 2006). Actin nucleator Spir creates actin cables at the vesicle membrane marked by Rab11, which is further transported by the myosin Vb (Schuh, 2011). A study in cultured cells showed that Spir directly interacts with the MyoV via its globular tail. Additionally, the same study also proposed a ternary complex consisting of Spir, MyoV and Rab11 (Pylypenko et al., 2016). These findings made me speculate that the DE-cadherin transport could be initiated by the Spir/MyoV/Rab11 complex. Preliminary results with the expression of the *Spir RNAi* showed that DE-cadherin still colocalizes with the HA-Rab11 and actin upon the Spir depletion. This implicates that there might be an additional factor recruiting Rab11 and MyoV to the nucleation center for the subsequent DE-cadherin transport.

Another actin nucleator, Cappuccino (Capu) directly interacts with Spir to build the actin network (Bradley et al., 2020). My initial results showed that in the cells lacking Capu, DE-cadherin was also still colocalizing with actin and HA-Rab11, implying that Rab11 can be recruited to the actin nucleation center in the absence of Capu. In addition to this, the cooperation between Spir and Capu has recently established suggested (Bradley et al., 2020; Dahlgaard et al., 2007). In line with this new finding, it would be interesting to see the effect of double knockdown of Spir and Capu on the recruitment of HA-Rab11 for DE-cadherin transport to the actin nucleation centers.

5.10 Evolutionary conservation of DE-cadherin transport pathway

The critical function of E-cadherin in cell-cell adhesion is conserved throughout species, which raises a question of extent to which my model for DE-cadherin transport can be applied to other organisms. Direct interaction between the MyoV, Sec15 and Rab11 has been identified in yeast (Jin et al., 2011). This shows that the established E-cadherin trafficking mechanism is

conserved in higher evolved organisms. Interestingly, even though three myosin V motors (Va, Vb and Vc) can be distinguished in mammalian cells, Rab11 was shown to bind only myosin Vb (Roland et al., 2009). This suggests that the specific interaction between Rab11 and the MyoV motor exists in the higher organisms. Another study in mammalian cells demonstrated that Sec15 is an effector of Rab11, and the Rab11 and Sec15 interaction has been confirmed *in vivo* (S. Wu et al., 2005; Zhang et al., 2004). This demonstrates possible interactions also between Rab11 and Sec15 in higher species. Taken together, this demonstrates that the complex consisting of MyoV, Sec15 and Rab11 evolved from a single-celled organism and that it is conserved in higher organisms as well.

The role of Rab11 in E-cadherin transport has also been well-documented in cultured mammalian cells. Firstly, E-cadherin was detected to pass through the apical endosomal compartment that is Rab11 positive (Stow & Lock, 2005). Secondly, E-cadherin localization to the plasma membrane is dependent on the human Rab11 orthologue Rab11a, since in its absence E-cadherin cannot be delivered to the plasma membrane (Desclozeaux et al., 2008; Stow & Lock, 2005). From these studies, it can be concluded that Rab11's critical involvement in E-cadherin trafficking has been preserved. Furthermore, studies in mammalian cells revealed that sorting signals for proper E-cadherin delivery are situated within the cytoplasmic tail (Y. T. Chen et al., 1999; Miranda et al., 2001), which is consistent with my findings in *Drosophila* epithelium. The endosomal retrieval mechanisms seem to be similar between flies and mammals too, since the interaction between E-cadherin and Snx16 has also been identified (Jinxin Xu et al., 2017). It would thus be interesting to test my proposed model for DE-cadherin transport in *Drosophila* epithelium and also in the mammalian system, using both experiments in fixed cells and live imaging techniques.

Altogether, my model for DE-cadherin trafficking in *Drosophila* follicular epithelium established a good foundation for further investigation of how changes in E-cadherin trafficking impact morphogenesis and how defective mechanisms of E-cadherin turnover and secretion promote disease progression.

6 List of abbreviations

DE-cadherin	*Drosophila* E-cadherin
Fas2	Fasciclin2
Fas3	Fasciclin3
ER	Endoplasmic reticulum
Dab2	Disabled-2
PALS1	Protein Associated with Lin Seven 1
BAR domain	Bin/Amphiphysin/Rvs domain
EMT	Epithelial-mesenchymal transition
ATP	Adenosine triphosphate
ADP	Adenosine diphosphate
MyoV	Myosin V
GTP	Guanosine-5`-triphosphate
GDP	Guanosine-5`-diphosphate
GEF	Guanine-nucleotide-exchange factor
GAP	GTPase activating protein
SNAREs	Soluble N-ethylmaleimide-Sensitive Factor Attachment Protein Receptors
ERES	ER exit sites
COPII	Coat protein complex II
GRASPs	Golgi Reassembly and Stacking Proteins
ILVs	Intraluminal vesicles
MVBs	Multivesicular bodies
Snx proteins	Sorting nexin proteins
PtdInsPs	Phosphatidylinositol phosphates
PM	Plasma membrane
UAS	Upstream Activating Sequence
EEA1	Early endosomal antigen 1
ORF	open reading frame
aPKC	Atypical protein kinase C
LT	Lysotracker
CC domain	Coiled-coil domain
RNAi	RNA interference
hpRNA	hairpin RNA
siRNA	short double-stranded RNA

RISC	RNA-induced silencing complex
bp	Base pairs
DMSO	Dimethyl sulfoxide
Crb	Crumbs
PIPKIγ	Iγ phosphatidylinositol-4-phosphate 5-kinase
VE-cadherin	Vascular endothelial cadherin
TRAPPII	Transport protein particle II
FERARI	Factors for endosome recycling and Rab interactions
Baz	Bazooka, *Drosophila* Par3 homolog
AQP3	Aquaporin3
RUSH	Retention using selective hooks
Capu	Cappuccino protein

7 List of Figures

8 References

Aberle, H., Butz, S., Stappert, J., Weissig, H., Kemler, R., & Hoschuetzky, H. (1994). Assembly of the cadherin-catenin complex in vitro with recombinant proteins. *Journal of Cell Science*, *107*(12), 3655–3663. https://doi.org/10.1242/jcs.107.12.3655

Aguilar-Aragon, M., Fletcher, G., & Thompson, B. J. (2020). The cytoskeletal motor proteins Dynein and MyoV direct apical transport of Crumbs. *Developmental Biology*, *459*(2), 126–137. https://doi.org/10.1016/j.ydbio.2019.12.009

Ahmed, S. M., & Macara, I. G. (2017). The Par3 polarity protein is an exocyst receptor essential for mammary cell survival. *Nature Communications*, *8*, 1–15. https://doi.org/10.1038/ncomms14867

Ahmed, S. M., Nishida-Fukuda, H., Li, Y., McDonald, W. H., Gradinaru, C. C., & Macara, I. G. (2018). Exocyst dynamics during vesicle tethering and fusion. *Nature Communications*, *9*(1). https://doi.org/10.1038/s41467-018-07467-5

Akhmanova, A., & Hammer III, J. A. (2010). Linking molecular motors to membrane cargo. *Current Opinion in Cell Biology*, *22*(4), 479–487.

Alexandrov, K., Horiuchi, H., Steele-Mortimer, O., Seabra, M. C., & Zerial, M. (1994). Rab escort protein-1 is a multifunctional protein that accompanies newly prenylated rab proteins to their target membranes. *EMBO Journal*, *13*(22), 5262–5273. https://doi.org/10.1002/j.1460-2075.1994.tb06860.x

Alory, C., & Balch, W. E. (2001). Organization of the Rab-GDI/CHM superfamily: The functional basis for choroideremia disease. *Traffic*, *2*(8), 532–543. https://doi.org/10.1034/j.1600-0854.2001.20803.x

Avrahami, L., Farfara, D., Shaham-Kol, M., Vassar, R., Frenkel, D., & Eldar-Finkelman, H. (2013). Inhibition of glycogen synthase kinase-3 ameliorates β-amyloid pathology and restores lysosomal acidification and mammalian target of rapamycin activity in the alzheimer disease mouse model: In vivo and in vitro studies. *Journal of Biological Chemistry*, *288*(2), 1295–1306. https://doi.org/10.1074/jbc.M112.409250

Babbey, C. M., Ahktar, N., Wang, E., Chen, C. C.-H., Grant, B. D., & Dunn, K. W. (2006). Rab10 Regulates Membrane Transport through Early Endosomes of Polarized Madin-Darby Canine Kidney Cells. *Molecular Biology of the Cell*, *17*, 3156–3175.

Balderhaar, H. J. K., Arlt, H., Ostrowicz, C., Bröcker, C., Sündermann, F., Brandt, R., Babst, M., & Ungermann, C. (2010). The Rab GTPase Ypt7 is linked to retromer-mediated receptor recycling and fusion at the yeast late endosome. *Journal of Cell Science*, *123*(23), 4085–4094. https://doi.org/10.1242/jcs.071977

Bannykh, S. I., Rowe, T., & Balch, W. E. (1996). The organization of endoplasmic reticulum export complexes. *Journal of Cell Biology*, *135*(1), 19–35. https://doi.org/10.1083/jcb.135.1.19

Barinaga-Rementeria Ramirez, I., & Lowe, M. (2009). Golgins and GRASPs: Holding the Golgi together. *Seminars in Cell and Developmental Biology*, *20*(7), 770–779. https://doi.org/10.1016/j.semcdb.2009.03.011

Bärlocher, K., Welin, A., & Hilbi, H. (2017). Formation of the Legionella replicative compartment at the crossroads of retrograde trafficking. *Frontiers in Cellular and Infection Microbiology*, *7*(NOV), 1–8. https://doi.org/10.3389/fcimb.2017.00482

Barlowe, C., Orci, L., Yeung, T., Hosobuchi, M., Hamamoto, S., Salama, N., Rexach, M. F., Ravazzola, M., Amherdt, M., & Schekman, R. (1994). COPII: A membrane coat formed by Sec proteins that drive vesicle budding from the endoplasmic reticulum. *Cell*, *77*(6), 895–907. https://doi.org/10.1016/0092-8674(94)90138-4

Barr, F., & Lambright, D. G. (2010). Rab GEFs and GAPs. *Current Opinion in Cell Biology*, *22*, 461–470.

Beronja, S., Laprise, P., Papoulas, O., Pellikka, M., Sisson, J., & Tepass, U. (2005). Essential function of Drosophila Sec6 in apical exocytosis of epithelial photoreceptor cells. *Journal of Cell Biology*, *169*(4), 635–646. https://doi.org/10.1083/jcb.200410081

Berx, G., Staes, K., van Hengel, J., Molemans, F., Bussemakers, M. J. G., van Bokhoven, A.,

& van Roy, F. (1995). Cloning and Characterization of the HUman Invasion Suppressor Gene E-cadherin (CDH1). *Genomics*, *26*(2), 281–289.
Biswas, K. H., & Zaidel-Bar, R. (2017). Early Events in the assembly of E-cadherin adhesions. *Experimental Cell Research*, *358*(1), 14–19.
Bogard, N., Lan, L., Xu, J., & Cohen, R. S. (2007). Rab11 maintains connections between germline stem cells and niche cells in the Drosophila ovary. *Development*, *134*(19), 3413–3418.
Boncompain, G., Divoux, S., Gareil, N., De Forges, H., Lescure, A., Latreche, L., Mercanti, V., Jollivet, F., Raposo, G., & Perez, F. (2012). Synchronization of secretory protein traffic in populations of cells. *Nature Methods*, *9*(5), 493–498. https://doi.org/10.1038/nmeth.1928
Borghi, N., Sorokina, M., Shcherbakova, O. G., Weis, W. I., Pruitt, B. L., Nelson, W. J., & Dunn, A. R. (2012). E-cadherin is under constitutive actomyosin-generated tension that is increased at cell-cell contacts upon externally applied stretch. *Proceedings of the National Academy of Sciences of the United States of America*, *109*(31), 12568–12573. https://doi.org/10.1073/pnas.1204390109
Boyd, C., Hughes, T., Pypaert, M., & Novick, P. (2004). Vesicles carry most exocyst subunits to exocytic sites marked by the remaining two subunits, Sec3p and Exo70p. *Journal of Cell Biology*, *167*(5), 889–901. https://doi.org/10.1083/jcb.200408124
Bradley, A. O., Vizcarra, C. L., Bailey, H. M., & Quinlan, M. E. (2020). Spire stimulates nucleation by Cappuccino and binds both ends of actin filaments. *Molecular Biology of the Cell*, *31*(4), 273–286. https://doi.org/10.1091/mbc.E19-09-0550
Brand, A. H., & Perrimon, N. (1993). Targeted gene expression as a means of altering cell fates and generating dominant phenotypes. *Development*, *2*, 401–415.
Brankatschk, B., Pons, V., Parton, R. G., & Gruenberg, J. (2011). Role of snx16 in the dynamics of tubulo-cisternal membrane domains of late endosomes. *PLoS ONE*, *6*(7). https://doi.org/10.1371/journal.pone.0021771
Bright, N. A., Davis, L. J., & Luzio, J. P. (2016). Endolysosomes Are the Principal Intracellular Sites of Acid Hydrolase Activity. *Current Biology*, *26*(17), 2233–2245. https://doi.org/10.1016/j.cub.2016.06.046
Brüser, L., & Bogdan, S. (2017). Adherens junctions on the move—membrane trafficking of E-cadherin. *Cold Spring Harbor Perspectives in Biology*, *9*(3). https://doi.org/10.1101/cshperspect.a029140
Bryant, D. M., Kerr, M. C., Hammond, L. A., Joseph, S. R., Mostov, K. E., Teasdale, R. D., & Stow, J. L. (2007). EGF induces macropinocytosis and SNX1-modulated recycling of E-cadherin. *Journal of Cell Science*, *120*(10), 1818–1828. https://doi.org/10.1242/jcs.000653
Bryant, D. M., Wylie, F. G., & Stow, J. L. (2005). Regulation of Endocytosis, Nuclear Translocation, and Signaling of Fibroblast Growth Factor Receptor 1 by E-Cadherin. *Mol Biol Cell*, *16*(January), 14–23. https://doi.org/10.1091/mbc.E04
Bucci, C., Thomsen, P., Nicoziani, P., McCarthy, J., & Van Deurs, B. (2000). Rab7: A key to lysosome biogenesis. *Molecular Biology of the Cell*, *11*(2), 467–480. https://doi.org/10.1091/mbc.11.2.467
Bulgakova, A. N., & Brown, H. N. (2016). Drosophila p120-catenin is crucial for endocytosis of the dynamic E-cadherin-Bazooka complex. *Journal of Cell Science*, *129*(3), 477–482.
Cetera, M., Ramirez-San Juan, G. R., Oakes, P. W., Lewellyn, L., Fairchild, M. J., Tanentzapf, G., Gardel, M. L., & Horne-Badovinac, S. (2014). Epithelial rotation promotes the global alignment of contractile actin bundles during Drosophila egg chamber elongation. *Nature Communications*, *5*, 5511. https://doi.org/10.1038/ncomms6511
Chappuis-Flament, S., Wong, E., Hicks, L. D., Kay, C. M., & Gumbiner, B. M. (2001). Multiple cadherin extracellular repeats mediate homophilic binding and adhesion. *Journal of Cell Biology*, *154*(1), 231–243. https://doi.org/10.1083/jcb.200103143
Chavrier, P., Parton, R. G., Hauri, H. P., Simons, K., & Zerial, M. (1990). Localization of low molecular weight GTP binding proteins to exocytic and endocytic compartments. *Cell*,

62(2), 317–329. https://doi.org/10.1016/0092-8674(90)90369-P
Chen, C. C.-H., Schweinsberg, P. J., Vashist, S., Mareiniss, D. P., Lambie, E. J., & Grant, B. D. (2006). RAB-10 Is Required for Endocytic Recycling in the Caenorhabditis elegans Intestine. *Molecular Biology of the Cell*, *17*, 1286–1297.
Chen, Y.-J., Huang, J., Huang, L., Austin, E., & Hong, Y. (2017). Phosphorylation potential of Drosophila E-cadherin intracellular domain is essential for development and adherens junction biosynthetic dynamics regulation. *Development*, *144*(7), 1242–1248.
Chen, Y. A., Scheller, R. H., & Medical, H. H. (2001). *SNARE-MEDIATED MEMBRANE FUSION*. *2*(February), 98–106.
Chen, Y. T., Stewart, D. B., & Nelson, W. J. (1999). Coupling assembly of the E-cadherin/β-catenin complex to efficient endoplasmic reticulum exit and basal-lateral membrane targeting of E-cadherin in polarized MDCK cells. *Journal of Cell Biology*, *144*(4), 687–699. https://doi.org/10.1083/jcb.144.4.687
Cheng, S. Bin, & Filardo, E. J. (2012). Trans-Golgi network (TGN) as a regulatory node for β1-adrenergic receptor (β1AR) down-modulation and recycling. *Journal of Biological Chemistry*, *287*(17), 14178–14191. https://doi.org/10.1074/jbc.M111.323782
Cheng, J., Grassart, A., & Drubin, D. G. (2012). Myosin 1E coordinates actin assembly and cargo trafficking during clathrin-mediated endocytosis. *Molecular Biology of the Cell*, *23*(15), 2891–2904. https://doi.org/10.1091/mbc.E11-04-0383
Cherry, S., Jin, E. J., Özel, M. N., Lu, Z., Agi, E., Wang, D., Jung, W.-H., Epstein, D., Meinertzhagen, I. A., Chan, C.-C., & Hiesinger, P. R. (2013). Charcot-Marie-Tooth 2B mutations in rab7 cause dosage-dependent neurodegeneration due to partial loss of function. *ELife*, *2*, 1–22. https://doi.org/10.7554/elife.01064
Choi, H. J., Loveless, T., Lynch, A. M., Bang, I., Hardin, J., & Weis, W. I. (2015). A conserved phosphorylation switch controls the interaction between cadherin and β-Catenin in vitro and in vivo. *Developmental Cell*, *33*(1), 82–93. https://doi.org/10.1016/j.devcel.2015.02.005
Classen, A. K., Anderson, K. I., Marois, E., & Eaton, S. (2005). Hexagonal packing of Drosophila wing epithelial cells by the planar cell polarity pathway. *Developmental Cell*, *9*(6), 805–817. https://doi.org/10.1016/j.devcel.2005.10.016
Csaba, Z., Lelouvier, B., Viollet, C., El Ghouzzi, V., Toyama, K., Videau, C., Bernard, V., & Dournaud, P. (2007). Activated somatostatin type 2 receptors traffic in vivo in central neurons from dendrites to the trans Golgi before recycling. *Traffic*, *8*(7), 820–834. https://doi.org/10.1111/j.1600-0854.2007.00580.x
Cullen, P. J., & Steinberg, F. (2018). To degrade or not to degrade: mechanisms and significance of endocytic recycling. *Nature Reviews Molecular Cell Biology*, *19*(11), 679–696. https://doi.org/10.1038/s41580-018-0053-7
Dahlgaard, K., Raposo, A. A. S. F., Niccoli, T., & St Johnston, D. (2007). Capu and Spire Assemble a Cytoplasmic Actin Mesh that Maintains Microtubule Organization in the Drosophila Oocyte. *Developmental Cell*, *13*(4), 539–553. https://doi.org/10.1016/j.devcel.2007.09.003
De Beco, S., Gueudry, C., Amblard, F., & Coscoy, S. (2009). Endocytosis is required for E-cadherin redistribution at mature adherens junctions. *Proceedings of the National Academy of Sciences of the United States of America*, *106*(17), 7010–7015. https://doi.org/10.1073/pnas.0811253106
Desclozeaux, M., Venturato, J., Wylie, F. G., Kay, J. G., Joseph, S. R., Le, H. T., & Stow, J. L. (2008). Active Rab11 and functional recycling endosome are required for E-cadherin trafficking and lumen formation during epithelial morphogenesis. In *American Journal of Physiology - Cell Physiology* (Vol. 295, Issue 2). https://doi.org/10.1152/ajpcell.00097.2008
Drees, F., Pokutta, S., Yamada, S., Nelson, W. J., & Weis, W. I. (2005). α-catenin is a molecular switch that binds E-cadherin-β-catenin and regulates actin-filament assembly. *Cell*, *123*(5), 903–915. https://doi.org/10.1016/j.cell.2005.09.021
Dunst, S., Kazimiers, T., von Zadow, F., Jambor, H., Sagner, A., Brankatschk, B., Mahmoud, A., Spannl, S., Tomancak, P., Eaton, S., & Brankatschk, M. (2015). Endogenously

Tagged Rab Proteins: A Resource to Study Membrane Trafficking in Drosophila. *Developmental Cell*, *33*(3), 351–365. https://doi.org/10.1016/j.devcel.2015.03.022
Eden, E. R., White, I. J., Tsapara, A., & Futter, C. E. (2010). Membrane contacts between endosomes and ER provide sites for PTP1B-epidermal growth factor receptor interaction. *Nature Cell Biology*, *12*(3), 267–272. https://doi.org/10.1038/ncb2026
Escola, J. M., Kuenzi, G., Gaertner, H., Foti, M., & Hartley, O. (2010). CC chemokine receptor 5 (CCR5) desensitization cycling receptors accumulate in the trans-Golgi network. *Journal of Biological Chemistry*, *285*(53), 41772–41780. https://doi.org/10.1074/jbc.M110.153460
Feinstein, T. N., & Listedt, A. D. (2008). GRASP55 Regulates Golgi Ribbon Formation. *Molecular Biology of the Cell*, *19*(July), 2696–2707. https://doi.org/10.1091/mbc.E07
Fili, N., & Toseland, C. P. (2020). Unconventional myosins: How regulation meets function. *International Journal of Molecular Sciences*, *21*(1), 1–25. https://doi.org/10.3390/ijms21010067
Frankel, E. B., & Audhya, A. (2018). ESCRT-dependent cargo sorting at multivesicular endosomes. *Seminars in Cell and Developmental Biology*, *74*, 4–10. https://doi.org/10.1016/j.semcdb.2017.08.020
Franz, A., & Riechmann, V. (2010). Stepwise polarisation of the Drosophila follicular epithelium. *Developmental Biology*, *338*, 136–147.
Friedrich, G. A., Hildebrand, J. D., & Soriano, P. (1997). The secretory protein sec8 is required for paraxial mesoderm formation in the mouse. *Developmental Biology*, *192*(2), 364–374. https://doi.org/10.1006/dbio.1997.8727
Fujita, Y., Krause, G., Scheffner, M., Zechner, D., Leddy, H. E. M., Behrens, J., Sommer, T., & Birchmeier, W. (2002). Hakai, a c-Cbl-like protein, ubiquitinates and induces endocytosis of the E-cadherin complex. *Nature Cell Biology*, *4*(3), 222–231. https://doi.org/10.1038/ncb758
Galletta, B. J., & Cooper, J. A. (2009). Actin and Endocytosis: Mechanisms and Phylogeny. *Current Opinion in Cell Biology*, *21*(1), 20–27. https://doi.org/10.1016/j.ceb.2009.01.006.Actin
Gomez, J. M., Wang, Y., & Riechmann, V. (2012). Tao controls epithelial morphogenesis by promoting fasciclin 2 endocytosis. *Journal of Cell Biology*, *199*(7), 1131–1143. https://doi.org/10.1083/jcb.201207150
Grant, B. D., & Donaldson, J. G. (2009). Pathways and mechanisms of endocytic recycling. *Nature Reviews. Molecular Cell Biology*, *10*(9), 597–608. https://doi.org/10.1038/nrm2755
Green, K. J., Getsios, S., Troyanovsky, S., & Godsel, L. M. (2010). Intercellular junction assembly, dynamics, and homeostasis. *Cold Spring Harbor Perspectives in Biology*, *2*(2), 1–22. https://doi.org/10.1101/cshperspect.a000125
Grenningloh, G., Rehm, E. J., & Goodman, C. S. (1991). Genetic analysis of growth cone guidance in Drosophila: fasciclin II functions as a neuronal recognition molecule. *Cell*, *67*(1), 45–57. https://doi.org/10.1016/0092-8674(91)90571-F
Grote, E., Carr, C. M., & Novick, P. J. (2000). Ordering the final events in yeast exocytosis. *Journal of Cell Biology*, *151*(2), 439–451. https://doi.org/10.1083/jcb.151.2.439
Guerra, F., & Bucci, C. (2016). Multiple Roles of the Small GTPase Rab7. *Cells*, *5*(3), 34. https://doi.org/10.3390/cells5030034
Guo, W., Sacher, M., Barrowman, J., Ferro-Novick, S., & Novick, P. (2000). Protein complexes in transport vesicle targeting. *Trends in Cell Biology*, *10*(6), 251–255. https://doi.org/10.1016/S0962-8924(00)01754-2
Gupta, T., & Schüpbach, T. (2003). Cct1, a phosphatidylcholine biosynthesis enzyme, is required for Drosophila oogenesis and ovarian morphogenesis. *Development*, *130*(24), 6075–6087. https://doi.org/10.1242/dev.00817
Haller, T., Dietl, P., Deetjen, P., & Völkl, H. (1996). The lysosomal compartment as intracellular calcium store in MDCK cells: a possible involvement in InsP3-mediated Ca2+ release. *Cell Calcium*, *19*(2), 157–165. https://doi.org/10.1016/S0143-4160(96)90084-6

Hammer, J. A., & Sellers, J. R. (2012). Walking to work: Roles for class v myosins as cargo transporters. *Nature Reviews Molecular Cell Biology*, *13*(1), 13–26. https://doi.org/10.1038/nrm3248
Hammer, J. A., & Wagner, W. (2013). Functions of class v myosins in neurons. *Journal of Biological Chemistry*, *288*(40), 28428–28434. https://doi.org/10.1074/jbc.R113.514497
Harris, T. J. C., & Tepass, U. (2010). Adherens junctions: From molecules to morphogenesis. *Nature Reviews Molecular Cell Biology*, *11*(7), 502–514. https://doi.org/10.1038/nrm2927
Hartman, M. A., & Spudich, J. A. (2012). The myosin superfamily at a glance. *Journal of Cell Science*, *125*(7), 1627–1632. https://doi.org/10.1242/jcs.094300
Hartsock, A., & Nelson, W. J. (2012). Competitive regulation of E-cadherin juxtamembrane domain degradation by p120-catenin binding and Hakai-mediated ubiquitination. *PLoS ONE*, *7*(5), 1–14. https://doi.org/10.1371/journal.pone.0037476
Hayashi, T., & Carthew, R. W. (2004). Surface mechanics mediate pattern formation in the developing retina. *Nature*, *431*(7009), 647–652. https://doi.org/10.1038/nature02952
He, B., & Guo, W. (2009). The Exocyst Complex in Polarized Exocytosis. *Current Opinion in Cell Biology*, *21*(4), 537–542. https://doi.org/10.1016/j.ceb.2009.04.007.The
He, L., Wang, X., Tang, H. L., & Montell, D. J. (2010). Tissue elongation requires oscillating contractions of a basal actomyosin network. *Nature Cell Biology*, *12*(12), 1133–1142. https://doi.org/10.1038/ncb2124
Heider, M. R., Gu, M., Duffy, C. M., Mirza, A. M., Marcotte, L. L., Walls, A. C., Farrall, N., Hakhverdyan, Z., Field, M. C., & Michael, P. (2016). Subunit connectivity, assembly determinants, and architecture of the yeast exocyst complex. *Nat Struct Mol Biol*, *23*(1), 59–66. https://doi.org/10.1038/nsmb.3146.Subunit
Heigwer, F., Port, F., & Boutros, M. (2018). RNA Interference (RNAi) Screening in Drosophila. *Genetics*, *208*, 853–874.
Heissler, S. M., & Sellers, J. R. (2016). Kinetic Adaptations of Myosins for their Diverse cellular Functions. *Traffic*, *17*(8), 839–859. https://doi.org/10.1016/j.physbeh.2017.03.040
Hesketh, G. G., Wartosch, L., Davis, L. J., Bright, N. A., & Luzio, J. P. (2018). The Lysosome and Intracellular Signalling. In *Progress in molecular and subcellular biology* (Vol. 57). Springer International Publishing. https://doi.org/10.1007/978-3-319-96704-2_6
Hill, E., Van Der Kaay, J., Downes, C. P., & Smythe, E. (2001). The role of dynamin and its binding partners in coated pit invagination and scission. *Journal of Cell Biology*, *152*(2), 309–323. https://doi.org/10.1083/jcb.152.2.309
Hirohashi, S. (1998). Inactivation of the E-Cadherin-Mediated Cell. *American Journal of Pathology*, *153*(2), 333–339.
Hoekstra, D., Tyteca, D., & van IJzendoorn, S. C. D. (2004). The subapical compartment: A traffic center in membrane polarity development. *Journal of Cell Science*, *117*(11), 2183–2192. https://doi.org/10.1242/jcs.01217
Hoepfner, S., Severin, F., Cabezas, A., Habermann, B., Runge, A., Gillooly, D., Stenmark, H., & Zerial, M. (2005). Modulation of receptor recycling and degradation by the endosomal kinesin KIF16B. *Cell*, *121*(3), 437–450. https://doi.org/10.1016/j.cell.2005.02.017
Hong, Y. (2018). aPKC: The Kinase that Phosphorylates Cell Polarity. *F1000Research*, *7*, 1–8. https://doi.org/10.12688/f1000research.14427.1
Hong, Y., Stronach, B., Perrimon, N., Jan, L. Y., & Jan, Y. N. (2001). Drosophila Stardust interacts with Crumbs to control polarity of epithelia but not neuroblasts. *Nature*, *414*(6864), 634–638. https://doi.org/10.1038/414634a
Horne-Badovinac, S., & Bilder, D. (2005). Mass transit: Epithelial morphogenesis in the Drosophila egg chamber. *Developmental Dynamics*, *232*(3), 559–574. https://doi.org/10.1002/dvdy.20286
Hsu, S. C., Ting, A. E., Hazuka, C. D., Davanger, S., Kenny, J. W., Kee, Y., & Scheller, R. H. (1996). The mammalian brain rsec6/8 complex. *Neuron*, *17*(6), 1209–1219. https://doi.org/10.1016/S0896-6273(00)80251-2

Huang, R. Y. J., Guilford, P., & Thiery, J. P. (2012). Early events in cell adhesion and polarity during epithelialmesenchymal transition. *Journal of Cell Science*, *125*(19), 4417–4422. https://doi.org/10.1242/jcs.099697

Huber, A. H., & Weis, W. I. (2001). The structure of the β-catenin/E-cadherin complex and the molecular basis of diverse ligand recognition by β-catenin. *Cell*, *105*(3), 391–402. https://doi.org/10.1016/S0092-8674(01)00330-0

Huotari, J., & Helenius, A. (2011). Endosome maturation. *EMBO Journal*, *30*(17), 3481–3500. https://doi.org/10.1038/emboj.2011.286

Ishiuchi, T., & Takeichi, M. (2011). Willin and Par3 cooperatively regulate epithelial apical constriction through aPKC-mediated ROCK phosphorylation. *Nature Cell Biology*, *13*(7), 860–866. https://doi.org/10.1038/ncb2274

Jan, C. H., Williams, C. C., & Weissman, J. S. (2015). Principles of ER coranslational translocation revealed by proximity-specific ribosome profiling. *Science*, *346*. https://doi.org/10.1126/science.1257521.Principles

Jaskulska, A., Janecka, A. E., & Gach-Janczak, K. (2021). Thapsigargin—from traditional medicine to anticancer drug. *International Journal of Molecular Sciences*, *22*(1), 1–12. https://doi.org/10.3390/ijms22010004

Jin, Y., Sultana, A., Gandhi, P., Franklin, E., Hamamoto, S., Khan, A. R., Munson, M., Schekman, R., & Weisman, L. S. (2011). Myosin V transports secretory vesicles via a Rab GTPase cascade and interaction with the exocyst complex. *Developmental Cell*, *21*(6), 1156–1170. https://doi.org/10.1016/j.devcel.2011.10.009

Johnson, D. E., Ostrowski, P., Jaumouillé, V., & Grinstein, S. (2016). The position of lysosomes within the cell determines their luminal pH. *The Journal of Cell Biology*, *212*(6), 677–692. https://doi.org/10.1083/jcb.201507112

Kametani, Y., & Takeichi, M. (2007). Basal-to-apical cadherin flow at cell junctions. *Nature Cell Biology*, *9*(1), 92–98. https://doi.org/10.1038/ncb1520

Katoh, Y., Nozaki, S., Hartanto, D., Miyano, R., & Nakayama, K. (2015). Architectures of multisubunit complexes revealed by a visible immunoprecipitation assay using fluorescent fusion proteins. *Journal of Cell Science*, *128*(12), 2351–2362. https://doi.org/10.1242/jcs.168740

Kelly, B. T., & Owen, D. J. (2011). Endocytic sorting of transmembrane protein cargo. *Current Opinion in Cell Biology*, *23*, 404–412.

Kelly, E. E., Horgan, C. P., Goud, B., & McCaffrey, M. W. (2012). The Rab family of proteins: 25 years on. *Biochemical Society Transactions*, *40*, 1337–1347.

Keppler, A., Gendreizig, S., Gronemeyer, T., Pick, H., Vogel, H., & Johnsson, K. (2003). A general method for the covalent labeling of fusion proteins with small molecules in vivo. *Nature Biotechnology*, *21*(1), 86–89. https://doi.org/10.1038/nbt765

Keppler, A., Kindermann, M., Gendreizig, S., Pick, H., Vogel, H., & Johnsson, K. (2004). Labeling of fusion proteins of O6-alkylguanine-DNA alkyltransferase with small molecules in vivo and in vitro. *Methods*, *32*(4), 437–444. https://doi.org/10.1016/j.ymeth.2003.10.007

Kerr, M. C., Lindsay, M. R., Luetterforst, R., Hamilton, N., Simpson, F., Parton, R. G., Gleeson, P. A., & Teasdale, R. D. (2006). Visualisation of macropinosome maturation by the recruitment of sorting nexins. *Journal of Cell Science*, *119*(19), 3967–3980. https://doi.org/10.1242/jcs.03167

Kirchhausen, T., Owen, D., & Harrison, S. C. (2014). Molecular Structure, Function, and Dynamics of Clathrin-Mediated Membrane Traffic. *Cold Spring Harbor Perspectives in Biology*, *6*.

Klumperman, J., & Raposo, G. (2014). The complex ultrastructure of the endolysosomal system. *Cold Spring Harbor Perspectives in Biology*, *6*(10), 1–22. https://doi.org/10.1101/cshperspect.a016857

Kobielak, A., & Fuchs, E. (2004). α-catenin: At the junction of intercellular adhesion and actin dynamics. *Nature Reviews Molecular Cell Biology*, *5*(8), 614–625. https://doi.org/10.1038/nrm1433

Kodera, N., & Ando, T. (2014). The path to visualization of walking myosin V by high-speed

atomic force microscopy. *Biophysical Reviews*, *6*(3–4), 237–260. https://doi.org/10.1007/s12551-014-0141-7
Kondylis, V., & Rabouille, C. (2009). The Golgi apparatus: Lessons from Drosophila. *FEBS Letters*, *583*(23), 3827–3838. https://doi.org/10.1016/j.febslet.2009.09.048
Korn, E. D. (2000). Coevolution of head, neck, and tail domains of myosin heavy chains. *The Proceedings of the National Academy of Sciences (PNAS)*, *97*(23), 12559–12564.
Kouranti, I., Sachse, M., Arouche, N., Goud, B., & Echard, A. (2006). Rab35 Regulates an Endocytic Recycling Pathway Essential for the Terminal Steps of Cytokinesis. *Current Biology*, *16*(17), 1719–1725. https://doi.org/10.1016/j.cub.2006.07.020
Krauss, J., López de Quinto, S., Nüsslein-Volhard, C., & Ephrussi, A. (2009). Myosin-V Regulates oskar mRNA Localization in the Drosophila Oocyte. *Current Biology*, *19*(12), 1058–1063. https://doi.org/10.1016/j.cub.2009.04.062
Krendel, M., & Mooseker, M. S. (2005). Myosins: Tails (and heads) of functional diversity. *Physiology*, *4*, 239–251. https://doi.org/10.1152/physiol.00014.2005
Kulkarni-Gosavi, P., Makhoul, C., & Gleeson, P. A. (2019). Form and function of the Golgi apparatus: scaffolds, cytoskeleton and signalling. *FEBS Letters*, *593*(17), 2289–2305. https://doi.org/10.1002/1873-3468.13567
Kurokawa, K., & Nakano, A. (2019). The ER exit sites are specialized ER zones for the transport of cargo proteins from the ER to the Golgi apparatus. *Journal of Biochemistry*, *165*(2), 109–114. https://doi.org/10.1093/jb/mvy080
Laiouar, S., Berns, N., Brech, A., & Riechmann, V. (2020). RabX1 Organizes a Late Endosomal Compartment that Forms Tubular Connections to Lysosomes Consistent with a “Kiss and Run” Mechanism. *Current Biology*, *30*(7), 1177-1188.e5. https://doi.org/10.1016/j.cub.2020.01.048
Laisne, M. C., Michallet, S., & Lafanechère, L. (2021). Characterization of microtubule destabilizing drugs: A quantitative cell-based assay that bridges the gap between tubulin based- and cytotoxicity assays. *Cancers*, *13*(20). https://doi.org/10.3390/cancers13205226
Langevin, J., Morgan, M. J., Rosse, C., Racine, V., Sibarita, J. B., Aresta, S., Murthy, M., Schwarz, T., Camonis, J., & Bellaïche, Y. (2005). Drosophila Exocyst Components Sec5, Sec6, and Sec15 Regulate DE-Cadherin Trafficking from Recycling Endosomes to the Plasma Membrane. *Developmental Cell*, *9*.
Langford, G. M. (2002). Myosin-V, a versatile motor for short-range vesicle transport. *Traffic*, *3*(12), 859–865. https://doi.org/10.1034/j.1600-0854.2002.31202.x
Lapierre, L. A., Kumar, R., Hales, C. M., Navarre, J., Bhartur, S. G., Burnette, J. O., Provance, J., Mercer, J. A., Bähler, M., & Goldenring, J. R. (2001). Myosin Vb is associated with plasma membrane recycling systems. *Molecular Biology of the Cell*, *12*(6), 1843–1857. https://doi.org/10.1091/mbc.12.6.1843
Lau, K. M., & McGlade, C. J. (2011). NUmb is a negative regulator of HGF dependent cell scattering and Rac1 activation. *Experimental Cell Research*, *317*(4), 539–551.
Le, T. L., Yap, A. S., & Stow, J. L. (1999). Recycling of E-cadherin: A potential mechanism for regulating cadherin dynamics. *Journal of Cell Biology*, *146*(1), 219–232. https://doi.org/10.1083/jcb.146.1.219
Lebo, D. P. V., & McCall, K. (2021). Murder on the ovarian express: A tale of non-autonomous cell death in the Drosophila ovary. *Cells*, *10*(6). https://doi.org/10.3390/cells10061454
Levayer, R., Pelissier-Monier, A., & Lecuit, T. (2011). Spatial regulation of Dia and Myosin-II by RhoGEF2 controls initiation of E-cadherin endocytosis during epithelial morphogenesis. *Nature Cell Biology*, *13*(5), 529–540. https://doi.org/10.1038/ncb2224
Li, B. X., Satoh, A. K., & Ready, D. F. (2007). Myosin V, Rab11, and dRip11 direct apical secretion and cellular morphogenesis in developing Drosophila photoreceptors. *Journal of Cell Biology*, *177*(4), 659–669. https://doi.org/10.1083/jcb.200610157
Lin, H. (2002). The stem-cell niche theory: Lessons from flies. *Nature Reviews Genetics*, *3*(12), 931–940. https://doi.org/10.1038/nrg952
Liu, T.-T., Gomez, T. S., Sackey, B. K., Billadeau, D. D., & Burd, C. G. (2012). Rab GTPase

regulation of retromer-mediated cargo export during endosome maturation. *Molecular Biology of the Cell*, *23*(13), 2505–2515. https://doi.org/10.1091/mbc.e11-11-0915
Lock, J. G., Hammond, L. A., Houghton, F., Gleeson, P. A., & Stow, J. L. (2005). E-cadherin transport from the trans-Golgi network in tubulovesicular carriers is selectively regulated by Golgin-97. *Traffic*, *6*(12), 1142–1156. https://doi.org/10.1111/j.1600-0854.2005.00349.x
Low, P., Varga, Á., Pircs, K., Nagy, P., Szatmári, Z., Sass, M., & Juhász, G. (2013). Impaired proteasomal degradation enhances autophagy via hypoxia signaling in Drosophila. *BMC Cell Biology*, *14*(1). https://doi.org/10.1186/1471-2121-14-29
Lu, Z., Ghosh, S., Wang, Z., & Hunter, T. (2003). Downregulation of caveolin-1 function by EGF leads to the loss of E-cadherin, increased transcriptional activity of β-catenin, and enhanced tumor cell invasion. *Cancer Cell*, *4*(6), 499–515. https://doi.org/10.1016/S1535-6108(03)00304-0
Lund, V. K., Madsen, K. L., & Kjaerulff, O. (2018). Drosophila Rab2 controls endosome-lysosome fusion and LAMP delivery to late endosomes. *Autophagy*, *14*(9), 1520–1542. https://doi.org/10.1080/15548627.2018.1458170
Magadán, J. G., Barbieri, M. A., Mesa, R., Stahl, P. D., & Mayorga, L. S. (2006). Rab22a Regulates the Sorting of Transferrin to Recycling Endosomes. *Molecular and Cellular Biology*, *26*(7), 2595–2614. https://doi.org/10.1128/mcb.26.7.2595-2614.2006
Margolis, J., & Spradling, A. (1995). Identification and behavior of epithelial stem cells in the Drosophila ovary. *Development*, *121*(11).
Maxfield, F. R., & McGraw, T. E. (2004). Endocytic recycling. *Nature Reviews Molecular Cell Biology*, *5*(2), 121–132. https://doi.org/10.1038/nrm1315
McNally, K. E., & Cullen, P. J. (2018). Endosomal Retrieval of Cargo: Retromer Is Not Alone. *Trends in Cell Biology*, *28*(10), 807–822. https://doi.org/10.1016/j.tcb.2018.06.005
Mehta A.D., Rock R.S., Rief M., Spudich J.A., Mooseker M.S., & Cheney R.E. (1999). Myosin-V is a processive actin-based motor. *Nature*, *400*(August 1999), 590–593.
Michel, M., Raabe, I., Kupinski, A. P., Pérez-Palencia, R., & Bökel, C. (2011). Local BMP receptor activation at adherens junctions in the Drosophila germline stem cell niche. *Nature Communications*, *2*(1). https://doi.org/10.1038/ncomms1426
Miranda, K. C., Khromykh, T., Christy, P., Le, T. L., Gottardi, C. J., Yap, A. S., Stow, J. L., & Teasdale, R. D. (2001). A Dileucine Motif Targets E-cadherin to the Basolateral Cell Surface in Madin-Darby Canine Kidney and LLC-PK1 Epithelial Cells. *Journal of Biological Chemistry*, *276*(25), 22565–22572. https://doi.org/10.1074/jbc.M101907200
Miyashita, Y., & Ozawa, M. (2007). A dileucine motif in its cytoplasmic domain directs β-catenin-uncoupled E-cadherin to the lysosome. *Journal of Cell Science*, *120*(24), 4395–4406. https://doi.org/10.1242/jcs.03489
Munro, S. (2011). The golgin coiled-coil proteins of the Golgi apparatus. *Cold Spring Harbor Perspectives in Biology*, *3*(6), 1–14. https://doi.org/10.1101/cshperspect.a005256
Murray, D. H., Jahnel, M., Lauer, J., Avellaneda, M. J., Brouilly, N., Cezanne, A., Morales-Navarrete, H., Perini, E. D., Ferguson, C., Lupas, A. N., Kalaidzidis, Y., Parton, R. G., Grill, S. W., & Zerial, M. (2016). *An endosomal tether undergoes an entropic collapse to bring vesicles together*.
Murthy, M., Garza, D., Scheller, R. H., & Schwarz, T. L. (2003). Mutations in the exocyst component Sec5 disrupt neuronal membrane traffic, but neurotransmitter release persists. *Neuron*, *37*(3), 433–447. https://doi.org/10.1016/S0896-6273(03)00031-X
Murthy, M., Ranjan, R., Denef, N., Higashi, M. E. L., Schupbach, T., & Schwarz, T. L. (2005). Sec6 mutations and the Drosophila exocyst complex. *Journal of Cell Science*, *118*(6), 1139–1150. https://doi.org/10.1242/jcs.01644
Myster, S. H., Cavallo, R., Anderson, C. T., Fox, D. T., & Peifer, M. (2003). Drosophila p120 catenin plays a supporting role in cell adhesion but is not an essential adherens junction component. *Journal of Cell Biology*, *160*(3), 433–449. https://doi.org/10.1083/jcb.200211083
Nagar, B., J, M. O., & Rini, J. M. (1996). *Structural basis of calcium- induced E-cadherin rigidification and dimerization*. *380*(March), 360–364.

Nanes, A. B., & Kowalczyk, P. A. (2012). Adherens junction turnover: regulating adhesion through cadherin endocytosis, degradation, and recycling. *Sub-Cellular Biochemistry*, *60*, 197–222. https://doi.org/10.1007/978-94-007-4186-7

Naslavsky, N., & Caplan, S. (2018). The enigmatic endosome - Sorting the ins and outs of endocytic trafficking. *Journal of Cell Science*, *131*(13). https://doi.org/10.1242/jcs.216499

Nejsum, L. N., & Nelson, W. J. (2007). A molecular mechanism directly linking E-cadherin adhesion to initiation of epithelial cell surface polarity. *Journal of Cell Biology*, *178*(2), 323–335. https://doi.org/10.1083/jcb.200705094

Nielsen, E., Severin, F., Backer, J. M., Hyman, A. A., & Zerial, M. (1999). Rab5 regulates motility of early endosomes on microtubules. *Nature Cell Biology*, *1*(6), 376–382. https://doi.org/10.1038/14075

O`Connell, C. B., Tyska, M. J., & Mooseker, M. S. (2007). Myosin at work: Motor adaptations for a variety of cellular functions. *Biochimica et Biophysica Acta (BBA) - Biomembranes*, *1773*(5), 615–630.

Oda, H., Uemura, T., Harada, Y., Iwai, Y., & Takeichi, M. (1994). A Drosophila homolog of cadherin associated with armadillo and essential for embryonic cell-cell adhesion. *Developmental Biology*, *165*(2), 716–726.

Ogata, T., & Yamasaki, Y. (1997). Ultra-high-resolution scanning electron microscopy of mitochondria and sarcoplasmic reticulum arrangment in human red, whote, and intermediate muscle fibers. *The Anatomical Recorc*, *248*(2), 214–223.

Olivieri, D., Sykora, M. M., Sachidanandam, R., Mechtler, K., & Brennecke, J. (2010). An in vivo RNAi assay identifies major genetic and cellular requirements for primary piRNA biogenesis in Drosophila. *The EMBO Journal*, *29*(19), 3301. https://doi.org/10.1038/EMBOJ.2010.212

Olkkonen, V. M., & Slenmark, H. (1997). Role of Rab GTPases in Membrane Traffic. *International Review of Cytology*, *176*, 1–85.

Pacquelet, A., Lin, L., & Rørth, P. (2003). Binding site for p120/δ-catenin is not required for Drosophila E-cadherin function in vivo. *Journal of Cell Biology*, *160*(3), 313–319. https://doi.org/10.1083/jcb.200207160

Pacquelet, A., & Rørth, P. (2005). Regulatory mechanisms required for DE-cadherin function in cell migration and other types of adhesion. *Journal of Cell Biology*, *170*(5), 803–812. https://doi.org/10.1083/jcb.200506131

Parsons, J. T., Horwitz, A. R., & Schwartz, M. A. (2010). Cell adhesion: Integrating cytoskeletal dynamics and cellular tension. *Nature Reviews Molecular Cell Biology*, *11*(9), 633–643. https://doi.org/10.1038/nrm2957

Patel, N. H., Snow, P. M., & Goodman, C. S. (1987). Characterization and cloning of fasciclin III: A glycoprotein expressed on a subset of neurons and axon pathways in Drosophila. *Cell*, *48*(6), 975–988. https://doi.org/10.1016/0092-8674(87)90706-9

Paterson, A. D., Parton, R. G., Ferguson, C., Stow, J. L., & Yap, A. S. (2003). Characterization of E-cadherin endocytosis in isolated MCF-7 and Chinese hamster ovary cells. The initial fate of unbound E-cadherin. *Journal of Biological Chemistry*, *278*(23), 21050–21057. https://doi.org/10.1074/jbc.M300082200

Pelham, H. R. B. (2002). Insights from yeast endosomes. *Current Opinion in Cell Biology*, *14*(4), 454–462. https://doi.org/10.1016/S0955-0674(02)00352-6

Peter, B. J., Kent, H. M., Mills, I. G., Vallis, Y., Butler, P. J. G., Evans, P. R., & McMahon, H. T. (2004). BAR Domains as Sensors of Membrane Curvature: The Amphiphysin BAR Structure. *Science*, *303*(5657), 495–499. https://doi.org/10.1126/science.1092586

Pfeffer, S., & Aivazian, D. (2004). Targeting Rab GTPases to distinct membrane compartments. *Nature Reviews Molecular Cell Biology*, *5*(11), 886–896. https://doi.org/10.1038/nrm1500

Pfeffer, S. R. (2005). Structural clues to Rab GTPase functional diversity. *The Journal of Biological Chemistry*, *280*(16), 15485–15488. https://doi.org/10.1074/jbc.R500003200

Pfeffer, S. R. (2013). Rab GTPase regulation of membrane identity. *Current Opinion in Cell Biology*, *25*(4), 414–419. https://doi.org/10.1016/j.ceb.2013.04.002

Phillips, M. J., & Voeltz, G. K. (2016). Structure and function of ER membrane contact sites with other organelles. *Nature Reviews Molecular Cell Biology*, *17*(2), 69–82. https://doi.org/10.1038/nrm.2015.8

Pocha, S. M., Wassmer, T., Niehage, C., Hoflack, B., & Knust, E. (2011). Retromer controls epithelial cell polarity by trafficking the apical determinant crumbs. *Current Biology*, *21*(13), 1111–1117. https://doi.org/10.1016/j.cub.2011.05.007

Pollard, T. D. (2016). Actin and Actin-Binding Proteins. *Cold Spring Harbor Perspectives in Biology*, *8*.

Prigent, M., Dubois, T., Raposo, G., Derrien, V., Tenza, D., Rossé, C., Camonis, J., & Chavrier, P. (2003). ARF6 controls post-endocytic recycling through its downstream exocyst complex effector. *Journal of Cell Biology*, *163*(5), 1111–1121. https://doi.org/10.1083/jcb.200305029

Priya, A., Kalaidzidis, I. V., Kalaidzidis, Y., Lambright, D., & Datta, S. (2015). Molecular Insights into Rab7-Mediated Endosomal Recruitment of Core Retromer: Deciphering the Role of Vps26 and Vps35. *Traffic*, *16*(1), 68–84. https://doi.org/10.1111/tra.12237

Puthenveedu, M. A., Bachert, C., Puri, S., Lanni, F., & Linstedt, A. D. (2006). GM130 and GRASP65-dependent lateral cisternal fusion allows uniform Golgi-enzyme distribution. *Nature Cell Biology*, *8*(3), 238–248. https://doi.org/10.1038/ncb1366

Pylypenko, O., Welz, T., Tittel, J., Kollmar, M., Chardon, F., Malherbe, G., Weiss, S., Michel, C. I. L., Samol-Wolf, A., Grasskamp, A. T., Hume, A., Goud, B., Baron, B., England, P., Titus, M. A., Schwille, P., Weidemann, T., Houdusse, A., & Kerkhoff, E. (2016). Coordinated recruitment of spir actin nucleators and myosin V motors to rab11 vesicle membranes. *ELife*, *5*(September), 1–25. https://doi.org/10.7554/eLife.17523

Qin, Y., Capaldo, C., Gumbiner, B. M., & Macara, I. G. (2005). The mammalian Scribble polarity protein regulates epithelial cell adhesion and migration through E-cadherin. *Journal of Cell Biology*, *171*(6), 1061–1071. https://doi.org/10.1083/jcb.200506094

Ravichandran, Y., Goud, B., & Manneville, J. B. (2020). The Golgi apparatus and cell polarity: Roles of the cytoskeleton, the Golgi matrix, and Golgi membranes. *Current Opinion in Cell Biology*, *62*, 104–113. https://doi.org/10.1016/j.ceb.2019.10.003

Reid, D. W. (2017). Diversity and selectivity in mRNA translation on the endoplasmic. *Physiology & Behavior*, *176*(10), 139–148. https://doi.org/10.1038/nrm3958.Diversity

Ridley, A. J. (2011). Life at the leading edge. *Cell*, *145*(7), 1012–1022. https://doi.org/10.1016/j.cell.2011.06.010

Riedel, F., Galindo, A., Muschalik, N., & Munro, S. (2018). The two TRAPP complexes of metazoans have distinct roles and act on different Rab GTPases. *Journal of Cell Biology*, *217*(2), 601–617. https://doi.org/10.1083/jcb.201705068

Riedel, F., Gillingham, A. K., Rosa-Ferreira, C., Galindo, A., & Munro, S. (2016). *An antibody toolkit for the study of membrane traffic in Drosophila melanogaster*. https://doi.org/10.1242/bio.018937

Riedl, J., Crevenna, A. H., Kessenbrock, K., Yu, J. H., Neukirchen, D., Bista, M., Bradke, F., Jenne, D., Holak, T. A., Werb, Z., Sixt, M., & Wedlich-Soldner, R. (2008). Lifeact: A versatile marker to visualize F-actin. *Nature Methods*, *5*(7), 605–607. https://doi.org/10.1038/nmeth.1220

Rimm, D. L., Koslov, E. R., Kebriaei, P., Cianci, C. D., & Morrow, J. S. (1995). α1(E)-catenin is an actin-binding and -bundling protein mediating the attachment of F-actin to the membrane adhesion complex. *Proceedings of the National Academy of Sciences of the United States of America*, *92*(19), 8813–8817. https://doi.org/10.1073/pnas.92.19.8813

Rink, J., Ghigo, E., Kalaidzidis, Y., & Zerial, M. (2005). Rab conversion as a mechanism of progression from early to late endosomes. *Cell*, *122*(5), 735–749. https://doi.org/10.1016/j.cell.2005.06.043

Rocha, N., Kuijl, C., Van Der Kant, R., Janssen, L., Houben, D., Janssen, H., Zwart, W., & Neefjes, J. (2009). Cholesterol sensor ORP1L contacts the ER protein VAP to control Rab7-RILP-p150Glued and late endosome positioning. *Journal of Cell Biology*, *185*(7), 1209–1225. https://doi.org/10.1083/jcb.200811005

Rodal, A. A., Blunk, A. D., Akbergenova, Y., Jorquera, R. A., Buhl, L. K., & Littleton, J. T.

(2011). A presynaptic endosomal trafficking pathway controls synaptic growth signaling. *Journal of Cell Biology*, *193*(1), 201–217. https://doi.org/10.1083/jcb.201009052
Rojas, R., van Vlijmen, T., Mardones, G. A., Prabhu, Y., Rojas, A. L., Mohammed, S., Heck, A. J. R., Raposo, G., van der Sluijs, P., & Bonifacino, J. S. (2008). Regulation of retromer recruitment to endosomes by sequential action of Rab5 and Rab7. *The Journal of Cell Biology*, *183*(3), 513–526. https://doi.org/10.1083/jcb.200804048
Roland, J. T., Lapierre, L. A., & Goldenring, J. R. (2009). Alternative splicing in class v myosins determines association with rab10. *Journal of Biological Chemistry*, *284*(2), 1213–1223. https://doi.org/10.1074/jbc.M805957200
Romani, P., Valcarcel-Jimenez, L., Frezza, C., & Dupont, S. (2021). Crosstalk between mechanotransduction and metabolism. *Nature Reviews Molecular Cell Biology*, *22*(1), 22–38. https://doi.org/10.1038/s41580-020-00306-w
Saftig, P., & Klumperman, J. (2009). Lysosome biogenesis and lysosomal membrane proteins: Trafficking meets function. *Nature Reviews Molecular Cell Biology*, *10*(9), 623–635. https://doi.org/10.1038/nrm2745
Sato, K., Watanabe, T., Wang, S., Kakeno, M., Matsuzawa, K., Matsui, T., Yokoi, K., Murase, K., Sugiyama, I., Ozawa, M., & Kaibuchi, K. (2011). Numb controls E-cadherin endocytosis through p120 catenin with aPKC. *Molecular Biology of the Cell*, *22*(17), 3103–3119. https://doi.org/10.1091/mbc.E11-03-0274
Sato, M., Sato, K., Liou, W., Pant, S., Harada, A., & Grant, B. D. (2008). Regulation of endocytic recycling by C. elegans Rab35 and its regulator RME-4, a coated-pit protein. *EMBO Journal*, *27*(8), 1183–1196. https://doi.org/10.1038/emboj.2008.54
Satoh, A. K., O'Tousa, J. E., Ozaki, K., & Ready, D. F. (2005). Rab11 mediates post-Golgi trafficking of rhodopsin to the photosensitive apical membrane of Drosophila photoreceptors. *Development*, *132*(7), 1487–1497. https://doi.org/10.1242/dev.01704
Sawyer, J. K., Harris, N. J., Slep, K. C., Gaul, U., & Peifer, M. (2009). The Drosophila afadin homologue Canoe regulates linkage of the actin cytoskeleton to adherens junctions during apical constriction. *Journal of Cell Biology*, *186*(1), 57–73. https://doi.org/10.1083/jcb.200904001
Schill, N. J., Hedman, A. C., Choi, S., & Anderson, R. A. (2014). Isoform 5 of PIPKIγ regulates the endosomal trafficking and degradation of E-cadherin. *Journal of Cell Science*, *127*(10), 2189–2203. https://doi.org/10.1242/jcs.132423
Schindelin, J., Arganda-Carreras, I., Frise, E., Kaynig, V., Longair, M., Pietzsch, T., Preibisch, S., Rueden, C., Saalfeld, S., Schmid, B., Tinevez, J. Y., White, D. J., Hartenstein, V., Eliceiri, K., Tomancak, P., & Cardona, A. (2012). Fiji: An open-source platform for biological-image analysis. *Nature Methods*, *9*(7), 676–682. https://doi.org/10.1038/nmeth.2019
Schneider-Poetsch, T., Ju, J., Eyler, D. E., Dang, Y. D., Bhat, S., Merrick, W. C., Green, R., Shen, B., & Liu, J. O. (2010). Inhibition of Eukaryotic Translation Elongation by Cycloheximide and Lactimidomycin. *Nat Chem Biol*, 209–217. https://doi.org/10.1038/nchembio.304.Inhibition
Schu, P. (2001). Vesicular protein transport. *Pharmacogenomics Journal*, *1*(4), 262–271. https://doi.org/10.1038/sj.tpj.6500055
Schuh, M. (2011). An actin-dependent mechanism for long-range vesicle transport. *Nature Cell Biology*, *13*(12), 1431–1436. https://doi.org/10.1038/ncb2353
Scott, C. C., Vacca, F., & Gruenberg, J. (2014). Endosome maturation, transport and functions. *Seminars in Cell and Developmental Biology*, *31*, 2–10. https://doi.org/10.1016/j.semcdb.2014.03.034
Seaman, M. N. J. (2004). Cargo-selective endosomal sorting for retrieval to the Golgi requires retromer. *Journal of Cell Biology*, *165*(1), 111–122. https://doi.org/10.1083/jcb.200312034
Seaman, M. N. J., Harbour, M. E., Tattersall, D., Read, E., & Bright, N. (2009). Membrane recruitment of the cargo-selective retromer subcomplex is catalysed by the small GTPase Rab7 and inhibited by the Rab-GAP TBC1D5. *Journal of Cell Science*, *122*(14), 2371–2382. https://doi.org/10.1242/jcs.048686

Seaman, M. N. J., Marcusson, E. G., Cereghino, J. L., & Emr, S. D. (1997). Endosome to Golgi retrieval of the vacuolar protein sorting receptor, Vps10p, requires the function of the VPS29, VPS30, and VPS35 gene products. *Journal of Cell Biology*, *137*(1), 79–92. https://doi.org/10.1083/jcb.137.1.79

Sellers, J. R. (1999). Myosins: a diverse superfamily. *Biochimica et Biophysica Acta (BBA) - Biomembranes*, *1496*, 3–22.

Shaaban, E. I. A., & Mohammed, S. A. (2021). Targeted liposomal nanodelivery of E-cadherin as potential therapy for acute myeloid leukaemia. *J Nanosci Nanomed*, *5*(3), 4–5.

Shafaq-Zadah, M., Gomes-Santos, C. S., Bardin, S., Maiuri, P., Maurin, M., Iranzo, J., Gautreau, A., Lamaze, C., Caswell, P., Goud, B., & Johannes, L. (2016). Persistent cell migration and adhesion rely on retrograde transport of β 1 integrin. *Nature Cell Biology*, *18*(1), 54–64. https://doi.org/10.1038/ncb3287

Sheff, D. R., Daro, E. A., Hull, M., & Mellman, I. (1999). The receptor recycling pathway contains two distinct populations of early endosomes with different sorting functions. *The Journal of Cell Biology*, *145*(1), 123–139. https://doi.org/10.1083/jcb.145.1.123

Silies, M., & Klämbt, C. (2010). APC/C(Fzr/Cdh1)-dependent regulation of cell adhesion controls glial migration in the Drosophila PNS. *Nature Neuroscience*, *13*(11), 1357–1364. https://doi.org/10.1038/nn.2656

Simonetti, B., & Cullen, P. J. (2019). Actin-dependent endosomal receptor recycling. *Current Opinion in Cell Biology*, *56*, 22–33. https://doi.org/10.1016/j.ceb.2018.08.006

Sirotkin, V., Beltzner, C. C., Marchand, J. B., & Pollard, T. D. (2005). Interactions of WASp, myosin-I, and verprolin with Arp2/3 complex during actin patch assembly in fission yeast. *Journal of Cell Biology*, *170*(4), 637–648. https://doi.org/10.1083/jcb.200502053

Skora, A. D., & Spradling, A. C. (2010). Epigenetic stability increases extensively during Drosophila follicle stem cell differentiation. *Proceedings of the National Academy of Sciences of the United States of America*, *107*(16), 7389–7394. https://doi.org/10.1073/pnas.1003180107

Snow, P. M., Bieber, A. J., & Goodman, C. S. (1989). Fasciclin III: A Novel Homophilic Adhesion Molecule in Drosophila. In *Cell* (Vol. 59).

Solinger, J. A., Rashid, H. O., Prescianotto-Baschong, C., & Spang, A. (2020). FERARI is required for Rab11-dependent endocytic recycling. *Nature Cell Biology*, *22*(2), 213–224. https://doi.org/10.1038/s41556-019-0456-5

Solis, G. P., Hülsbusch, N., Radon, Y., Katanaev, V. L., Plattner, H., & Stuermer, C. A. O. (2013). Reggies/flotillins interact with Rab11a and SNX4 at the tubulovesicular recycling compartment and function in transferrin receptor and E-cadherin trafficking. *Molecular Biology of the Cell*, *24*(17), 2689–2702. https://doi.org/10.1091/mbc.E12-12-0854

Srahna, M., Leyssen, M., Ching, M. C., Fradkin, L. G., Noordermeer, J. N., & Hassan, B. A. (2006). A signaling network for patterning of neuronal connectivity in the Drosophila brain. *PLoS Biology*, *4*(11), 2076–2090. https://doi.org/10.1371/journal.pbio.0040348

Stow, J. L., & Lock, J. G. (2005). Rab11 in Recycling Endosomes Regulates the Sorting and Basolateral Transport of E-Cadherin. *Molecular Biology of the Cell*, *16*(1), 1744–1755. https://doi.org/10.1091/mbc.E04

Sun, Y., Martin, A. C., & Drubin, D. G. (2006). Endocytic Internalization in Budding Yeast Requires Coordinated Actin Nucleation and Myosin Motor Activity. *Developmental Cell*, *11*(1), 33–46. https://doi.org/10.1016/j.devcel.2006.05.008

Szafranski, P., & Goode, S. (2004). A Fasciclin 2 morphogenetic switch organizes epithelial cell cluster polarity and motility. *Development*, *131*(9), 2023–2036. https://doi.org/10.1242/dev.01097

Takeichi, M. (2014). Dynamic contacts: Rearranging adherens junctions to drive epithelial remodelling. *Nature Reviews Molecular Cell Biology*, *15*(6), 397–410. https://doi.org/10.1038/nrm3802

Tepass, U, Tanentzapf, G., Ward, R., & Fehon, R. (2001). Epithelial cell polarity and cell junctions in Drosophila. *Annu. Rev. Dev. Biol.*, *16*, 423–457.

Tepass, Ulrich, Gruszynski-DeFeo, E., Haag, T. A., Omatyar, L., Török, T., & Hartenstein, V.

(1996). shotgun encodes Drosophila E-cadherin and is preferentially required during cell rearrangement in the neurectoderm and other morphogenetically active epithelia. In *Genes and Development* (Vol. 10, Issue 6). https://doi.org/10.1101/gad.10.6.672
Tepass, Ulrich, Theres, C., & Knust, E. (1990). crumbs encodes an EGF-like protein expressed on apical membranes of Drosophila epithelial cells and required for organization of epithelia. *Cell*, *61*(5), 787–799.
TerBush, D. R., Maurice, T., Roth, D., & Novick, P. (1996). The Exocyst is a multiprotein complex required for exocytosis in Saccharomyces cerevisiae. *EMBO Journal*, *15*(23), 6483–6494. https://doi.org/10.1002/j.1460-2075.1996.tb01039.x
Thiery, J. P., & Sleeman, J. P. (2006). Complex networks orchestrate epithelial-mesenchymal transitions. *Nature Reviews Molecular Cell Biology*, *7*(2), 131–142. https://doi.org/10.1038/nrm1835
Thoreson, M. A., Anastasiadis, P. Z., Daniel, J. M., Ireton, R. C., Wheelock, M. J., Johnson, K. R., Hummingbird, D. K., & Reynolds, A. B. (2000). Selective uncoupling of p120(ctn) from E-cadherin disrupts strong adhesion. *Journal of Cell Biology*, *148*(1), 189–201. https://doi.org/10.1083/jcb.148.1.189
Touchot, N., Chardin, P., & Tavitian, A. (1987). Four additional members of the ras gene superfamily isolated by an oligonucleotide strategy: molecular cloning of YPT-related cDNAs from a rat brain library. *Proceedings of the National Academy of Sciences of the United States of America*, *84*(23), 8210–8214. https://doi.org/10.1073/pnas.84.23.8210
Traer, C. J., Rutherford, A. C., Palmer, K. J., Wassmer, T., Oakley, J., Attar, N., Carlton, J. G., Kremerskothen, J., Stephens, D. J., & Cullen, P. J. (2007). SNX4 coordinates endosomal sorting of TfnR with dynein-mediated transport into the endocytic recycling compartment. *Nature Cell Biology*, *9*(12), 1370–1380. https://doi.org/10.1038/ncb1656
Van der Sluijs, P., Hull, M., Webster, P., Mâle, P., Goud, B., & Mellman, I. (1992). The small GTP-binding protein Rab4 controls an early sorting event on the endocytic pathway. *Cell*, *70*(5), 729–740. https://doi.org/10.1016/0092-8674(92)90307-X
Van Roy, F., & Berx, G. (2008). The cell-cell adhesion molecule E-cadherin. *Cellular and Molecular Life Sciences*, *65*(23), 3756–3788. https://doi.org/10.1007/s00018-008-8281-1
Vonderheit, A., & Helenius, A. (2005). Rab7 Associates with Early Endosomes to Mediate Sorting and Transport of Semliki Forest Virus to Late Endosomes. *PLoS Biology*, *3*(7), e233. https://doi.org/10.1371/journal.pbio.0030233
Wandinger-Ness, A., & Zerial, M. (2014). Rab proteins and the compartmentalization of the endosomal system. *Cold Spring Harbor Perspectives in Biology*, *6*(11), a022616. https://doi.org/10.1101/cshperspect.a022616
Wang, Q., Chen, X.-W., & Margolis, B. (2007). PALS1 Regulates E-Cadherin Trafficking in Mammalian Epithelial Cells. *Molecular Biology of the Cell*, *18*(March), 874–885. https://doi.org/10.1091/mbc.E06
Wang, S. Y., Zhao, Z., & Rodal, A. A. (2019). Higher-order assembly of Sorting Nexin 16 controls tubulation and distribution of neuronal endosomes. *Journal of Cell Biology*, *218*(8), 2600–2618. https://doi.org/10.1083/JCB.201811074
Wang, Y., Seemann, J., Pypaert, M., Shorter, J., & Warren, G. (2003). A direct role for GRASP65 as a mitotically regulated Golgi stacking factor. *EMBO Journal*, *22*(13), 3279–3290. https://doi.org/10.1093/emboj/cdg317
Wang, Z., Sandiford, S., Wu, C., & Li, S. S. C. (2009). Numb regulates cell-cell adhesion and polarity in response to tyrosine kinase signalling. *EMBO Journal*, *28*(16), 2360–2373. https://doi.org/10.1038/emboj.2009.190
Weeratunga, S., Paul, B., & Collins, B. M. (2020). Recognising the signals for endosomal trafficking. *Current Opinion in Cell Biology*, *65*, 17–27. https://doi.org/10.1016/j.ceb.2020.02.005
Weigert, R. (2014). Live Mammalian Tissues. *Cold Spring Harbor Perspectives in Biology*, 1–12.
West, M., Zurek, N., Hoenger, A., & Voeltz, G. K. (2011). A 3D analysis of yeast ER structure reveals how ER domains are organized by membrane curvature. *Journal of Cell*

Biology, *193*(2), 333–346. https://doi.org/10.1083/jcb.201011039
Wheelock, M. J., Shintani, Y., Maeda, M., Fukumoto, Y., & Johnson, K. R. (2008). Cadherin switching. *Journal of Cell Science*, *121*(6), 727–735. https://doi.org/10.1242/jcs.000455
Wiederkehr, A., De Craene, J. O., Ferro-Novick, S., & Novick, P. (2004). Functional specialization within a vesicle tethering complex: Bypass of a subset of exocyst deletion mutants by Sec1p or Sec4p. *Journal of Cell Biology*, *167*(5), 875–887. https://doi.org/10.1083/jcb.200408001
Woichansky, I., Beretta, C. A., Berns, N., & Riechmann, V. (2016). Three mechanisms control E-cadherin localization to the zonula adherens. *Nature Communications*, *7*. https://doi.org/10.1038/ncomms10834
Worby, C. A., & Dixon, J. E. (2002). Sorting out the cellular functions of sorting nexins. *Nature Reviews Molecular Cell Biology*, *3*(12), 919–931. https://doi.org/10.1038/nrm974
Wu, S., Mehta, S. Q., Pichaud, F., Bellen, H. J., & Quiocho, F. A. (2005). Sec15 interacts with Rab11 via a novel domain and affects Rab11 localization in vivo. *Nature Structural and Molecular Biology*, *12*(10), 879–885. https://doi.org/10.1038/nsmb987
Wu, X., Bowers, B., Rao, K., & Wei, Q. (1998). *Visualization of Melanosome Dynamics within Wild-Type and Dilute Melanocytes Suggests a Paradigm for Myosin V Function In Vivo*. *143*(7), 1899–1918.
Wucherpfennig, T., Wilsch-Brauninger, M., & González-Gaitán, M. (2003). Role of Drosophila Rab5 during endosomal trafficking at the synapse and evoked neurotransmitter releaase. *Journal of Cell Biology*, *161*, 609–624. https://doi.org/10.1083/jcb.200211087
Xiong, X., Xu, Q., Huang, Y., Singh, R. D., Anderson, R., Leof, E., Hu, J., & Ling, K. (2012). An association between type Iγ PI4P 5-kinase and Exo70 directs E-cadherin clustering and epithelial polarization. *Molecular Biology of the Cell*, *23*(1), 87–98. https://doi.org/10.1091/mbc.E11-05-0449
Xu, Jiang, Lan, L., Bogard, N., Mattione, C., & Cohen, R. S. (2011). Rab11 Is Required for Epithelial Cell Viability , Terminal Differentiation , and Suppression of Tumor-Like Growth in the Drosophila Egg Chamber. *PLoS ONE*, *6*(5). https://doi.org/10.1371/journal.pone.0020180
Xu, Jinxin, Zhang, L., Ye, Y., Shan, Y., Wan, C., Wang, J., Pei, D., Shu, X., & Liu, J. (2017). SNX16 Regulates the Recycling of E-Cadherin through a Unique Mechanism of Coordinated Membrane and Cargo Binding. *Structure*, *25*, 1251–1263.
Xu, T., & Rubin, G. M. (1993). Analysis of genetic mosaics in developing and adult Drosophila tissues. *Development*, *117*(4), 1223–1237.
Yang, D. H., Cai, K. Q., Roland, I. H., Smith, E. R., & Xu, X. X. (2007). Disabled-2 is an epithelial surface positioning gene. *Journal of Biological Chemistry*, *282*(17), 13114–13122. https://doi.org/10.1074/jbc.M611356200
Yeaman, C., Grindstaff, K. K., & Nelson, W. J. (2004). Mechanism of recruiting Sec6/8 (exocyst) complex to the apical junctional complex during polarization of epithelial cells. *Journal of Cell Science*, *117*(4), 559–570. https://doi.org/10.1242/jcs.00893
Yilmaz, M., & Christofori, G. (2009). EMT, the cytoskeleton, and cancer cell invasion. *Cancer and Metastasis Reviews*, *28*(1–2), 15–33. https://doi.org/10.1007/s10555-008-9169-0
Yilmaz, M., & Christofori, G. (2010). Mechanisms of motility in metastasizing cells. *Molecular Cancer Research*, *8*(5), 629–642. https://doi.org/10.1158/1541-7786.MCR-10-0139
Yonemura, S., Wada, Y., Watanabe, T., Nagafuchi, A., & Shibata, M. (2010). α-Catenin as a tension transducer that induces adherens junction development. *Nature Cell Biology*, *12*(6), 533–542. https://doi.org/10.1038/ncb2055
Zeigerer, A., Gilleron, J., Bogorad, R. L., Marsico, G., Nonaka, H., Seifert, S., Epstein-Barash, H., Kuchimanchi, S., Peng, C. G., Ruda, V. M., Conte-Zerial, P. Del, Hengstler, J. G., Kalaidzidis, Y., Koteliansky, V., & Zerial, M. (2012). Rab5 is necessary for the biogenesis of the endolysosomal system in vivo. *Nature*, *485*(7399), 465–470. https://doi.org/10.1038/nature11133
Zerial, M., & McBride, H. (2001). Rab proteins as membrane organizers. *Nature Reviews Molecular Cell Biology*, *2*(2), 107–117. https://doi.org/10.1038/35052055
Zhang, J., Schulze, K. L., Hiesinger, P. R., Suyama, K., Wang, S., Fish, M., Acar, M.,

Hoskins, R. A., Bellen, H. J., & Scott, M. P. (2007). Thirty-one flavors of Drosophila rab proteins. *Genetics*, *176*(2), 1307–1322. https://doi.org/10.1534/genetics.106.066761

Zhang, M., Chen, L., Wang, S., & Wang, T. (2009). Rab7: Roles in membrane trafficking and disease. *Bioscience Reports*, *29*(3), 193–209. https://doi.org/10.1042/BSR20090032

Zhang, X. M., Ellis, S., Sriratana, A., Mitchell, C. A., & Rowe, T. (2004). Sec15 is an effector for the Rab11 GTPase in mammalian cells. *Journal of Biological Chemistry*, *279*(41), 43027–43034. https://doi.org/10.1074/jbc.M402264200

Zhitomirsky, B., Farber, H., & Assaraf, Y. G. (2018). LysoTracker and MitoTracker Red are transport substrates of P-glycoprotein: implications for anticancer drug design evading multidrug resistance. *Journal of Cellular and Molecular Medicine*, *22*(4), 2131–2141. https://doi.org/10.1111/jcmm.13485

Zobel, T., Brinkmann, K., Koch, N., Schneider, K., Seemann, E., Fleige, A., Qualmann, B., Kessels, M. M., & Bogdan, S. (2015). Cooperative functions of the two F-BAR proteins Cip4 and Nostrin in the regulation of E-cadherin in epithelial morphogenesis. *Journal of Cell Science*, *128*(7), 1453–1453. https://doi.org/10.1242/jcs.170944